Journal Pre-proof

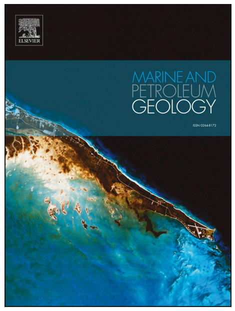

Nature and preservation of Late Jurassic breakup-related volcanism in the carnarvon basin, North West shelf, Australia

Michael S. Curtis, Simon P. Holford, Mark A. Bunch, Nick Schofield

PII: S0264-8172(23)00210-6

DOI: https://doi.org/10.1016/j.marpetgeo.2023.106304

Reference: JMPG 106304

To appear in: *Marine and Petroleum Geology*

Received Date: 5 July 2022

Revised Date: 26 April 2023

Accepted Date: 27 April 2023

Please cite this article as: Curtis, M.S., Holford, S.P., Bunch, M.A., Schofield, N., Nature and preservation of Late Jurassic breakup-related volcanism in the carnarvon basin, North West shelf, Australia, *Marine and Petroleum Geology* (2023), doi: https://doi.org/10.1016/j.marpetgeo.2023.106304.

Nature and preservation of Late Jurassic breakup-related volcanism in the Carnarvon Basin, North West Shelf, Australia.

Michael S. Curtis[a*], Simon P. Holford[a], Mark A. Bunch[a] & Nick Schofield[b]

[a]Australian School of Petroleum and Energy Resources, University of Adelaide, North Terrace, Adelaide, South Australia, 5005, Australia

[b]Department of Geology and Geophysics, University of Aberdeen, King's College, Aberdeen, AB24 3FX, Scotland

*Corresponding Author: michael.curtis@adelaide.edu.au

+61 (0) 452 327 771

Other author contact details: simon.holford@adelaide.edu.eu

mark.bunch@adelaide.edu.au

n.schofield@abdn.ac.uk

Competing Interests

The authors hereby declare that they have no competing interests.

Funding

This work was funded through a postgraduate scholarship from the University of Adelaide, Faculty of Engineering Computer and Mathematical Sciences, and also by ASEG Research Foundation Grant no. RF19P01. These funding sources had no involvement in study design; in the collection, analysis and interpretation of data; in the writing of the report; or in the decision to submit the article for publication.

ABBREIVATIONS[1]

[1] Abbreviations (in order of first appearance in text and figures): ESB – Exmouth Sub-Basin; NCB – Northern Carnarvon Basin; TVC – Toro Volcanic Complex; LIP – Large Igneous Province; WAM – West Australian Margin; Mt.A – the Pyrenees Volcano; CRFZ – Cape Range Fracture Zone; KVU – Valanginian (Cretaceous) 'KV' Unconformity; IHU – Intra-Hauterivian (Cretaceous) Unconformity; EP – Exmouth Plateau; NiA – Ningaloo Arch; NoA – Novara Arch; ResA – Resolution Arch; Fm – Formation, Sst. Sandstone; LBG – Lower Barrow Group, UBG – Upper Barrow Group; ODP – Offshore Drilling Program; TWT – Two-way seismic time; msTWT – Milliseconds two-way seismic time; RMS – Root Mean Square; Ma – Million years ago; SVP – Southern Volcanic Province.

HIGHLIGHTS

Two Late Jurassic volcanic centres: the Pyrenees Volcano and the Toro Volcanic Complex, are present in the inboard Exmouth Sub-Basin (ESB), part of the Carnarvon Basin, Western Australia.

The Pyrenees Volcano is well preserved, whilst the Toro Volcanic Complex has been peneplaned following Late Jurassic to Early Cretaceous uplift and erosion.

The proximity of preserved volcanic centres to arches uplifted from the Late Jurassic to the Early Cretaceous suggests a broader volcanic province in the southern ESB was uplifted and eroded.

Geologists may be underestimating the significance of pre-breakup extrusive volcanic rocks on magma-rich rifted margins worldwide.

ABSTRACT

The North West Australian Margin, which formed as Greater India rifted from Australia during the Jurassic to Early Cretaceous, is recognised as an archetypal magma-rich rifted margin, with records of extensive igneous activity in the Exmouth Plateau and Exmouth Sub-Basin (ESB) of the Northern Carnarvon Basin (NCB). Pre-breakup magmatism is manifested by a large ~400 x 150 km intrusive sill complex, emplaced into Triassic and Jurassic strata in the Late Jurassic and Early Cretaceous. An apparent lack of extrusive igneous rocks has caused previous works to describe the region as a large *intrusive* igneous province. Here, we describe two recently identified Upper Jurassic volcanic centres: the Pyrenees Volcano in the eastern ESB (first reported here), and the Toro Volcanic Complex (TVC), in the western ESB. Although offset by Early Cretaceous normal faulting, the edifice of the Pyrenees Volcano and associated lava flows are well preserved beneath a protective carapace of Upper Jurassic strata below the angular Intra-Hauterivian Unconformity on the Novara Arch. In contrast, a significant proportion of the TVC was peneplaned beneath an intra-Valanginian (Early Cretaceous) unconformity following breakup-related uplift. As Upper Triassic to Lower Cretaceous strata appear to have been eroded over the Ningaloo Arch in the southern ESB, we postulate that Late Jurassic extrusive volcanism may have been more spatially extensive, prior to erosion associated with Early Cretaceous exhumation in the southern NCB. Hence our findings suggest that the NCB was potentially host to significantly more extrusive volcanism than has been preserved within basin fill. Our findings also have broader implications for the conditions required to preserve extrusive igneous material in sedimentary

basins within large igneous provinces that have undergone complex histories of rift-related vertical motion.

KEYWORDS

Volcano, intrusion, erosion, unconformity, Northern Carnarvon Basin, Large Igneous Province (LIP), volcanic rifted margin.

1. INTRODUCTION

The northern part of the West Australian Margin (WAM), which formed as a result of Mesozoic rifting and break-up of Greater India and the Australian continent, is widely considered to be an archetypal example of a volcanic or magma-rich rifted continental margin (White and McKenzie, 1989, Planke et al., 2000). Breakup-related magmatism along the margin is evidenced by the presence of a large igneous province (LIP) focused on the Northern Carnarvon Basin (NCB) (Figure 1) covering an area of ~45 000 km^2 (Frey et al., 1998, Rohrman, 2013). Seismic reflection data shows that the Exmouth LIP is characterised by extensive pre-breakup intrusions in the Exmouth Sub-Basin and Exmouth Plateau, syn-breakup extrusive igneous rocks on the Gascoyne and Cuvier margins, and a post-breakup volcanic plateau further outboard on the Cuvier Abyssal Plain (Symonds et al., 1998). The origin of this LIP has been variably ascribed to mantle plume activity (Rohrman, 2015), mantle convection (Mihut and Müller, 1998) and rift-related decompressional melting (Mutter and Larson, 1989).

Much of the recent work on the magmatic history of the WAM (e.g. Frey et al., 1998, Mihut and Müller, 1998, Symonds et al., 1998, Müller et al., 2002, Holford et al., 2013, Magee et al., 2013a, McClay et al., 2013, Rohrman, 2013, Rohrman, 2015, Magee et al., 2017, Magee and Jackson, 2020, Mark et al., 2020) has focused on the Northern Carnarvon Basin (NCB). Whilst there is abundant evidence for extensive occurrence of intrusive igneous rock (dominantly expressed by interconnected sill complexes) within the Exmouth LIP (Figure 1), a defining characteristic of this igneous province is the paucity of extrusive rocks, with Rohrman (2013) proposing the term Large *Intrusive* Igneous Province to define the magmatism in this region. Though variable, the volumetric ratio of intrusive to extrusive rock associated with magmatic systems is typically 2-3:1 (White et al., 2006). Hence, one would expect that between one-quarter to one-third of the total volume of igneous material in the NCB might be extrusive. However, there is scant present-day evidence for extrusive rock in the NCB. The basin lacks extensive syn-rift basaltic sequences that have been observed in analogous inboard basins at volcanic margins (e.g. the Faroe-Shetland and Rockall basins, offshore UK; (Schofield et al., 2017, Jolley et al., 2021)). Only isolated well penetrations of pre-breakup extrusive igneous rocks are observed (Tithonian basaltic volcanics in Toro-1; (Curtis et al., 2022); and thin Tithonian to Valanginian ashfall deposits in Enfield-3, Enfield-4, and Stybarrow-2; (Curtis et al., 2022); Figure 1).

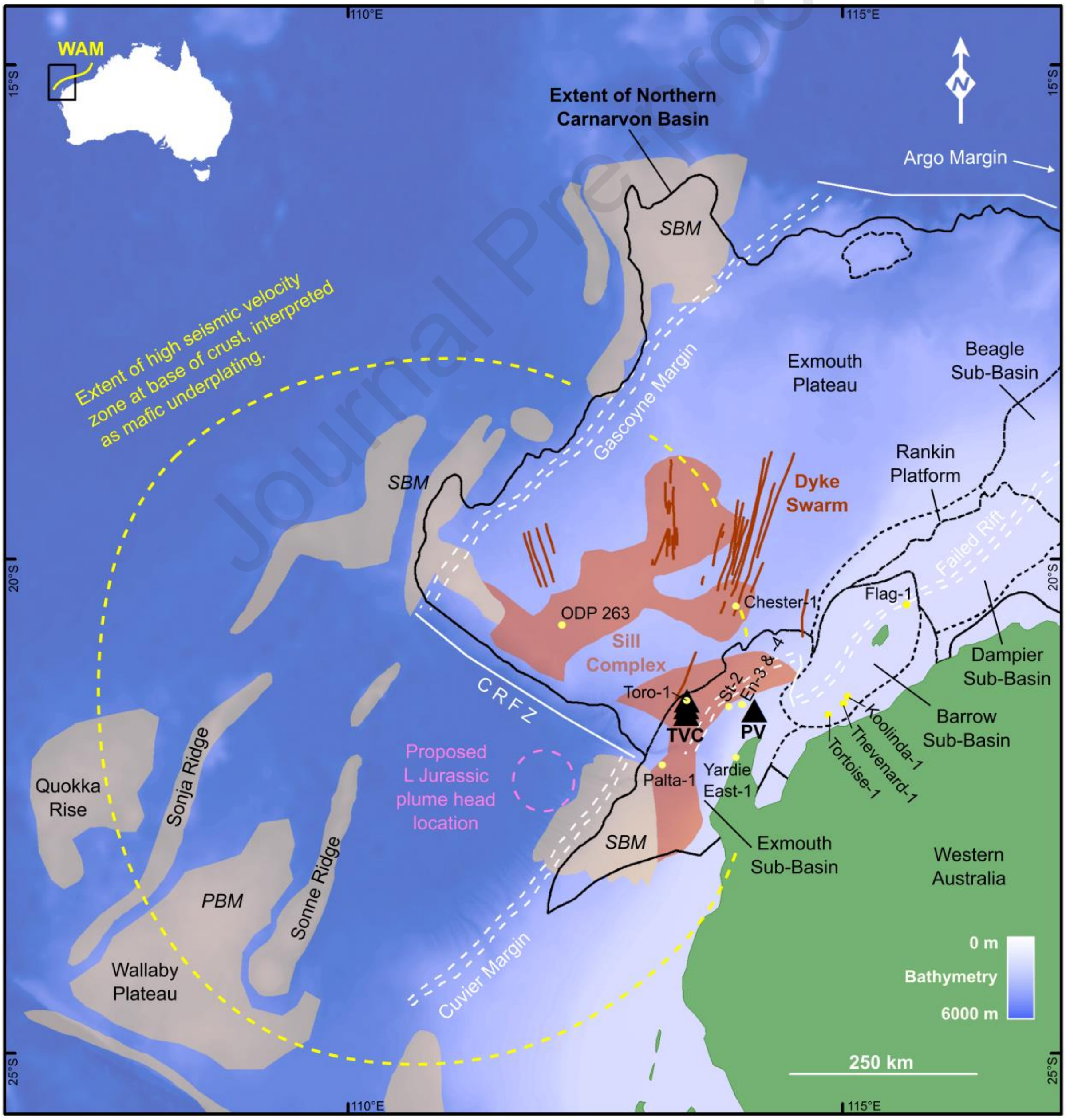

Figure 1: Regional map of Northern Carnarvon Basin, showing locations of major igneous centres, Middle Jurassic to Early Cretaceous rift zones and Sub-Basin outlines. Yellow dots are locations of petroleum exploration wells that have penetrated igneous material. Orange shaded areas denote intrusion locations as defined by Frey et al (1998). Pale brown shaded areas indicate regions of syn- (SBM) and post- (PBM) breakup magmatism (after Frey et al., 1998, Symonds et al., 1998, Rey et al., 2008 and Holford et al., 2013). Stippled black lines are positive magnetic anomalies in the Cuvier Abyssal Plain, interpreted from the AGSO 2000 Magnetic Anomaly Grid. WAM - North West Australian Margin; CRFZ - Cape Range Fracture Zone; TVC - Toro Volcanic Complex; PV - Pyrenees Volcano; black triangles represent volcanic centres. Well abbreviations: St-2 – Stybarrow 2; En-3 & -4 – Enfield-3 and Enfield-4.

The focus of this study is to determine the possible processes responsible for the enigma that is an apparent absence of syn-rift extrusive volcanism in the NCB. We investigate the preservation histories of the only known syn-rift volcanic centres within the NCB, both of which were emplaced in the Late Jurassic. First, we first evaluate the Pyrenees Volcano, located in the eastern Exmouth Sub-Basin (Figure 1), which we find was protected from breakup-related uplift and erosion by downfaulting and a thick covering of Tithonian deltaic sedimentary rocks. We then evaluate the Toro Volcanic Complex (TVC), located in the western Exmouth Sub-Basin (Figure 1), where our seismic mapping indicates the volcanic complex was peneplaned beneath a Valanginian-aged breakup unconformity accounting for Jurassic and Triassic strata that were removed across much of the Exmouth Sub-Basin. Our findings imply that a large area in the southern Exmouth Sub-basin, possibly host to extrusive igneous rock, was subject to erosion during breakup-related uplift. If volcanic rocks from this region were indeed eroded, this would contribute to re-balancing the currently skewed intrusive:extrusive igneous rock ratio of the Exmouth LIP.

2. GEOLOGICAL SETTING

2.1 Tectonostratigraphy of the Northern Carnarvon Basin

The Northern Carnarvon Basin (NCB) is part of the West Australian Margin and is a product of Jurassic rifting and Early Cretaceous breakup between Greater India and the Australian Continent. It is bound by the Argo Margin to the north, the Gascoyne Margin to the west, the Cuvier Margin to the South and the Australian Continent to the East (Figure 1). The Exmouth Sub-Basin, which is the focus of this study, is one of a series of NE-SW trending Sub-Basins within the inboard NCB (Figure 1). A simplified stratigraphic column for the NCB is provided in Figure 2; a detailed stratigraphic column for the Late Jurassic and Early Cretaceous, the period in which magmatic activity took place, is provided in Figure 3.

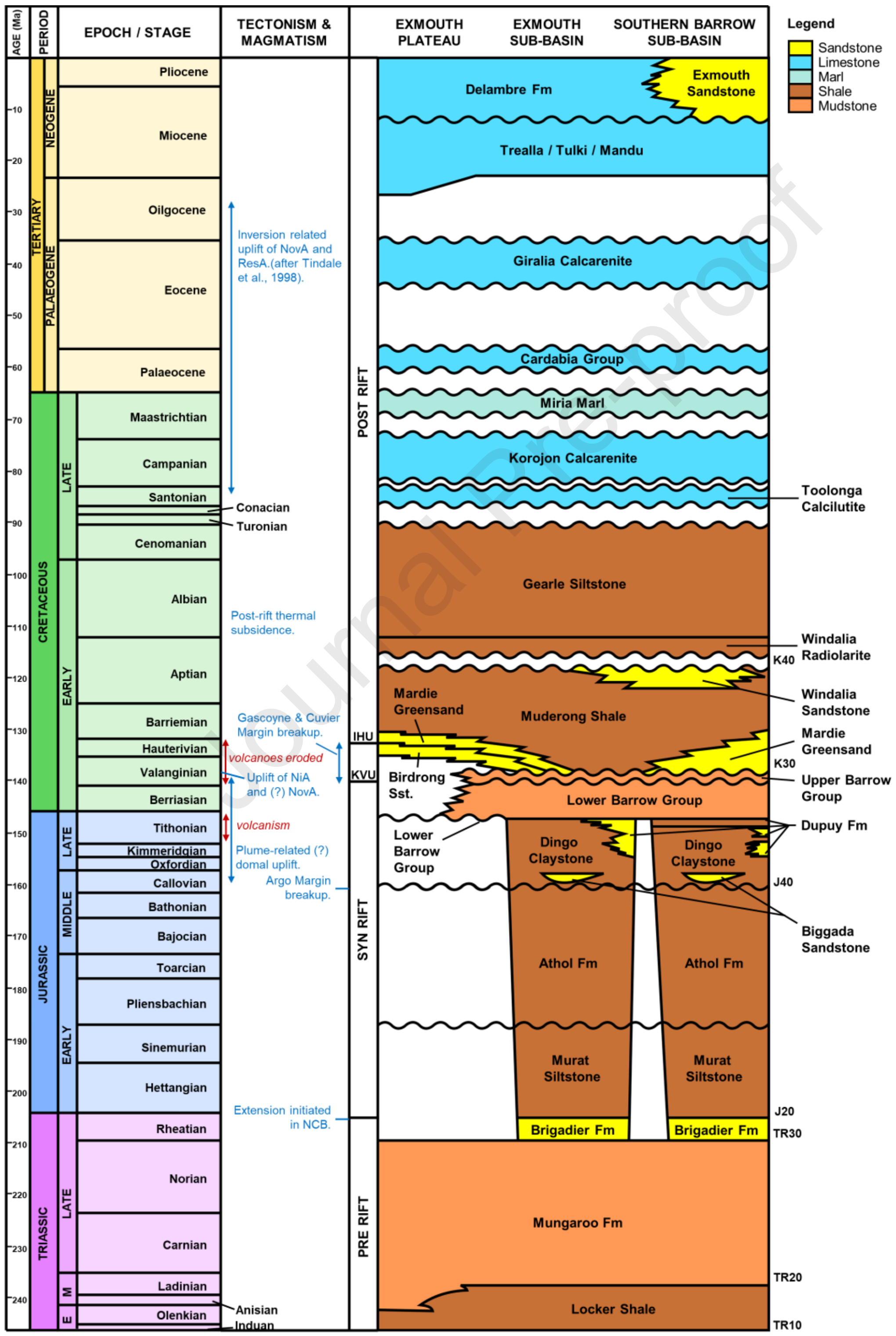

Figure 2: Stratigraphic column for the Northern Carnarvon Basin, modified from Wilkins (2002). NCB – Northern Carnarvon Basin; EP – Exmouth Plateau; ESB – Exmouth Sub-Basin; NiA – Ningaloo Arch; NoA – Novara Arch; IHU – Intra-Hauterivian (Cretaceous) Unconformity; KVU – Valanginian (Cretaceous) 'KV' Unconformity; Fm – Formation; Sst. – Sandstone; DCy – Dingo Claystone; TVC – Toro Volcanic Complex; PV – Pyrenees Volcano. Sequence boundaries (TR10, TR20 etc) after Longley et al. (2002) and Marshall and Lang (2013).

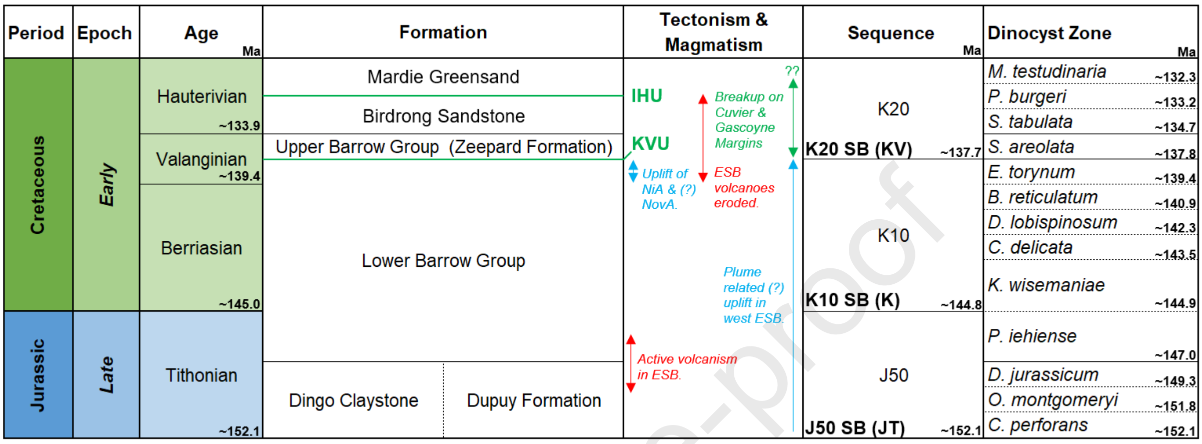

Figure 3: Detailed stratigraphic column for the Exmouth Sub-Basin and Exmouth Plateau spanning the Tithonian (Late Jurassic) to the Hauterivian (Early Cretaceous). Sequences, sequence boundaries and dinocyst zones after Longley et al. (2002) and Marshall and Lang (2013). ESB – Exmouth Sub-Basin; IHU – Intra-Hauterivian (Cretaceous) Unconformity; KVU – Valanginain (Cretaceous) 'KV' Unconformity; NiA – Ningaloo Arch; NovA – Novara Arch.

2.1.1 Early deposition and rifting

The oldest sedimentary rocks in the NCB are found within the Locker Shale, a roughly 5 km thick package of deep marine shales and silts, deposited from the Early to the Middle Triassic (Lipski, 1993). The Locker Shale is unconformably overlain by the Mungaroo Formation, an extensive fluvio-deltaic sequence deposited through the Middle and Late Triassic, containing up to 6 km of fluvial channel sandstones, floodplain deposits, and lower delta plain channel soils and coals, and is present throughout the NCB (Adamson et al., 2013, Heldreich et al., 2017, Payenberg et al., 2019). Following flooding of the Mungaroo Delta through the Rhaetian, a fining up sequence of sandstones to siltstones was deposited as the Brigadier Formation. (Hocking, 1992).

The onset of rifting between Greater India and the Australian continent in the Earliest Jurassic caused rapid subsidence, initiating a chain of northeast-southwest oriented Sub-Basins: the Exmouth Sub-Basin, the Barrow Sub-Basin, the Dampier Sub-Basin and the Beagle Sub-Basin (Jablonski, 1997, Longley et al., 2002, Chongzhi et al., 2013). A structural high named the Alpha Arch developed during this episode, separating the Exmouth and Barrow Sub-Basins (Figure 4). Within the Sub-Basins, deep marine shales of the Murat and Athol formations were deposited until the end of the Callovian (Hocking, 1992). Inboard, this rifting generated NNE-SSW oriented normal faults with offsets of ~300 to ~800 m in the Exmouth Sub-Basin (Black et al., 2017, Dempsey et al., 2019) and Exmouth Plateau (Barber, 1982, Velayatham et al., 2018). This first stage of extension was focussed to the northeast of the Exmouth Plateau and culminated in breakup on the Argo Margin in the Callovian to Oxfordian (Tindale et al., 1998).

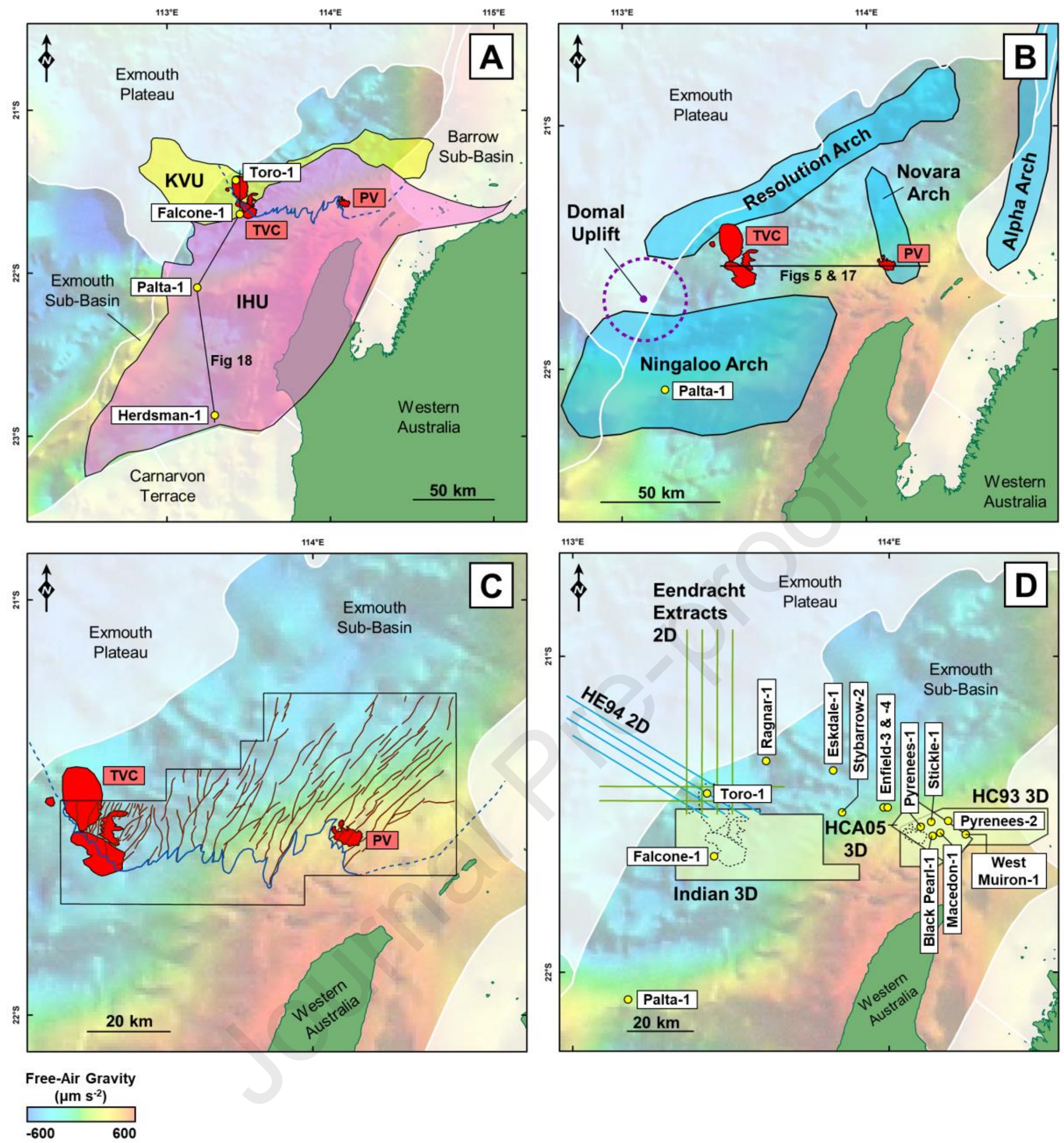

Figure 4: Maps showing structural elements within the Exmouth Sub-Basin. The background is the Global Gravity Map (v10.1) of Sandwell and Smith (1997), which highlights the Ningaloo Arch in the southern Exmouth Sub-Basin. The locations of the Pyrenees Volcano (PV) and the Toro Volcanic Complex (TVC) are shown on each map. (A) Map showing areas where Jurassic and Early Cretaceous rocks are eroded beneath the Valanginian 'KV' Unconformity (KVU) and Intra-Hauterivian Unconformity (IHU) in the Exmouth Sub-Basin, after Reeve et al. (2022). The dark blue line represents the intersection of the subcrop of the top volcanics horizon with the KVU and IHU. Also shown is the line of section for Figure 18. (B) Map showing areas of uplift within the Exmouth Sub-Basin after Tindale et al. (1998), Reeve et al. (2022) and seismic mapping conducted as part of this study. Also shown is the line of section for Figures 5 and 17. (C) Map showing locations of major faults in Late Jurassic strata within the Exmouth-Sub-Basin. The black box is the combined study areas of Underschultz et al. (2008) and Black et al. (2017). The dark blue line represents the intersection of the subcrop of the top volcanics horizon with the KVU and IHU. (D) Map showing the locations of seismic reflection survey data and petroleum exploration wells that provided sources analysed in this study.

Rifting continued through the Late Jurassic (Jablonski, 1997) while the Exmouth, Barrow and Dampier Sub-Basins were filled with deep marine shales of the Dingo Claystone (Hocking, 1992), followed by turbidite deposits of the Dupuy Formation (Tait, 1985, Hocking, 1992). There was little deposition on the Exmouth Plateau during this time (Exon et al., 1992, Tindale et al., 1998, Reeve et al., 2016).

2.1.2 Breakup and unconformity development

Regional uplift, centred on the Cape Range Fracture Zone (CRFZ) (Figure 1), the Gascoyne Block (the rifted-continental block to the west of the CRFZ) and the Australian hinterland (to the south), was initiated during the Tithonian to Berriasian (from 146.7-144.5 Ma) (Reeve et al., 2016), possibly due to mantle plume-related thermal doming (Rohrman, 2015) (Figure 1), mantle convection (Braun and Beaumont, 1989), depth-dependent extension (Driscoll and Karner, 1998) or a combination of these processes (Reeve et al., 2016). Black et al. (2017) identified a link between a sub-circular region of uplift, roughly 70 km in diameter, centred approximately 100 km west of the Exmouth Peninsula, and plume related uplift based on the work of Rohrman (2015) (Figure 4).

This regional uplift exposed Jurassic rocks which became the source for an extensive system of rivers that supplied sediment northwards and westwards onto a prograding siliciclastic shoreline and shelf (Paumard et al., 2018). The sedimentary rocks deposited through the Late Tithonian and Valanginian by these rivers and associated shelf deltas make up the Lower Barrow Group (LBG) (Reeve et al., 2016, Paumard et al., 2018). The thickness of the LBG across the Exmouth Sub-Basin reaches up to 3 km (Reeve et al., 2016), with clinoforms varying in height from ~100 to ~550 m (Paumard et al., 2018). Paumard et al. (2018) have sub-divided the LBG into six sequences calibrated to the P. iehiense, K. wiseamaniae, C. delicata, D. lobispinosum, B. reticulatum and E. torynum dinocyst zones, which vary in thickness and spatial extent across depocentres in the Exmouth Plateau, Exmouth Sub-Basin and Barrow Sub-Basin as a result of dynamic variations in accommodation space and sediment supply. This recent re-interpretation has superseded the earlier concept that the LBG represents sedimentary rocks deposited in a single delta system, as postulated by previous workers (e.g. Tait (1985) and, to an extent, Reeve et al. (2016)). Within the Exmouth Sub-Basin, the LBG conformably overlies Jurassic strata of the Dingo Claystone and Dupuy Formations.

The Ningaloo Arch is an east-west striking anticlinal structure with a long axis of roughly 130 km that separates the central and southern sections of the Exmouth Sub-Basin (Figure 4). Uplift along the Ningaloo Arch occurred in the Valanginian causing erosion, generating the "KV" (K: Cretaceous; V: Valanginian) Unconformity (KVU) between 134.98 and 133.74 Ma (Tindale et al., 1998, Reeve et al., 2022) (Figure 4). The KVU is manifested as an angular unconformity in the Exmouth Sub-Basin, and as a disconformity across the south-eastern Exmouth Plateau as a result of non-deposition (Reeve et al., 2022). Many workers have concluded that this unconformity formed as a result of breakup on the Cuvier margin (occurring contemporaneously with breakup on the Gascoyne margin) (Tindale et al., 1998, Longley et al., 2002, Marshall and Lang, 2013, Black et al., 2017). Most recently, Alves et al. (2023) have specifically defined this surface as a 'Lithospheric Breakup *Surface*' representing the <u>*onset*</u> of lithospheric breakup, above which a series of sequentially backstepping sequences, related to increasing water depths, are deposited that collectively form a 'Breakup *Sequence*' (representing the period between the onset of lithospheric breakup and a time when subsidence is controlled predominantly by thermal relaxation). In this paper, whilst we recognise the application of the new terminology of Alves et al. (2023), to keep in line with language used in previous work and that used by the local petroleum industry, we continue to use the term 'unconformity' to describe this surface in the sense that, in our study area (the central Exmouth Sub-Basin), it represents a surface of contact between two groups of unconformable strata.

We also note that Reeve et al. (2022) disagree with the notion that the KVU represents breakup. They present palynological analyses that suggests its age is contemporaneous with the formation of magnetic stripes at the outboard edge of the Gascoyne Margin, which they postulate formed before the full rupture of lithosphere. They instead associate the KVU with localisation of extension along narrow continental rift zones. Two additional uplifted arches are present within the Exmouth Sub-Basin: the Resolution Arch (with a long axis of roughly 125 km), which forms the northern boundary of the Exmouth Sub-Basin, and the Novara Arch (with a long axis of roughly 50 km), which crosses the central Exmouth Sub-Basin (Figure 4). Tindale et al. (1998) suggested that the formation of these arches was much later, associated with inversion during the Santonian to Oligocene. However recent work by Reeve et al. (2022) mapping the KVU erosional surface (Figure 4) suggests that these arches might possibly have been uplifted and eroded, along with the Ningaloo Arch, during the Valanginian.

Eroded material from the uplifted Ningaloo, (and possibly also the Novara and Resolution arches, after Reeve et al. (2022)) was redeposited as the deltaic Zeepard Formation, which has also been defined as the Upper Barrow Group (UBG), in the Middle Valanginian (Arditto, 1993, Reeve et al., 2016, Paumard et al., 2018). The UBG is equivalent to a seventh, E. torynum, dinocyst sequence of Paumard et al. (2018). The UBG is thickest (~200 m) over a 50 km wide region on the Exmouth Plateau immediately north of the Exmouth Sub-Basin. Following deposition of the UBG, a marine transgression reworked the UBG and deposited shoreface sands of the Birdrong Sandstone (Hocking et al., 1988).

It has recently been suggested that continental breakup between Greater India and Australia, and the eventual initiation of oceanic crust formation along the Cuvier and Gascoyne margins, occurred over a period of 4-5 million years from the Hauterivian to the Barriemian (Early Cretaceous) (Robb et al., 2005, Direen et al., 2008, Reeve et al., 2021). Robb et al. (2005), Direen et al. (2008) and Reeve et al, (2021) define an Intra-Hauterivian Unconformity (IHU), at the top surface of the Birdrong Sandstone (Reeve et al., 2016). They argue that the IHU is expressed as an angular unconformity across much of the southern Exmouth Sub-Basin, truncating the KVU both in the eastern Exmouth Sub-Basin above the Novara and Resolution arches, and southern Exmouth Sub-Basin across the Ningaloo Arch (Reeve et al., 2022) (Figure 4). In their model, the IHU forms a disconformity across the southeastern Exmouth Plateau and represents a period of non-deposition (Reeve et al., 2022). In Reeve et al. (2022)'s model, the IHU is the main breakup unconformity, not the KVU. They suggest this surface, representing uplift and erosion in the Exmouth Sub-Basin, formed as a result of the final stages of breakup on the outboard edge of the Gascoyne Margin (northwest of the Exmouth Plateau) during the Hauterivian and Barriemian from 132.5 to 131 Ma. This timing is based on the age of magnetic stripes in the Gascoyne abyssal plain (Reeve et al., 2021).

An alternative model is proposed by Alves et al. (2023). As mentioned previously, they define the KVU as a surface that formed contemporaneously with the *onset* of lithospheric breakup in the nearby Cuvier Margin. Alves et al. (2023) refute the idea that far-field stresses, such as those along the Gascoyne Margin, could have initiated unconformities impacting strata so far inboard as the Exmouth Sub Basin. Hence, they do not recognise the IHU proposed by Reeves et al. (2022). Alves et al. (2023) instead note that Marshall and Lang (2013) and Smith et al. (2003) show that the Zeepard and Birdrong formations (bounded by the KVU beneath and IHU above in the model of Reeve et al. (2022)) are separated by flooding surfaces and are progressively backstepping above the LBG; and that another flooding surface separates the Birdrong Sandstone from the overlying Mardie Greensand. They suggest it is not necessary to invoke the presence of an unconformity such as Reeve et al. (2022)'s IHU to explain the upward transition from the Birdrong Sandstone to the Mardie Greensand. Seemingly cross cutting relationships and apparent truncations might instead be explained by differing directions of progradation following flood events. Alves et al. (2023) define the progressively deepening upwards stacking pattern represented by the Zeepard and Birdrong formations as forming the first part of a *Breakup Sequence*, occurring between the initiation of breakup and a time when thermal relaxation dominates subsidence.

Regardless of which model is correct, the KVU and/or the IHU record a maximum of over 2 km of erosion in the southern Exmouth Sub-Basin (Rohrman, 2015), and at least 900 m in the central Exmouth Sub-Basin (Black et al., 2017). At the Palta-1 petroleum exploration well in the southern Exmouth Sub-Basin (Figure 1), vitrinite reflectance data suggest that up to ~2.5 km of sedimentary rocks have been eroded beneath the unconformities (Gibson, 2014). This removed section includes the entire Lower Cretaceous and Jurassic syn-rift sequences, and part of the Triassic pre-rift sequence.

The period of rifting leading to breakup on the Gascoyne and Cuvier margins is associated with a second episode of faulting across the NCB (Figure 4): some of the earlier NNE-SSW oriented normal faults were reactivated, with offsets of 150 m recorded in Callovian to Tithonian strata in the Exmouth Sub-Basin (Black et al., 2017). NE-SW oriented faults were also initiated in this period, with displacements of 5 to 60 m within Oxfordian to Valanginian strata (Black et al., 2017). Some of the

NE-SW oriented faults link with the NNE-SSW oriented faults in Callovian strata. Most upper fault tips terminate at the KVU or IHU, while a minority extend upwards above these unconformities where minor offsets are visible (Black et al., 2017).

The Mardie Greensand was deposited across the NCB above the Birdrong Sandstone from the Late Hauterivian to the Barremian following a marine incursion (Hocking et al., 1988, Reeve et al., 2016). Reeve et al. (2022) note that the ages of deposited sediments above their IHU are older over the Exmouth Plateau than over the Novara Arch, possibly representing the effect of ongoing uplift and erosion.

2.1.3 Post-breakup

Post-breakup, the NCB entered a thermal sag phase. Predominantly deep marine shales of the Muderong Formation were deposited from the Barremian until the Late Cretaceous, except for the Aptian Windalia Sandstone, which represents regression and deposition of a delta sourced from the northwest Australian continent (Felton et al., 1992). The uppermost strata of the Northern Carnarvon Basin comprise a series of carbonate units, deposited from the Late Cretaceous through to the present day (Quilty, 1977, McCaffrey et al., 2020, Riera, 2020).

2.2 Magmatic record of the Northern Carnarvon Basin

The magmatic record of the Northern Carnarvon Basin can be divided into three distinct phases, the first of which is the focus of our study:

2.2.1 Phase I: Pre-breakup magmatism

The first phase concerns pre-breakup magmatism, which began during rifting in the Late Jurassic and terminated at the time of breakup in the Early Cretaceous (Symonds et al., 1998, Müller et al., 2002, Magee et al., 2013c, Rohrman, 2013, Mark et al., 2020). The intrusive component of the pre-breakup magmatism is most clearly expressed by a ~150 x 400 km complex of intrusions that has been documented on seismic reflection data from the Exmouth Plateau and Exmouth Sub-Basin (Symonds et al., 1998) (Figure 1). Intrusions vary in morphology, from relatively small (3-5 km diameter) isolated saucer-shaped sills that are common within Jurassic strata of the Exmouth Sub-Basin (e.g. Magee et al., 2013a), to interconnected and stacked complexes of sheet intrusions, some of which are over 100 km in length, hosted in Triassic strata of the Exmouth Plateau (Holford et al., 2013). The presence of a dyke swarm, possibly sourced by Late Jurassic to Early Cretaceous mantle plume impingement, has been recently suggested (Magee and Jackson, 2020). This dyke swarm is centred on the central southern Exmouth Sub-Basin, extending northwards and radially across the western Exmouth Plateau (Figure 1). Intrusive igneous rocks have been penetrated by petroleum exploration wells Yardie East-1 and Palta-1 in the Exmouth Sub-Basin, and Chester-1 and Rimfire-1 in the Exmouth Plateau (Figure 1) (Kjellgren, 1982, Gibson, 2014, Magee and Jackson, 2020).

Despite the broad spatial extent of the pre-breakup intrusive complex (Figure 1), very little associated contemporaneous extrusive volcanism in the Exmouth Plateau and Exmouth Sub-Basin has been identified. The only reported well penetrations of Late Jurassic to Early Cretaceous pre-breakup extrusive igneous rocks are from the Toro-1 petroleum exploration well (Figure 1 and Figure 4), where ~200 m of heavily altered volcanic rocks of basaltic composition have been described within a sequence of Tithonian marine sedimentary rocks (Sturrock, 2014, Grain et al., 2015, Curtis et al., 2022). Three wells in the central Exmouth Sub-Basin (Enfield-3, Enfield-4, and Stybarrow-2), four wells in the adjacent Barrow Sub-Basin (Tortoise-1, Thevenard-1, Koolinda-1 and Flag-1) and ODP 263 in the Exmouth Plateau (Figure 1) have penetrated bentonitic and smectitic clays that have been interpreted to be weathered ashfall deposits (Tait, 1985, Shipboard Scientific Party, 1990, Willis, 2001, Willis, 2002, Locke, 2004). Sampling of the ashfall deposits in each well is from side wall cores taken during drilling, which does not allow for accurate recording of bed thicknesses. Palynological evidence suggests that the altered ashfall deposits in Stybarrow-2 and Enfield-3 are also Tithonian in age (Willis, 2001, Locke, 2004), and hence similar to the volcanic rocks penetrated at Toro-1. The bentonite layer in Enfield-4 is hosted within Lower Cretaceous Lower Barrow Group rocks (Willis, 2002), and implies extrusive volcanism was still active at this time.

2.2.2 Phase II: Syn-breakup magmatism

The second phase encompasses breakup-related extrusive igneous activity along the Gascoyne Margin (the north western margin of the Exmouth Plateau) and Cuvier Margin (the margin to the southwest of the southern Exmouth Sub-Basin (Figure 1; (Symonds et al., 1998, Rey et al., 2008). On the Gascoyne Margin, accumulations of both subaerial and submarine flood basalts and hyaloclastites erupted from volcanic fissures have been interpreted as up to 1.9 km thick, with magma emplaced into, and onto, a 100 to 200 km wide zone of transitional crust along the margin (Rey et al., 2008). On the Cuvier Margin, submarine flood basalt sequences are interpreted to be much thicker, reaching up to 8 km over an area of 150 x 200 km (Sayers et al., 2002).

2.2.3 Phase III: Post-breakup magmatism

The Cuvier Abyssal Plain (northwest of the Cuvier Margin) hosts a series of post-breakup volcanic highs at the Wallaby Plateau, the Quokka Rise and the Sonne and Sonja ridges (e.g. Symonds et al., 1998) (Figure 1). The Wallaby Plateau and the adjacent Quokka Rise are roughly 70,000 km^2 in area and are composed of a sequence of mafic lava flows and volcaniclastic rocks 4-5 km in thickness and roughly 320,000 km^3 in volume (Symonds et al., 1998, Müller et al., 2002, Olierook et al., 2015). Absolute Pb^{206}/U^{238} and Ar^{40}/Ar^{39} age-dating of dredge samples constrains the age of extrusive activity at the Wallaby Plateau to 124 ± 0.5 Ma (Olierook et al., 2015), which is at least 5 million years after breakup on the Cuvier and Gascoyne margins (Reeve et al., 2021). The northern Sonja and southern Sonne ridges represent extinct spreading ridges (Robb et al., 2005), and extend roughly 200 km northeast from the Wallaby Plateau. Dredging has confirmed they are composed of basalt, volcanic breccia and tuff (Von Stackelberg et al., 1980). These ridges formed between 128 and 125 Ma (Robb et al., 2005) to bisect oceanic crust that was at least 10 million years old (Mihut and Müller, 1998), implying a post-breakup setting.

2.2.4 Lower crustal underplating

At the base of the crust (~18 km) beneath the Exmouth Plateau is a lens-shaped body of high seismic velocity (7 to 8 km/s) (Mutter and Larson, 1989, Fomin et al., 2000, Rohrman, 2015). This feature occurs over a roughly circular area ~750 km in diameter (Figure 1), and is up to 4 km thick beneath the Cape Range Fracture Zone (CRFZ; (Rohrman, 2015). This addition to the base of the crust is estimated to have caused ~500 m of uplift of the CRFZ, and between 500 and 1,800 m uplift on the Greater Indian continental block in the region of the present-day Sonne and Sonja ridges during the Early Cretaceous (Rohrman, 2015). Associated erosion represents a possible sediment source for the Barrow Delta (Ghori, 1999, Reeve et al., 2016). The feature has been interpreted as mafic underplating (a lower crustal mafic intrusion sourced by partial melting of the upper mantle (Fomin et al., 2000)) comprising gabbro, which would explain the high seismic velocity anomaly (Mutter and Larson, 1989, Fomin et al., 2000, Rohrman, 2015). Underplating may have occurred in the Late Jurassic, providing a possible source for the pre-breakup magmatism expressed in the Exmouth Plateau and Exmouth Sub-Basin (Rohrman, 2013).

3. DATA AND METHODS

3.1 Seismic and well data

This study was undertaken through the interpretation of petrophysical and palynological data acquired at the Pyrenees-1, Pyrenees-2, Stickle-1, West Muiron-1, Macedon-1, Black Pearl-1 and Toro-1 petroleum exploration wells, and through mapping of the open file HE94 2D, Eendracht Extract 2D, HC93 2D, HCA05 3D, and Indian 3D seismic reflection survey datasets (Table 1, Figure 2D). Seismic and well data were downloaded from the National Offshore Petroleum Information Management System (NOPIMS), operated by Geoscience Australia (GA, 2022). Details of the vertical resolution of the 3D surveys host to the volcanic centres we studied are presented in Table 2.

Survey Name	Type	Acquired by	Acquisition year	Area (km^2)	Max TWT (s)	Line / Inline & Crossline spacing
HE94	2D	BHP Petroleum & Geco-Prakla	1994	~15,000	8	~25 km
Eendracht Extracts	2D extracts from multiclient 3D	Spectrum Geo	2010	7920	7	~5 km
HC93	3D	Schlumberger & Geco Prakla	1993	606	12	12.5 m
HCA05	3D	BHP Petroleum & Veritas DGC	2005	253	3.4	12.5 m
Indian	3D	Woodside & CGG	2001	1,307	6	14 m (Inline) 12.5 m (Crossline)

Table 1: Acquisition details of seismic reflection surveys interpreted in this study.

Name of 3D survey	Sample interval (msTWT)*	Average frequency (Hz)	Average velocity (ms-1)	Dominant wavelength, λ_{dom} (m)	Vertical resolution	
					Limit of separability (λ_{dom} / 4) (m)	*Limit of detection (λ_{dom} / 30) (m)*
HC93	1040 - 1310	~16.5	~2040	~123	~31	~4
HCA05	1040 - 1310	~36	~2040	~56	~14	~2
Indian	2160 - 2980	~40	~2800	~65	~16	~2

Table 2: Vertical resolution in the 3D seismic reflection surveys used in this study. *Sample intervals reported here are from the depth range that host the Pyrenees Volcano (HC93 & HCA05 surveys) and Toro Volcanic Complex (Indian survey). In the HC93 and HCA05 surveys, average velocities are from the Pyrenees-1 petroleum exploration well; in the Indian survey, the average velocity is the mean of velocities over the volcano host interval from both the Toro-1 well and Falcone-1A wells.

3.2 Methods

Dinocyst zones from the palynological reports from the Pyrenees-1, Pyrenees-2, Stickle-1, West Muiron-1, Macedon-1, Black Pearl-1 petroleum exploration wells were integrated with regional dynocyst zone interpretation by Helby et al. (2004) and Marshall and Lang (2013), and tied to seismic reflection data. This provided biostratigraphic constraints and guided the identification of key formations and seismic horizons proximal to the Pyrenees Volcano, imaged within the HC93 and HCA05 3D seismic reflection surveys. In the same manner, biostratigraphic constraint near the Toro Volcanic Complex, imaged within the Indian 3D seismic reflection survey, was provided by palynological data from the Toro-1 petroleum exploration well which directly penetrates the Toro Volcano, and the Falcone-1A well.

Seismic interpretation was undertaken using Schlumberger's Petrel seismic-to-simulation modelling software. Whilst a number of seismic horizons were mapped, three in particular underpin the regional structural and stratigraphic framework for our study: (1) The base of the LBG, (2) the KVU and (3) the IHU, as identified by Reeve et al. (2022). These were mapped in detail across the study area using the principles of seismic stratigraphy outlined by Mitchum et al. (1977a), (Mitchum et al., 1977b) and Mitchum et al. (1977b), integrating the interpretation with dinocyst zones taken from palynology reports from local petroleum exploration wells. A semi-automated picking method was utilised to increase efficiency in interpreting the surfaces at a regional scale. As the LBG is conformable with the underlying Dingo Claystone and Dupuy Formation, the surface was mapped along seismic reflections marking the interface between the D. jurassicum and P iehiense dinocyst zones. The KVU and IHU (which are angular unconformities in the study area) were identified from reflection terminations representing the truncation of underling strata. Further to these key seismic surfaces, major faults were also interpreted in the vicinity of the volcanic centres. Within this regional seismic-stratigraphic and structural context, the top and bottom surfaces of features interpreted to be volcanoes and associated lava flows were interpreted at single line spacing in the 3D seismic reflection survey datasets. The criteria that were used in the identification and interpretation of extrusive and intrusive igneous features within the seismic reflection survey data are shown in Table 3.

Volcanic edifices		**Lava flows**		**Intrusions**	
Observation	Reference	Observation	Reference	Observation	Reference
Cone shaped morphology.	*(Calvès et al., 2012, Magee et al., 2013b)*	*High seismic amplitude on top extrusive surface reflection and reduced quality of seismic imaging beneath.*	*(Kiørboe, 1999, Holford, 2012, Reynolds et al., 2017b)*	*A characteristic high amplitude (generated by their higher acoustic impedance than host sedimentary rocks).*	*(Symonds et al., 1998, Planke et al., 2005)*
High acoustic impedance reflector marking a hard and dense surface, indicating transition to mafic volcanogenic rock units from relatively soft sedimentary rocks.	*(Holford et al., 2017)*	*Clear definition of flow lobes on spectral decomposition imaging of the feature's surface.*	*(Holford, 2012)*	*Vertical transgression of stratigraphy.*	*(Hansen and Cartwright, 2006b, Schmiedel et al., 2019)*
Weak seismic signal below feature due to attenuation.	*(Holford et al., 2017)*	*Feature spatially associated with nearby volcanic edifice.*	*(Reynolds et al., 2017b)*	*Share morphologies with intrusions recorded elsewhere, e.g. stepped or saucer shapes.*	*(Schofield et al., 2012b)*
Onlapping seismic reflections of low amplitude, indicating the feature formed above the seabed and was subsequently overlain by sedimentary rocks.	*(Magee et al., 2013b)*			*Abrupt lateral termination.*	(Smallwood and Maresh, 2002, Planke et al., 2005, McClay et al., 2013, Schofield et al., 2017, Mark et al., 2018, Mark et al., 2020)
Distinct seismic facies within the feature, possibly due to vents, pipes, plugs and lava flows overlapping one another.	*(Davies et al., 2002, Bischoff et al., 2017, Reynolds et al., 2017c)*			*Presence of a zone of low seismic signal beneath the intrusion.*	(McClay et al., 2013)
Amorphous, low amplitude seismic character within the feature, possibly representative alteration of mafic	*(Reynolds et al., 2017c, Toro 1 Well Completion Report)*				

volcanic rocks to clay minerals or the presence of hyaloclastite.			
Igneous intrusions beneath the feature, possibly acting as magma feeder pathways.	*(Magee et al., 2013b, Holford et al., 2017, Reynolds et al., 2017c)*		

Table 3: Seismic characteristics of volcanic edifices, lava flows and igneous intrusions.

Spectral decomposition analysis (after Sinha et al. (2005)) is a useful tool for highlighting igneous features in seismic reflection survey data (e.g. Reynolds et al. (2017b) in the Bight Basin, and Holford et al. (2017) in the Bass Basin, both offshore southern Australia). In this study, spectral decomposition analysis was undertaken on the seismic surface defining the Pyrenees Volcano and associated lava flows using GeoTeric software. Spectral decomposition (or time-frequency decomposition) is a seismic data analysis technique that isolates for display the amplitude of specific frequency components of the seismograms within a processed seismic reflection survey dataset. These amplitudes are typically mapped as normalised primary colour channel textures projected to seismic data probes such as vertical cross-sections, two-way time slices or an interpreted seismic horizon. Visualising seismic reflection survey data this way can demonstrate a range of vertical (TWT) scales of seismic reflection interference. These reflection events often highlight or reveal sometimes-subtle geological features (both structural features and 'geobody' rock units). In this study, frequencies of 14, 24 and 46 Hz were assigned to red, green and blue colour channels respectively over the Pyrenees Volcano structure and regions of high seismic amplitude to the northwest and southeast. This combination of frequencies was selected to best highlight volcanic features within the data.

4. OBSERVATIONS AND INTERPRETATION

4.1 Seismic stratigraphic framework

Figure 5 shows a regional seismic line across the central Exmouth Sub-Basin that links the Indian 3D seismic reflection survey in the west to the HCA03 and HC93 3D seismic surveys in the east. This highlights the regional setting of the volcanic centres that are the focus of this study. The seismic surfaces of the Base LBG, the KVU and the IHU are highlighted. Also interpreted are the top volcanics surface, top Athol Formation (Middle Jurassic) and top Mungaroo Formation (Uppermost Triassic).

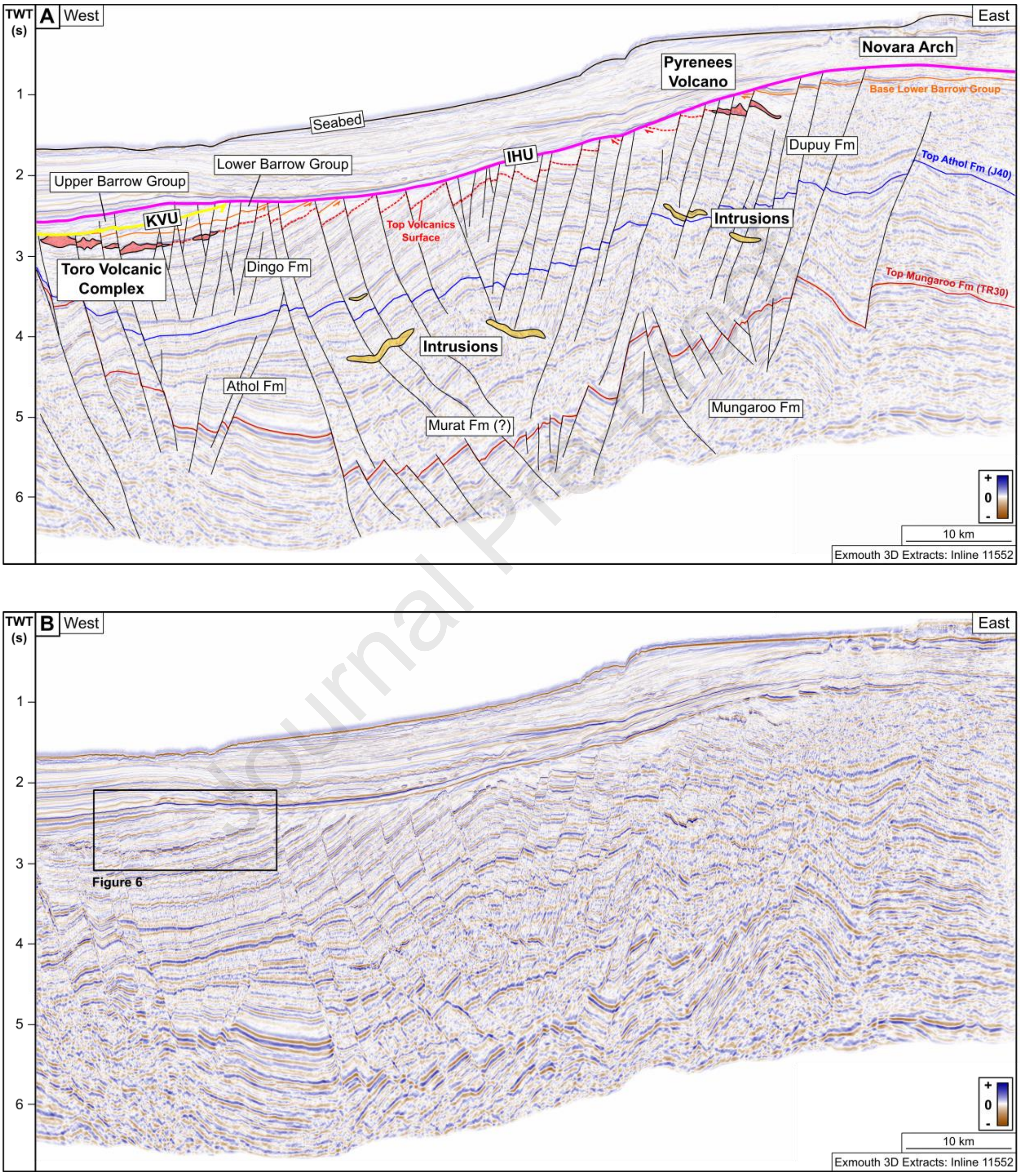

Figure 5: (A) Interpreted and (B) uninterpreted seismic section of Inline 11552 from the Exmouth Extract 3D seismic reflection survey through the central Exmouth Sub-Basin, showing regional structure and the relative locations of the Toro Volcanic Complex and the Pyrenees Volcano. Line of section shown on Figure 4B. The key seismic surfaces interpreted across the study area are highlighted, including the top volcanic surface, which is correlated between the two volcanic centres

suggesting contemporaneous volcanism across the Exmouth Sub-Basin. The Novara Arch is a major structural high in the east of the study area. IHU – Intra-Hauterivian (Cretaceous) Unconformity; KVU – Valanginian (Cretaceous) 'KV' Unconformity.

4.1.1 Base Lower Barrow Group

The bottom-most part of the P. iehiense sequence within the Lower Barrow Group has a moderate impedance contrast with the underlying Dingo Formation (close to the TVC) (Figure 5 and Figure 6) and stronger acoustic impedance contrast with the Dupuy Formation (close to the Pyrenees Volcano) (Figure 5). This impedance contrast, along with correlation from intersections of the base P. iehiense dinocyst zone in nearby petroleum exploration wells were used to map the surface across the study area. The Base LBG surface is present in the vicinity of both volcanic centres, however, it is absent where truncated by the IHU in the centre of the study area (Figure 5).

4.1.2 Intra-Valanginian 'KV' Unconformity

We interpret the Intra-Valanginian 'KV' Unconformity, or 'KVU', representing Valanginian uplift, to be present in the north of the Indian 3D seismic reflection survey, and the northeast of the HC93 survey, in line with previous work undertaken by Reeve et al. (2022) (Figure 4). The surface representing the KVU has a negative amplitude and is defined by the abrupt termination of underlying faults and underlying seismic reflections, truncation of the TVC, and by correlation from penetrations in the Toro-1 and Falcone-1A petroleum exploration wells.

4.1.3 Intra-Hauterivian Unconformity

We interpret the Intra-Hauterivian Unconformity or 'IHU', representing the top of the Birdrong and Zeepard formations, to be present throughout the entire study area. The IHU surface is marked by the lowest of a set of high amplitude seismic reflection events representing the Muderong Shale and Windalia Radiolarite across the study area. The IHU surface is characterised by a negative seismic amplitude. In the study area, the IHU surface is expressed as both a disconformity (or possibly simply as a conformable flooding surface (after Alves et al. (2023)) e.g. immediately above the TVC, and as an angular unconformity, e.g. along the western portion of the seismic line shown in Figure 5. Figure 6 highlights this duality, showing the IHU to be conformable with the Birdrong and Zeepard formations in the west but changing in character, to truncate the KVU (as well as strata both above and below) to the east. In this part of the Exmouth Sub-Basin, this interpretation appears consistent with observations by Paumard et al. (2018), Reeve et al. (2022), and Alves et al. (2023).

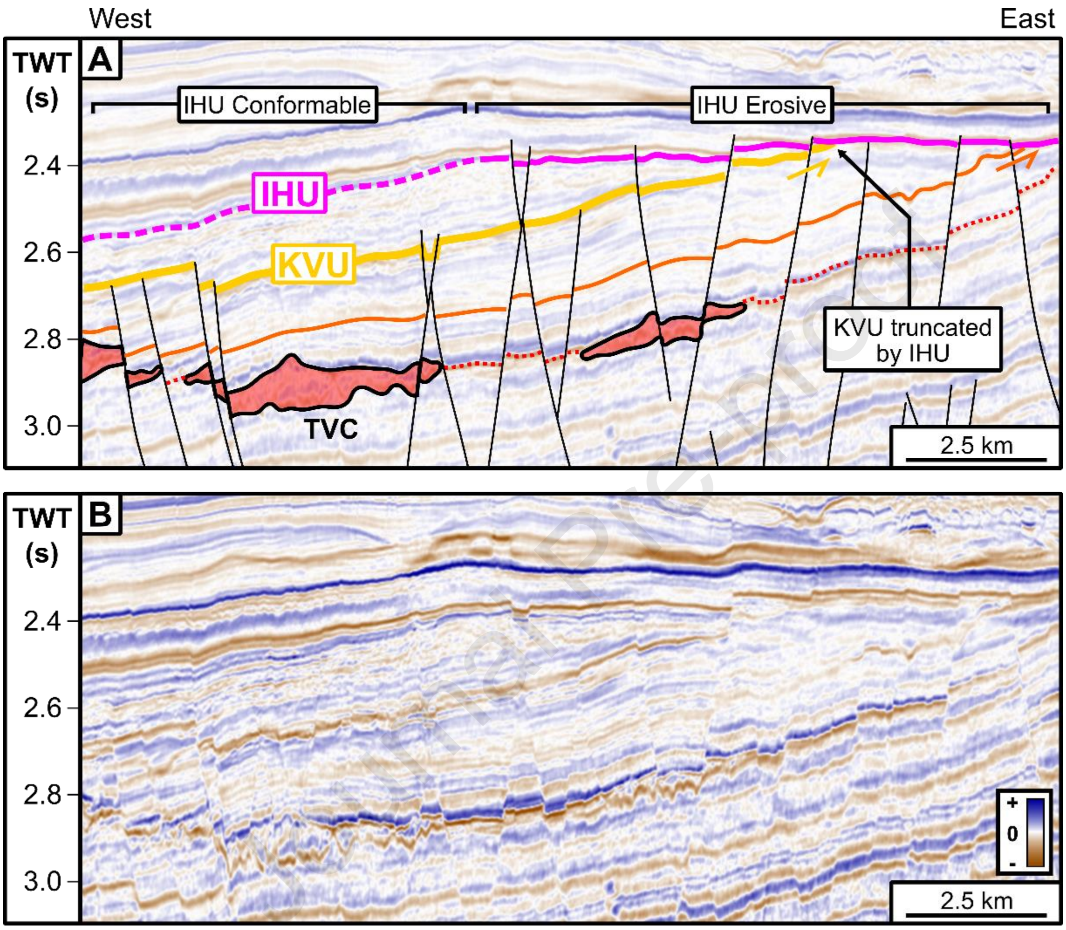

Figure 6: (A) Interpreted and (B) uninterpreted seismic section highlighting the nature of the Valanginian (Cretaceous) 'KV' Unconformity (KVU) and the Intra-Hauterivian (Cretaceous) Unconformity (IHU) in the western part of the study area. The IHU surface is conformable with underlying strata directly above the Toro Volcanic Complex (TVC), however, to the east, strata beneath are eroded. The KVU and Base Lower Barrow Group (orange line) surfaces are truncated by the IHU. Location of section shown on Figure 5B.

4.2 Eastern Exmouth Sub-Basin: Extrusive Magmatism

4.2.1 Description of the Pyrenees Volcano

4.2.1.1 Dimensions

A high seismic amplitude, mound-shaped feature (MSF) is observed in both the HC93 3D and HCA05 3D seismic reflection survey datasets (Figure 7, Figure 8 and Figure 9), roughly 4.5 km southwest of the Pyrenees-1 petroleum exploration well, and situated on the Novara Arch . The maximum height of the feature is ~170 msTWT (milliseconds, two-way-time), from its base at ~1,300 msTWT. The MSF base has a footprint covering ~2.5 x 3.3 km (Figure 9). At the top of the MSF there is a bright reflection event with a concave depression, ~25 msTWT deep and ~460 m in diameter (Figure 7). A smaller mound, ~350 m in diameter and ~30 msTWT in height, is present on the northeastern flank of the MSF (Figure 7). The top surface of the MSF is elongate, forming a ridge striking NNE-SSW at a bearing of ~35° from North (Figure 7).

4.2.1.2 Well constraint and host rocks

Sedimentary rocks intersected in the Pyrenees-1 petroleum exploration well can be correlated south-westwards to the MSF (Figure 8). Dupuy Formation siltstones intersected at the bottom of the well, constrained to the Tithonian by palynology data (Spry, 1994), onlap the MSF ~150 msTWT from its base. The contact between Dupuy Formation and the overlying Lower Barrow Group (LBG) is ~40 msTWT above the MSF's Peak. A thickness of ~50 msTWT of LBG rests beneath the intra-Hauterivian Unconformity (Figure 8). Palynological data from Pyrenees-1 constrains the timing of the Lower Barrow Group above the MSF as Tithonian to Berriasian (Spry, 1994). Vertical seismic profile data from the Pyrenees-1 well indicate that average seismic velocities are ~2,200 ms^{-1} within the Dupuy Formation and 2,130 ms^{-1} within the Barrow Group (Spry, 1994). This indicates thicknesses of ~90 m for the Dupuy Formation and ~110 m for the Barrow Group Formation components of strata overlying the peak of the MSF.

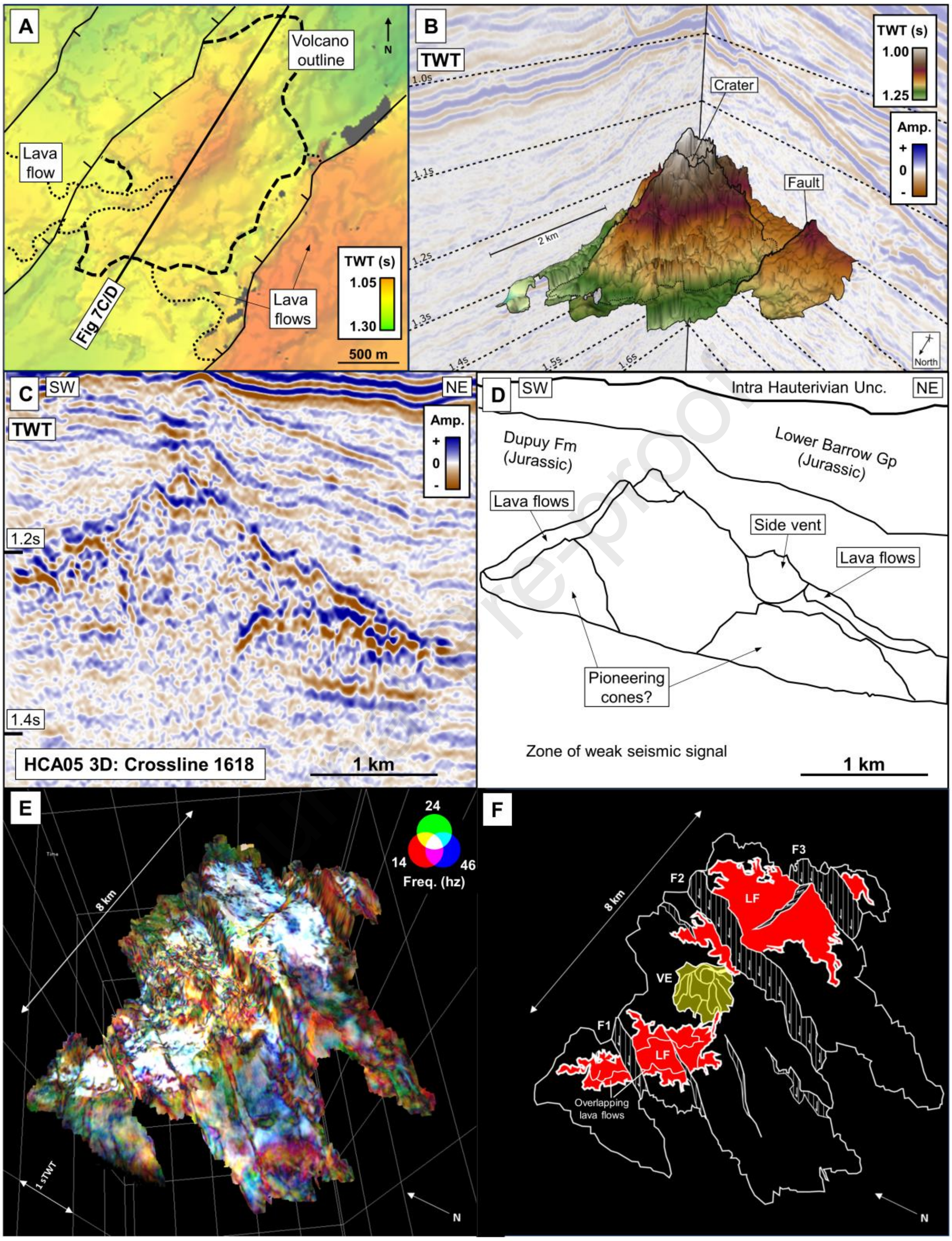

Figure 7: (A) Plan view of top the Pyrenees Volcano surface within the HC93 3D seismic reflection survey. (B) Birds-eye view of top the Pyrenees Volcano surface. Adjacent seismic reflection lines are Inline 1906 and Crossline 2102 of the HCA05 3D seismic reflection survey. (C) Close up of the Pyrenees Volcano on Crossline 1618 of the HCA05 3D seismic reflection survey. Line of section shown in Figure 7A. (D) Interpretation of seismic reflection data shown in Figure 7C, including internal structures (possibly representing early-stage volcanic edifices) within the Pyrenees Volcano. (E) Spectral decomposition image over the top of the Pyrenees Volcano surface. White regions indicate

high amplitude seismic reflections we interpret as lava flows. (F) Interpretation of spectral decomposition image showing lava flows (LF, red) flowing away from volcanic edifice (VF). Individual lava lobes are visible at edges of flows. Normal faults trending NE-SW (F1 to F3) are evident, crosscutting lava flows, indicating displacement during the early Cretaceous.

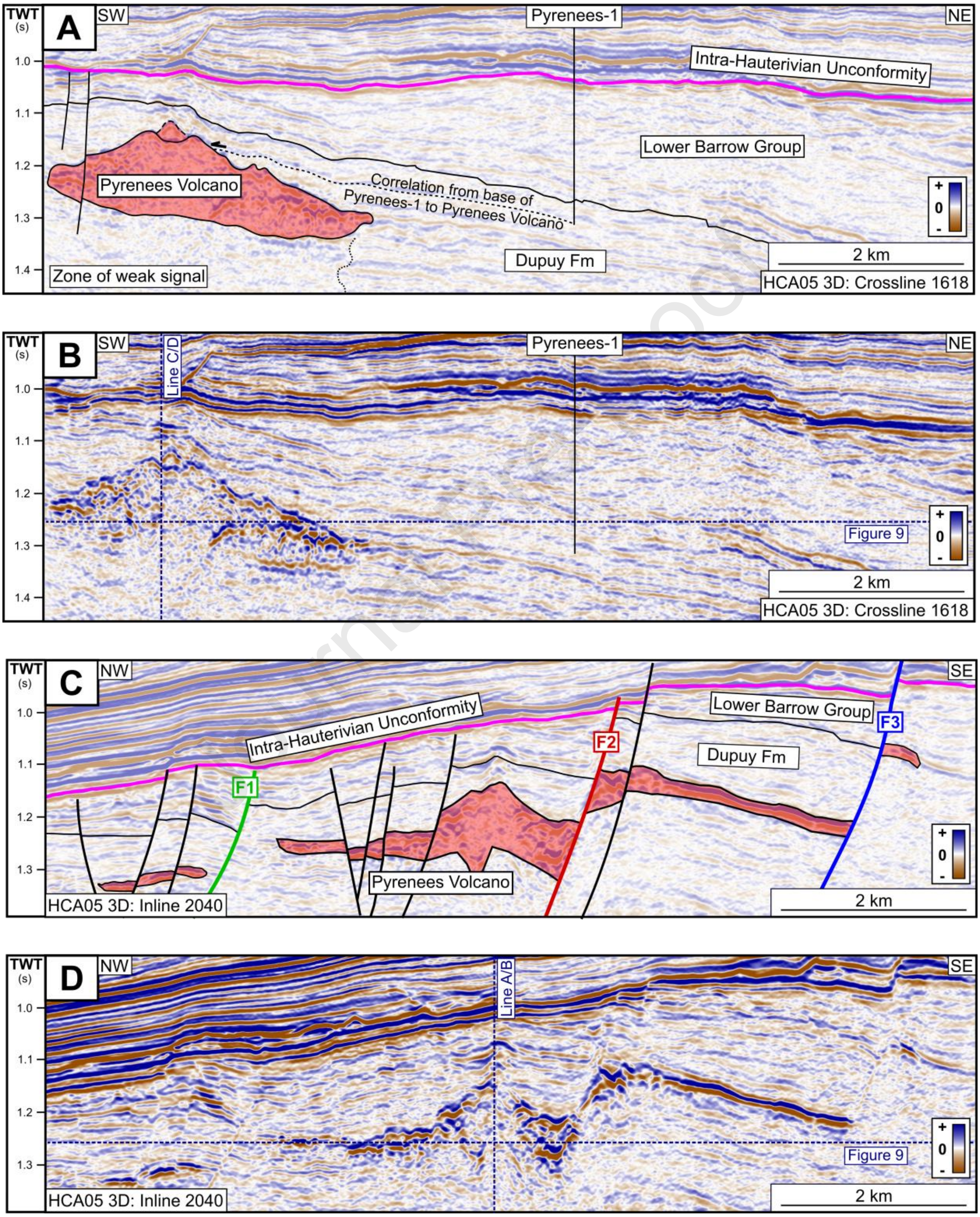

Figure 8: (A) Interpreted, and (B) uninterpreted seismic sections of part of Crossline 1618 from the HCA05 3D seismic reflection survey, which passes through the Pyrenees Volcano. The line of section

is shown on Figure 9. The Pyrenees Volcano is overlain by the Dupuy Formation, which lies below the Lower Barrow Group. In this vicinity, the Lower Barrow Group is subdivided into the Macedon, Muiron and Pyrenees members, representing the early stage delta bottomsets, foresets and topsets respectively. In this part of the seismic line, the Lower Barrow Group is eroded beneath the Intra-Hauterivian Unconformity. Also shown is the seismic correlation from the bottom of the Pyrenees-1 well to the Pyrenees Volcano, where palynological data help constrain sedimentary rock onlapping the Pyrenees Volcano flank to the Tithonian. (C) Interpreted, and (D) uninterpreted seismic sections of part of Inline 2040 from the HCA05 3D seismic reflection survey, which passes through the Pyrenees Volcano, and highlights offset of the volcanic edifice and lava flows by normal faults. Offset along major faults F1, F2 and F3 is recorded in Figure 9. The timeslice shown in Figure 9 is also highlighted.

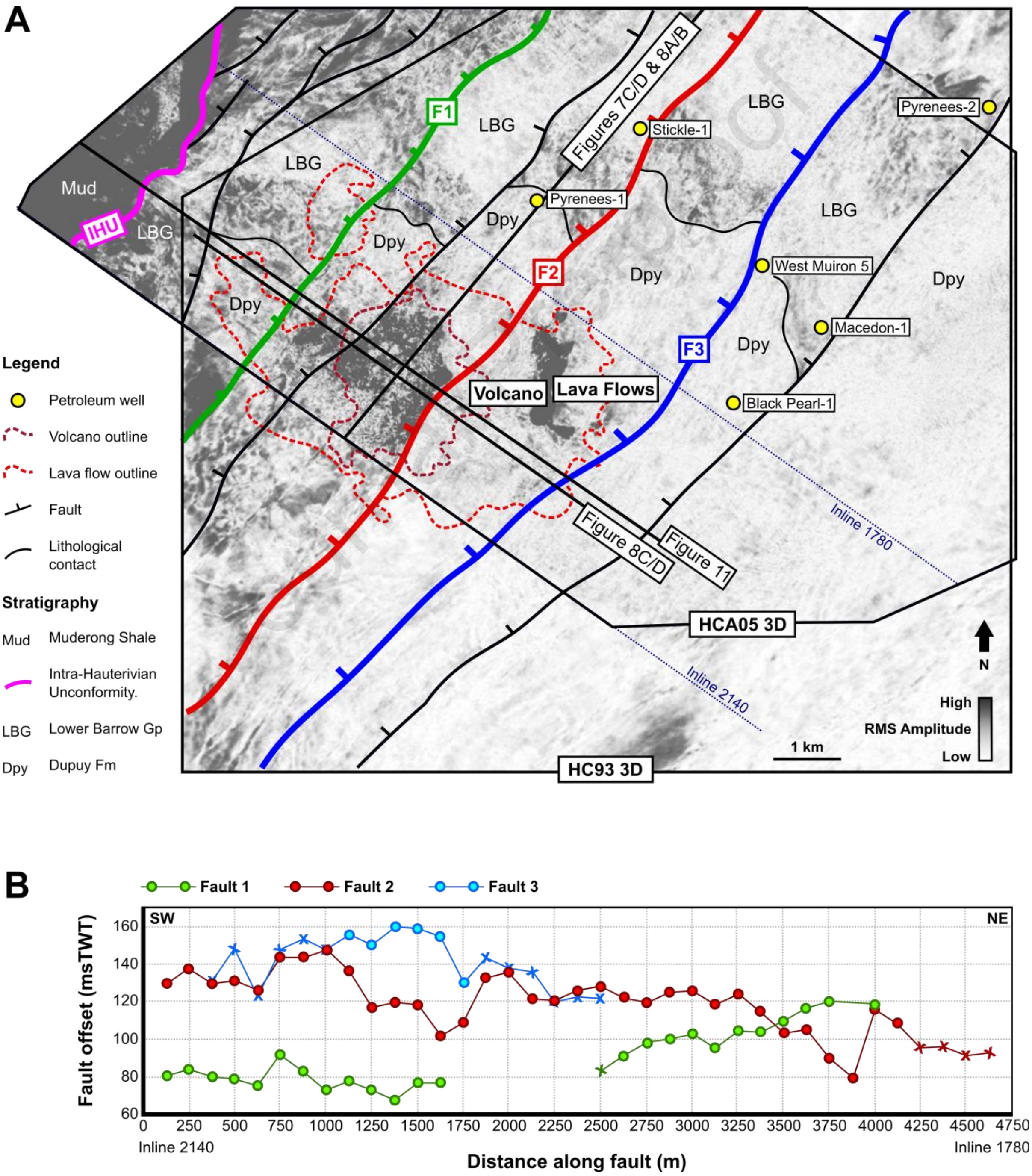

Figure 9: (A) Composite RMS Amplitude attribute on time slice at 1260 msTWT on the HC93 and HCA05 3D seismic reflection surveys. Outlines of the Pyrenees Volcano (dark red) and lava flows (pale red) are shown. Offset on NE-SW trending normal faults is towards the NW. Section lines for Figures 7C/D, 8A-D, and 11 are shown. Fault 1 (F1), Fault 2 (F2), and Fault 3 (F3) are labelled. Location of timeslice shown on Figure 8A & C. (B): Graph showing offset of volcano and lava flows along Faults 1, 2 and 3. Points are averages of 3x measurements of fault offset made on every 10th inline (between inlines 1780 and 2140) of the HCA05 3D seismic reflection survey. Inlines are ~90° to fault orientation, and are spaced at 12.5 m. "O" points represent volcano and lava flow offset, "X" points represent offset of sedimentary rocks where igneous rocks are not present.

4.2.1.3 Seismic expression

The top surface of the MSF is represented by a high amplitude seismic reflector (Figure 7). The character of the seismic reflections within the MSF is highly variable. We observed a roughly 1,000 m x ~120 msTWT zone of highly disorganised, low amplitude, amorphous seismic response in the centre of the MSF, with brighter dome shaped reflectors on either side ~50 msTWT in height (Figure 7). There is a zone of weak seismic signal beneath the MSF where the lateral continuity of seismic reflections becomes difficult to discern (Figure 7 and Figure 8).

Regions of high seismic amplitude extend laterally from the MSF (Figure 8). Bright reflectors extend furthest to the northwest and southeast, ~2,500 and ~2,350 m respectively from the base of the MSF, covering an area of ~25 km^2, concordant with the strata beneath and above them. In contrast to the MSF, the bright reflectors have very little internal variation in seismic facies (Figure 8). Spectral decomposition imaging of the reflectors shows that they are characterised by curved, lobe-shaped edges (Figure 7E and F). Both bright reflections extend onto the flanks of the MSF. These reflectors are of a similar seismic expression and morphology to those confirmed to represent lava flows elsewhere, e.g. in the Bight Basin, on the Southern Australian Margin (Reynolds et al., 2017a).

4.2.1.4 Structure

Both the MSF, and the surrounding strata have been offset by three major, and several minor, NE-SW striking normal faults (Figure 4A, Figure 7, Figure 8 and Figure 11). The average displacement of the MSF on each of the three major faults, Fault 1, Fault 2 and Fault 3, is 90, 118, and 141 msTWT respectively (Figure 9B). In the vicinity of the MSF these faults have greatest offset below the Intra-Hauterivian Unconformity, with limited displacement above (Figure 8).

4.2.2 Interpretation of the Pyrenees Volcano

The MSF shares many characteristics with volcanoes interpreted on seismic data in other sedimentary basins (e.g. Collier and Watts, 2001, Somoza et al., 2003, Thomson, 2005, Calvès et al., 2012, Magee et al., 2013b, Bischoff et al., 2017, Holford et al., 2017, Reynolds et al., 2017c, Reynolds et al., 2018). These include a broadly conical shape, a top surface marked by high seismic amplitude, variable internal seismic facies including a zone of amorphous seismic response, a region of weak seismic signal beneath, and bright seismic reflections emanating from the sides of the conical feature. Hence, we interpret the MSF to be a volcano, and proximal flat-lying high amplitude seismic reflections to represent lava flows. Due to its location immediately south of the Pyrenees oil field, we have named the feature the Pyrenees Volcano. Mafic volcanism is considered most likely as (1) mafic magmatism is common in rift settings elsewhere, e.g. the Central North Sea (Quirie et al., 2019), as its primary source is decompression melting of the mantle (Johnson et al., 2005, Lebedev et al., 2006) (and potentially plume-related in the NCB; Rohrman, 2015), and (2) although the Pyrenees Volcano has not been sampled, every contemporaneous igneous rock recovered from the Exmouth Sub-Basin (including those from the TVC), and the wider NCB, is mafic in composition (Curtis et al. 2022).

4.1.2.1 High amplitude top surface on the Pyrenees Volcano

The acoustic impedance contrast between strata overlying the Pyrenees Volcano, and the top surface of the volcano (Figure 7 and Figure 8) is consistent with a transition from relatively soft and low density sandstones and siltstones of turbidite deposits within the Dupuy Formation (Tait, 1985, Hocking, 1992) to harder mafic volcanic and volcaniclastic rocks with higher densities.

4.1.2.2 Crater-like depressions on the Pyrenees Volcano's top surface

The concave depression at the top of the Pyrenees Volcano (Figure 7) likely represents its main eruptive crater. Craters are ubiquitously present at the top of volcanoes, and are frequently imaged on seismic reflection surveys (e.g. Bischoff et al., 2017, Reynolds et al., 2017b, Reynolds et al., 2017c). The similarly-shaped depression observed on the northeastern flank of the Pyrenees Volcano (Figure 7) may represent a side vent, similar to those observed on the sides of the Kora Volcano in New Zealand (Bischoff et al., 2017).

4.2.2.3 Varied internal seismic facies

Within the Pyrenees Volcano there is a zone of low seismic amplitude (Figure 7 and Figure 8), similar in appearance to the seismic reflection expression of the Toro Volcano penetrated by the Toro-1 petroleum exploration well on the western side of the Exmouth Sub-Basin. This may be the result of seismic signal attenuation due to the highly reflective top surface of the Pyrenees Volcano. The two dome shaped features within the Pyrenees Volcano possibly represent small early-stage eruptive centres that were later buried as the main vent became dominant. If so, this suggests the Pyrenees Volcano may have formed in multiple stages.

4.2.2.4 Origin of the bright reflections surrounding the Pyrenees Volcano

Regions of high seismic amplitude emanate from the crater-like depressions and extend from the base of the Pyrenees Volcano. These are visible in the original seismic reflection survey datasets (Figure 8) and also in the spectral decomposition imaging (Figure 7E and F). Their outline is shown on Figure 9**Error! Reference source not found.**. Mafic lavas such as basalt are crystalline and have a high density, which produces a high contrast in acoustic impedance with overlying sedimentary rocks, as observed here (Figure 8). Thus, we believe these high amplitude reflections likely represent mafic lava flows. Furthermore, the high amplitude reflection events are paired with underlying reflectors; these pairs exhibit a consistent TWT thickness (Figure 8), implying flat lying, planar features such as lava flows (Reynolds et al., 2017b).

When visualised using spectral decomposition imaging (Figure 7E & F), regions of white in Figure 7E exhibit maximal impedance contrast within the image and minimal destructive interference caused by seismic reflection from the base of the underlying unit at all scales up to the bed resolution limit of the low frequency band (red). In other words, the white regions show where the thickest homogeneous units of most acoustically distinctive rock underlie the seismic reflector. These regions appear to emanate from the Pyrenees Volcano (Figure 5), suggesting it is the source of this material. Laterally, the reflection events terminate in curved lobes similar in nature to lava flows identified in 3D seismic reflection data within the Bight Basin, on the Southern Australian Margin by Reynolds et al. (2017b), and observed in the field on Payan Matru Volcano in Argentina (Wadge and Lopes, 1991). The flows at the Pyrenees Volcano appear to be layered, overlapping one another (Figure 7E) and implying that multiple events led to their formation, a feature also noted by Bischoff et al. (2017) at the Kora Volcano in New Zealand.

4.2.2.5 Interpretation of the Pyrenees Volcano's dimensions

At its peak, the Pyrenees Volcano is ~170 msTWT high, with its base at ~1300 msTWT. Seismic velocities of mafic volcanic rock at this depth, range from 3,500 to 6,000 ms^{-1} (Lesage et al., 2018). This suggests the Pyrenees Volcano could be ~300 to 500 m in height. However, all igneous rocks penetrated in petroleum exploration wells and scientific boreholes in the Northern Carnarvon basin are heavily altered (Curtis et al., 2022). Mafic volcanic rocks intersected at Toro-1 (Figure 4) were altered to clay with average seismic velocity of ~2,850 ms^{-1} (Sturrock, 2014, Taylor, 2014). If similar alteration processes have occurred at the Pyrenees Volcano, its maximum height could be as low as ~240 m. In calculating the Pyrenees Volcano volume we have approximated the volcano shape to be a cone of radius ~1.5 km. The equation for the volume of a cone is $1/3\ \pi r^2 h$ (where 'r' is radius, and 'h' is height). With a height range of ~240 to ~500 m, the volume of the Pyrenees Volcano is likely between 0.6 and 1.2 km^3.

4.2.3 Interpretation of the timing of volcanic activity

The Pyrenees-1 petroleum exploration well (Figure 9) intersects the Tithonian aged Dupuy Formation at 1,163 m below the seafloor (1,242 msTWT), where it continues below the borehole total depth at 1,277 m below the seafloor (1,316 msTWT) (Spry, 1994). The Dupuy Formation sequence intersected by the Pyrenees-1 well can be correlated to overlie the top section of the Pyrenees Volcano (Figure 8). West Murion-5, located ~7.5 km ENE from the Pyrenees Volcano (Figure 9**Error! Reference source not found.**), intersects 293 m of the Dupuy Formation, within which the well reaches its total depth. At the Pyrenees-1 well, the seismic velocity of the Dupuy Formation is ~2,200 m/s. Assuming a fairly constant thickness between the two wells, the Dupuy Formation is present to at least 1,580 msTWT below the base of the Pyrenees-1 well. Strata at this depth below Pyrenees-1 correlate to those beneath the base of the Pyrenees Volcano (Figure 8). This suggests the volcano formed, erupted and was buried during deposition of the Dupuy Formation in the Tithonian, during the pre-breakup phase of magmatism.

4.2.4 Interpretation of environment of deposition and water depth during volcanic activity

The Pyrenees volcano is completely buried by the Dupuy formation. Palynological analyses of the Dupuy Formation intersected in petroleum exploration wells in the vicinity of the Pyrenees Volcano (e.g. Pyrenees-1, Pyrenees-2, Black Pearl-1, Macedon-1, Stickle-1 and West Muiron-5) (Figure 4 and Figure 9) supports an open marine setting for the deposition of the Dupuy Formation. Subsequent regional palaeogeographic reconstructions by (Longley et al., 2002) for the J50 interval (Early Tithonian, during Dupuy Formation and Dingo Claystone deposition, and incorporating the C. perforans to D. jurassicum dinocyst zones) place the Pyrenees Volcano in the centre of Exmouth Sub-Basin depocentre at the time (Figure 10A), where water depths would have been hundreds of metres. This implies that the Pyrenees Volcano, which is likely altered to clay and ~240 m in height, formed in a submarine environment.

Reflection patterns in the Dupuy Formation adjacent to the Pyrenees Volcano are suggestive of onlap of strata onto the edifice (Figure 7 and Figure 8). This is similar to the volcano-host rock configurations described by Magee et al. (2013b) in seismic reflection data from the Bight Basin, offshore South Australia. The lava flows surrounding the Pyrenees Volcano would have been erupted into seawater, and subsequently flowed on the seabed. Upon eruption, lava would have fragmented due to rapid cooling and quenching, forming hyaloclastite (Batiza et al., 2000), similar to lavas sourced from submarine volcanoes in the Bass Basin, offshore southeast Australia (Reynolds et al., 2018).

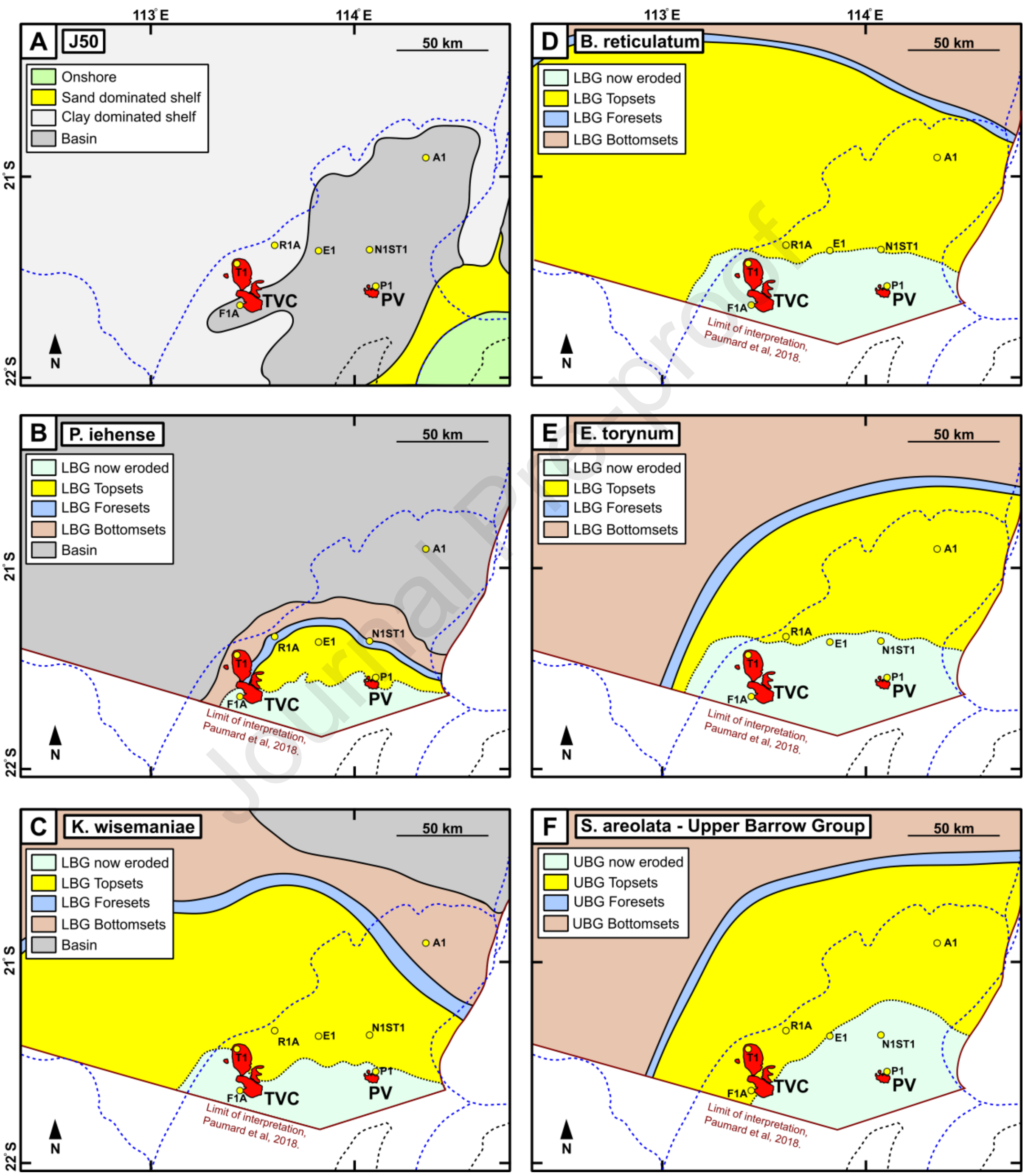

Figure 10: Maps showing the palaeogeographic setting of the Toro Volcanic Complex (TVC) and the Pyrenees Volcano (PV) at (A) the J50 sequence boundary (~152.1 Ma) (after Longley et al., 2002); at the end of the (B) P. iehiense (~144.9 Ma), (C) K.wisemaniae (~143.5 Ma), (D) E. torynum (~137.8 Ma) depositional phases of the Lower Barrow Group (after Paumard et al., 2018); and (F) at the end of the S. areolata depositional phase, marking the end of deposition of the Upper Barrow Group at

~134.7 Ma (after Paumard et al., 2018). Also shown are the locations of the Altair 1 (A1), Eskdale 1 (E1), Falcone-1A (F1A), Novara-1 ST1 (N1ST1) Toro-1 (T1) and Ragnar 1A (R1A) petroleum exploration wells.

4.2.5 Interactions between volcanic rocks and faults

The Pyrenees Volcano and its associated lava flows are offset by NE-SW striking faults (Figure 8 and Figure 9). NE-SW oriented faults affecting Upper Jurassic strata have been reported within the Exmouth Sub-Basin by Underschultz et al. (2008) and Black et al. (2017). Faults of this orientation are associated with the second stage of rift-related faulting and formed between 145 and 138 Ma (Berriasian to Valanginian) (Black et al., 2017). In other words, normal faulting followed deposition of the Dupuy Formation and Lower Barrow Group above the Pyrenees Volcano, but occurred before the termination of erosion associated with the IHU in the Barriemian (Reeve et al., 2022) (Figure 8). This is coeval with uplift of the Ningaloo, Resolution and Novara arches (Tindale et al., 1998, Reeve et al., 2022). Limited displacement above the IHU in Barriemian to Cenomanian age strata (Figure 8) suggests minor reactivation during the thermal sag phase following continental breakup on the Gascoyne and Cuvier margins.

In the vicinity of the Pyrenees Volcano, average displacement along faults is 1, 2 and 3 is 90, 118, and 141 msTWT respectively (Figure 8C and D, and Figure 9B). The Pyrenees Volcano is bound by the Dupuy Formation, which has an average internal seismic velocity of 2,200 ms^{-1} (Pyrenees 1 WCR). Average displacements of ~200, ~260 and ~310 m have been calculated on faults 1, 2 and 3 respectively using the Dupuy Formation average internal velocity of 2,200 ms^{-1}. Along some sections of the faults, e.g. as in Figure 8, a proportion of the offset applies to seismic reflectors representing the volcano and lava flows. Total displacement in these areas will be greater as seismic velocities are higher (at least ~2,850 ms^{-1} if the Pyrenees Volcano is altered, and higher if not altered).

4.3 Eastern Exmouth Sub-Basin: Intrusive magmatism

4.3.1 Description of sub-volcanic feature

Beneath the Pyrenees Volcano, at a depth of ~2,600 msTWT is a discrete, high amplitude seismic reflector (Figure 11). The reflection is visible in both the HC93 3D and HCA05 seismic reflection surveys, although it extends beyond the northern extent of the HC93 3D survey and the western extent of the HCA05 3D survey (Figure 9). Within the bounds of the seismic reflection datasets, the bright reflector is 12.5 km long (north to south) and 7.5 km wide (east to west). The reflector has a stepped morphology, which appears to be related to downward offset to the NW by several normal faults that strike NNE-SSW (Figure 11). Offset of the sub-volcanic feature along each of the faults is between ~40 and ~100 msTWT.

The reflector comprises two distinct segments: a broad 7.5 x 5 km segment to the northwest, and a narrower 2 x 5 km segment to the southeast. The broader north-western segment is parallel to host strata and has an average thickness of 40 msTWT. The narrow south-eastern segment has an average thickness of 30 msTWT and is also strata-concordant but has been tilted towards the southeast within a rotated fault block (Figure 11).

An RMS amplitude map highlights the internal structure of this feature (Figure 11). The highest amplitudes (yellow) are observed within the northwestern segment of the feature, and a branching network of interconnected corridors of high amplitude with average widths of up to 180 m are observed on the top surface of the feature. These high amplitude corridors often terminate in lobate structures of lower amplitude. The southeastern segment is characterised by lower seismic amplitudes.

728 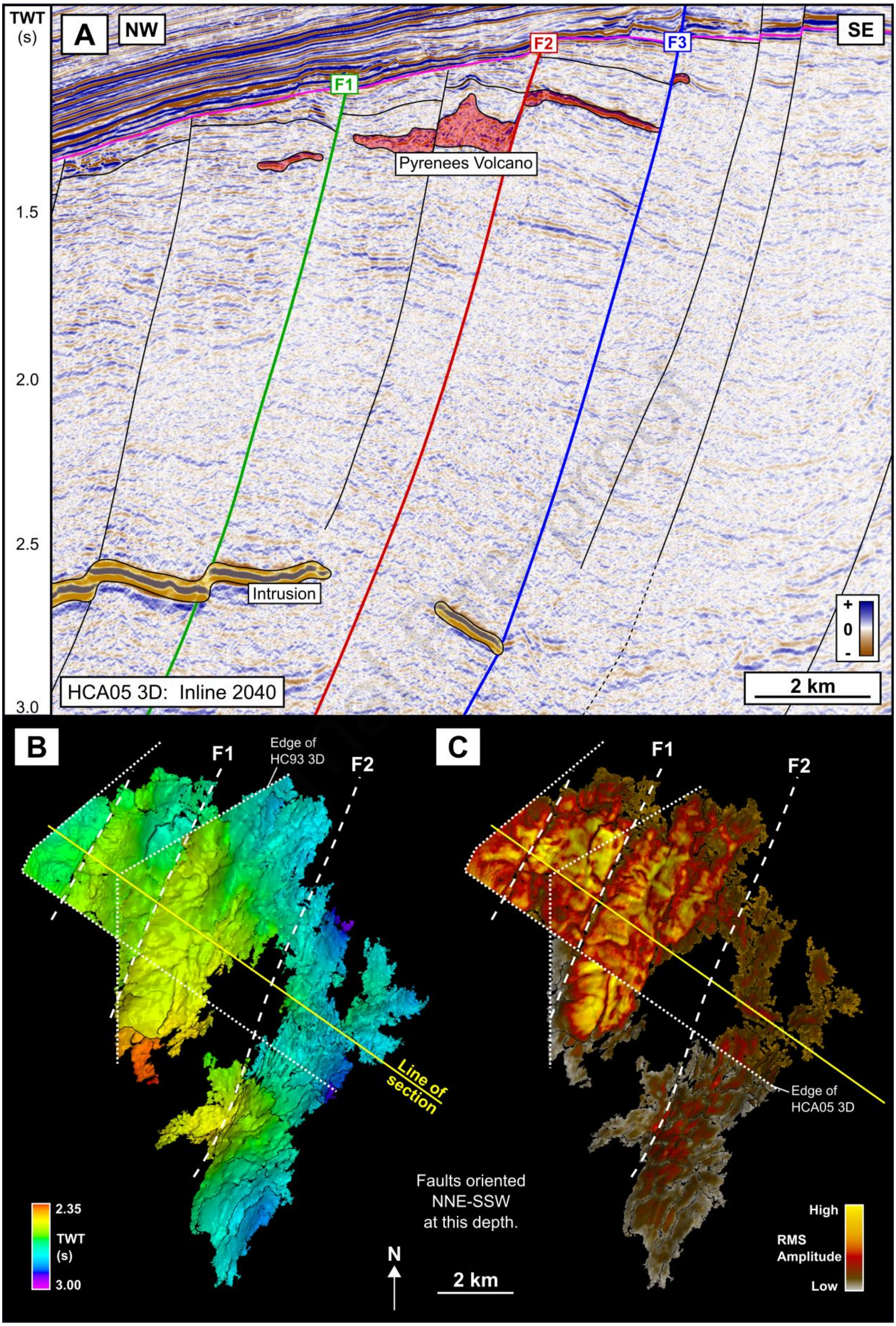

TWT (s)
A
NW
SE
F1
F2
F3
Pyrenees Volcano
Intrusion
1.5
2.0
2.5
3.0
HCA05 3D: Inline 2040
2 km
+
0
-
B
F1
F2
Edge of HC93 3D
Line of section
2.35
TWT (s)
3.00
C
F1
F2
Edge of HCA05 3D
Faults oriented NNE-SSW at this depth.
N
2 km
High
RMS Amplitude
Low

Figure 11: (A) Interpreted section of part of Inline 2040 from the HCA05 Seismic Reflection survey. The line of section is shown in bottom part of the figure. This figure shows the presence of an igneous intrusion at ~2.7 sTWT depth beneath the Pyrenees Volcano. The intrusion is offset by the same generation of normal faults that offset the Pyrenees Volcano. Faults (F1 to F3) are labelled. Time structure (B) and RMS amplitude (C) maps of top surface of the intrusion below the Pyrenees Volcano. Movement on the faults has rotated strata, including the intrusion, to dip towards the SE. High amplitude (yellow) zones within the intrusion show likely paths of dominant magma transport within the intrusion, terminating at lobe shaped features at the intrusion's edges. At this depth, the faults are oriented NNE-SSW, whereas they are oriented NE-SW at the level of the Pyrenees Volcano. Black lines denote the edges of the HC93 and HCA05 3D seismic reflection surveys.

4.3.2 Interpretation of sub-volcanic feature

The seismic amplitude characteristics and abrupt lateral termination of lobe-shaped edges of the sub-volcanic feature strongly suggest that it is an igneous intrusion. Similar structures have been reported in igneous intrusions observed in seismic reflection data by Smallwood and Maresh (2002), Planke et al. (2005), Hansen and Cartwright (2006a), McClay et al. (2013), Schofield et al. (2017a), Mark et al. (2018) and Mark et al., (2020), amongst others. The high amplitude corridors on the top surface may represent channels that fed magma through the intrusion as it was emplaced (e.g. Magee et al., 2016b).

The intrusion is offset by the same set of normal faults that offset the Pyrenees Volcano (Figure 11). However, at this depth (~2,600 msTWT) the faults have a different orientation, striking NNE-SSW. In contrast, at the level of the Pyrenees Volcano (~1300 msTWT) these faults strike NE-SW. This suggests these faults initially formed during rifting that led to Callovian breakup along the Argo Margin to the North, where normal faults became oriented NNE-SSW and offset was between 300 and 800 m (Black et al., 2017, Dempsey et al., 2019). In order to have also offset Late Jurassic strata at the level of the Pyrenees Volcano, the faults in the study area must have been later reactivated during uplift and rifting that led to breakup on the Gascoyne and Cuvier margins, where extension was oriented NW-SE. This is likely what led to the change in orientation of the faults observed at shallower depths.

Emplacement of a single intrusion at different levels within the host strata (e.g. Schofield et al., 2012a, Schofield et al., 2012b, Magee et al., 2016b) can also lead to vertical offset of magma lobes within a sill. However, lateral overlap of magma lobes is also commonly observed (Schofield et al., 2012a, Schofield et al., 2012b, Magee et al., 2016b), but is not apparent here. Furthermore, several of the high seismic amplitude magma conduits connect across faults (Figure 11), which implies that the intrusion was once continuous.

Other studies on igneous intrusions in the central Exmouth Sub-Basin have estimated that their ages range from Kimmeridgian (Magee et al., 2013a) to Berriasian, based primarily on the observations of onlap onto forced folds (Magee et al., 2016a, O'Halloran et al., 2019). We do not observe forced folding above the intrusion beneath the Pyrenees Volcano, but since it is offset by faults that were active between 145 and 138 Ma, it must have been emplaced prior to the cessation of fault movement. Hence we suggest that the intrusion beneath the Pyrenees Volcano was likely emplaced sometime between the Kimmeridgian and the Berriasian, and certainly before fault movement terminated at ~138 Ma (Valanginian). Whilst we cannot determine whether this intrusion contributed to the formation of the Pyrenees Volcano, both the spatial correspondence and the relationship between the observed igneous rocks and the faulting suggest this is a possibility.

4.4 Western Exmouth Sub-Basin: Extrusive Magmatism

4.4.1 The Toro Volcano

The only other confirmed example of extrusive magmatism in the inboard Carnarvon Basin is the Toro Volcano (Black et al., 2017), which is located on the western side of the Exmouth Sub-Basin roughly 75 km WNW of the Pyrenees Volcano (Figure 1), within the bounds of the Indian 3D and the Endracht Extracts and HE94 3D seismic reflection surveys (Figure 4 and Figure 12).

Partly altered lava flows in the western flank of the Toro Volcano were intersected in the Toro-1 petroleum exploration well between 1,441.4 and 1,602.6 m below the seafloor (Figure 13) (Taylor, 2014, Grain et al., 2015, Curtis et al., 2022). The well intersects strata from the O. montgomeryi dinocyst zone below the Toro Volcano, and strata from the D. jurassicum dinocyst zone immediately above the Toro Volcano (Taylor, 2014, Grain et al., 2015). This constrains the timing of volcanism to the Tithonian, between ~151.8 and ~147 Ma (Marshall and Lang, 2013). Hence, the Toro Volcano is of a similar age to the Pyrenees Volcano. The top section of the Toro Volcano is onlapped by deltaic siltstones, claystones/shales and sandstones of the Lower Barrow Group (Taylor, 2014), above which it is truncated beneath the KV Unconformity (KVU) (Figure 13 and Figure 14). Seismic profile lines through the volcano show that its top surface is defined by a high-amplitude reflector, whilst its internal structure is defined by amorphous and chaotic reflection events (Figure 13 and Figure 14).

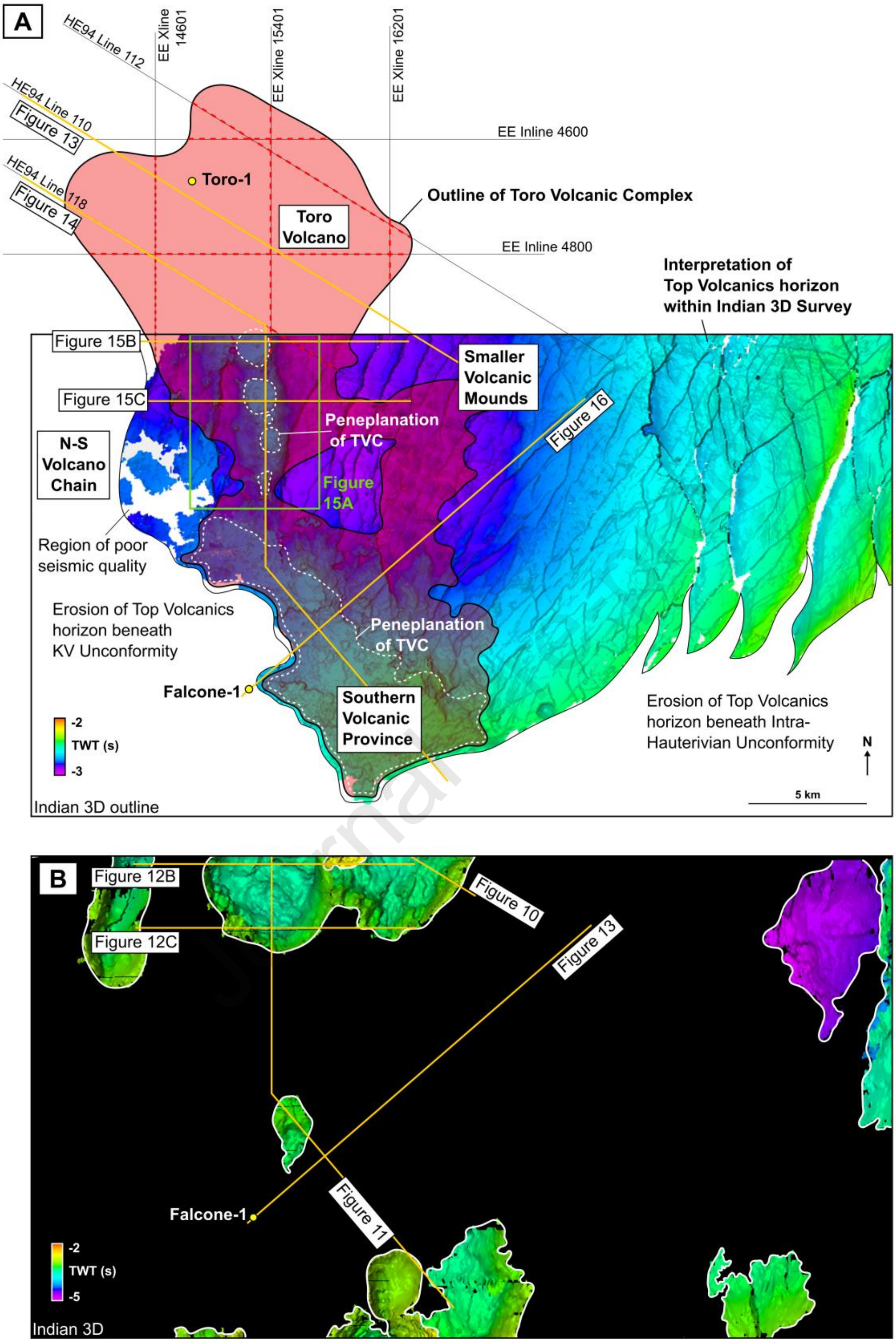

Figure 12: (A) Map showing the extent of the Toro Volcanic Complex (TVC; Pink shaded area) within the Indian 3D, HE94 and Eendracht Extract 2D seismic reflection surveys. Interpreted 3D surface within part of the Indian 3D seismic reflection survey is the top TVC surface (time), mapped as part of this study. The white region denotes an area where top TVC surface is eroded beneath the KV and Intra-Hauterivian unconformities. White dotted lines denote regions where the TVC is truncated beneath the KV and Intra-Hauterivian unconformities. Black lines show locations of 2D seismic

reflection survey lines from the Eendracht Extracts (EE) 2D and HE94 2D seismic reflection surveys that intersect the TVC (intersections represented by red overprint). Orange lines are lines of section for Figures 13, 14, 15 and 16. Also shown are the locations of the Toro-1 and Facone-1 petroleum exploration wells. (B) Map showing locations and depths of intrusions below the TVC, and seismic section lines, within the Indian 3D seismic reflection survey.

The Toro Volcano is at least 10 km in diameter and has a 'height' of at least 330 msTWT (Figure 13). VSP velocities over the 161.2 m section of the volcano intersected in Toro-1 have an average of 2,850 m/s, which translates to a current height of ~470 m for the Toro Volcano. As the Toro Volcano is truncated beneath the KVU, the Toro Volcano was likely higher prior to erosion. An extrapolation from the flanks upwards to a possible peak spans ~420 msTWT (Figure 13), suggesting the height prior to truncation may have been ~630 m. This volcano is ~3 times wider than the Pyrenees Volcano at its base (10 vs 3.5 km) and was potentially originally ~2.5 times higher (~630 vs ~240 m). Assuming a conical geometry to the eroded section, we estimate that ~0.21 km^3 of extrusive rock may have been eroded from the Toro Volcano.

Analysis of rock cuttings indicates that the volcano comprises highly altered basaltic rock (Grain et al., 2015, Curtis et al., 2022). The intense alteration to clay minerals is responsible for the relatively low seismic velocity of the volcanic sequence (~2,850 m/s), lower than the surrounding sedimentary rocks where velocities are between 3,000-3,250 m/s, and hence may account for the lower acoustic impedance contrast with the overlying sedimentary rocks at the Toro Volcano than observed at the Pyrenees Volcano (Figure 7, Figure 13 and Figure 14).

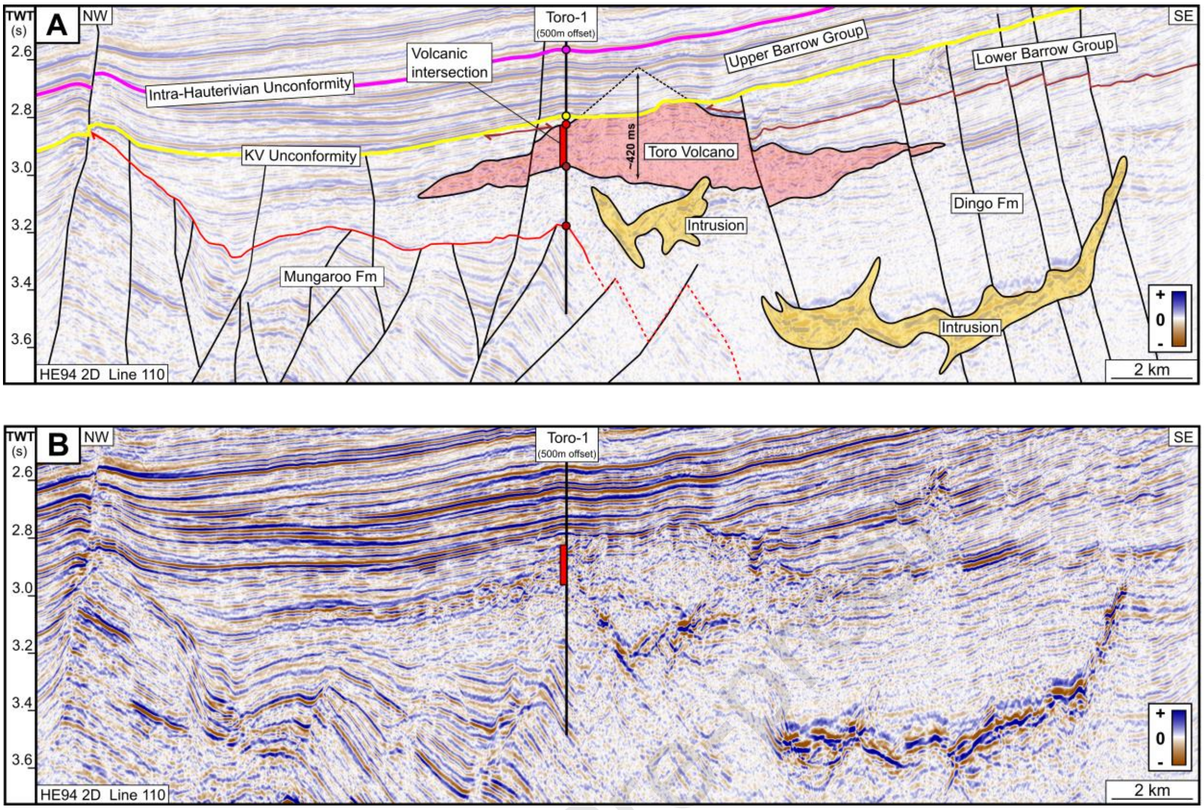

Figure 13: (A) Interpreted and (B) uninterpreted section of Line 110 from the HE94 2D seismic reflection survey, through Toro Volcano. The line of section is shown on Figure 9. The Toro Volcano is intersected by Toro-1, which is offset 500 m to the northeast. The lower section of the Toro Volcano is overlain by the Dingo Formation, and the uppermost section is overlain by the Lower Barrow Group. The KV Unconformity truncates the Toro Volcano suggesting the top section of the edifice was eroded following Early Cretaceous uplift. The eastern flank of the Toro volcano is downthrown ~100 msTWT by a normal fault. Intrusions beneath the volcano cross-cut the faults with no apparent offset, suggesting their emplacement post-dates faulting and volcanism. Poor seismic signal beneath the Toro Volcano makes it difficult to continue interpretation of the top Mungaroo Formation surface.

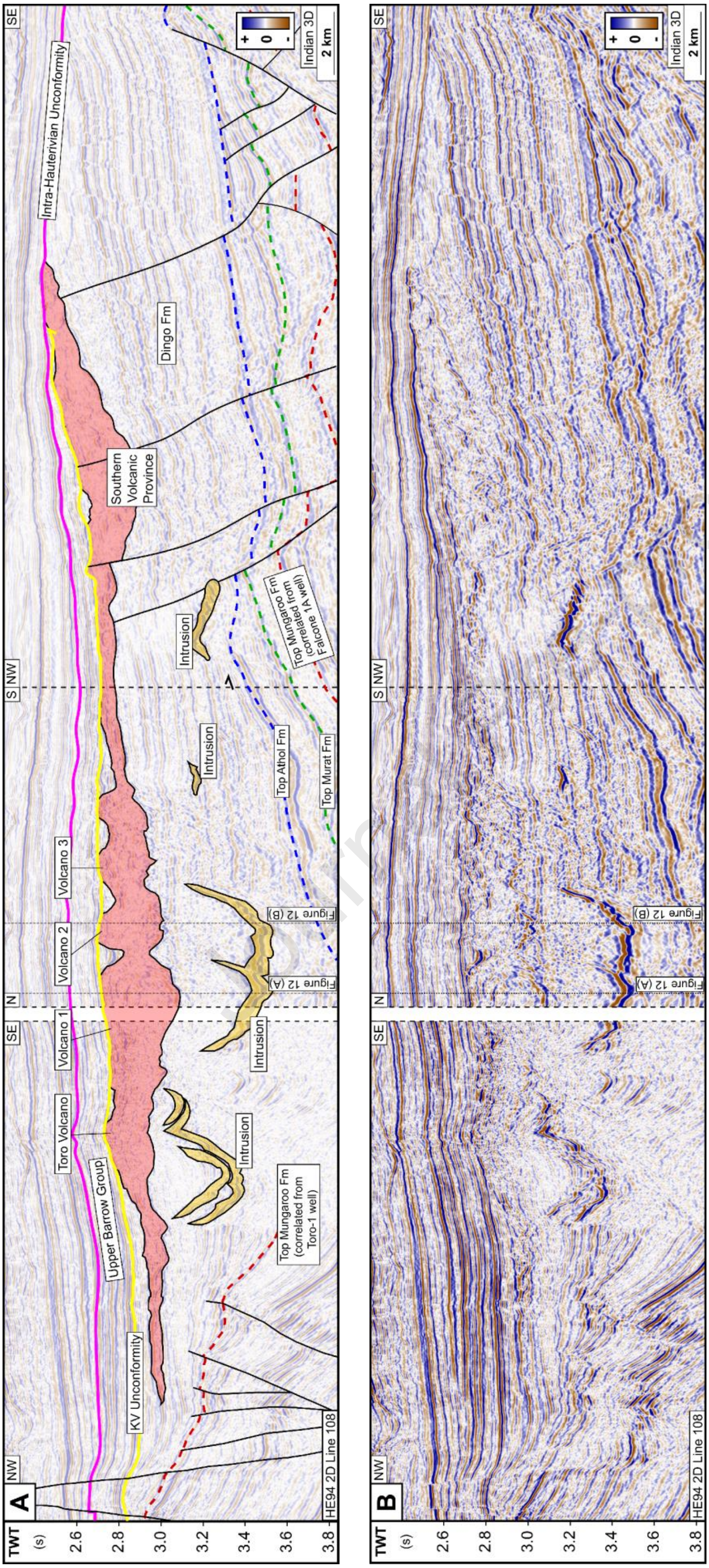
A
B
TWT
(s)
2.6
2.8
3.0
3.2
3.4
3.6
3.8
NW
SE
N
S NW
Intra-Hauterivian Unconformity
Dingo Fm
Southern Volcanic Province
Intrusion
Top Mungaroo Fm (correlated from Falcone 1A well)
Top Athol Fm
Top Murat Fm
Volcano 3
Volcano 2
Volcano 1
Toro Volcano
Upper Barrow Group
KV Unconformity
Top Mungaroo Fm (correlated from Toro-1 well)
Figure 12 (A)
Figure 12 (B)
HE94 2D Line 108
Indian 3D
2 km

Figure 14: (A) Interpreted and (B) uninterpreted seismic lines through the Toro Volcanic Complex (TVC) from the HE94 2D (Line 108) and Indian 3D seismic reflection surveys. The line of section is shown on Figure 9. The top sections of the Toro Volcano, Volcanoes 1, 2 and 3, and the Southern Volcanic Province are truncated beneath the KV (yellow) and Intra-Hauterivian (pink) unconformities. Several saucer shaped intrusions are located beneath the TVC. Lithological contacts below the TVC on the right hand side are correlated from the Falcone-1A well, whilst the Top Mungaroo Formation surface on the left hand side of the figure is correlated from the Toro-1 well.

4.4.2 Truncated mounds to the south of the Toro Volcano

4.4.2.1 Description of truncated mounds to south of Toro Volcano

A chain of three, N-S aligned truncated and flat-topped mound-shaped structures is observed within the Indian 3D seismic reflection survey, to the south of the Toro Volcano (Figure 12 and Figure 15). The structures are characterised by a bright uppermost reflector and a chaotic internal structure of low seismic amplitude (Figure 15), which connects the base of each structure (Figure 14). This amorphous seismic facies continues northwest from the Indian 3D seismic reflection survey, along Line 110 of the HE94 2D seismic reflection survey, to connect with the Toro Volcano (Figure 14). The bases of the flat-topped mound shaped structures are located at a depth of ~3,000 msTWT in the Indian 3D seismic reflection survey, within the Upper Jurassic Dingo Formation. Their tops are at ~2,700 msTWT, and are each truncated beneath the KV Unconformity. The structures are up to 330 msTWT thick, and taper outwards in a concave downwards fashion from their truncated surfaces to their bases. The flat-topped surfaces of the two northernmost mounds are circular in shape with a diameter of ~1.4 km, whist the most southern has an oval-shaped top surface, with a north-south oriented long axis of ~1.35 km and an east-west oriented short axis of ~650 m. From north to south, the structures are ~8, 7.5 and 5 km wide at their bases, respectively. In the immediate vicinity of the southernmost mound are three smaller mound structures, with diameters between 300 and 350 m.

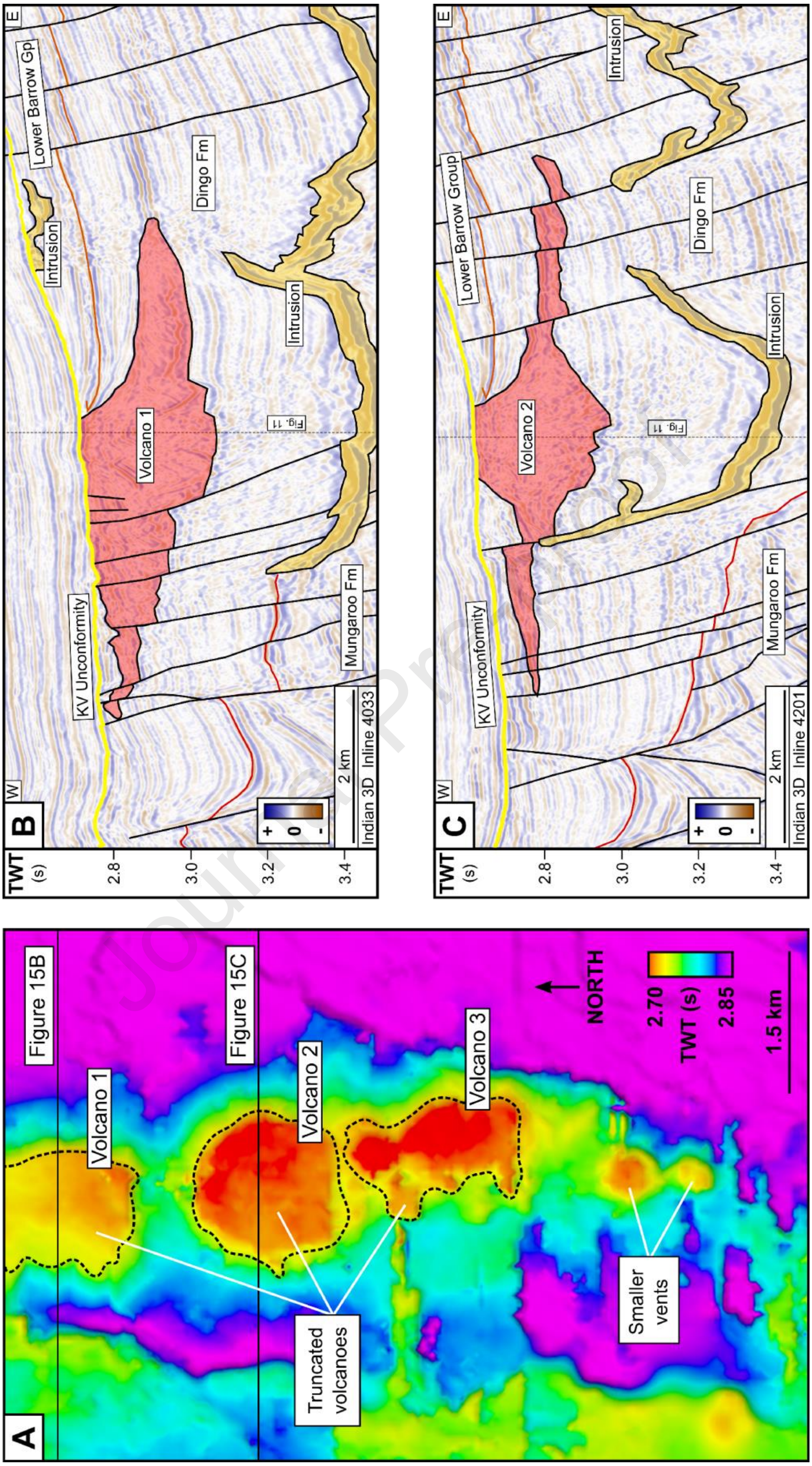
A
Figure 15B
Figure 15C
Volcano 1
Volcano 2
Volcano 3
Truncated volcanoes
Smaller vents
NORTH
2.70
TWT (s)
2.85
1.5 km
B
W
E
TWT (s)
2.8
3.0
3.2
3.4
Lower Barrow Gp
Intrusion
Dingo Fm
Volcano 1
Fig. 11
KV Unconformity
Mungaroo Fm
2 km
Indian 3D Inline 4033
C
Lower Barrow Group
Volcano 2
Indian 3D Inline 4201

Figure 15: (A) Two-way time structure map of Top Volcanic surface in the region of the flat-topped mound structures. (B) & (C) show interpreted seismic sections from the Indian 3D seismic reflection survey through Volcano 1 and Volcano 2. Lines of section are shown on Figure 9. Like the Toro Volcano, these volcanoes are overlain by Dingo Formation and Lower Barrow Group strata, and are peneplaned beneath the KV Unconformity. The volcanic edifices have been subject to minor (~50 msTWT) offset on NNE-SSW striking normal faults. Saucer-shaped intrusions below the volcanoes cross-cut, and are intruded into the faults; one intrusion above the volcano is truncated beneath the KV Unconformity. This suggests that the volcano was displaced on the faults prior to intrusive emplacement. Subsequently, uplift and associated erosion likely exposed both the volcanoes and intrusions prior to the onset of deposition following final development of the KV Unconformity.

4.4.2.2 Interpretation of truncated mounds to south of Toro Volcano

Magee et al. (2016a) have interpreted these features to be the largest of several chains of crater-hosted mounds, situated above fluid escape vents and emanating from normal faults that terminate beneath them. They postulate that hydrothermal fluids were explosively expelled at the seabed, forming craters that were then rapidly infilled. Magee et al. (2016a) classify these crater-hosted mounds as being formed by hydrothermal vents on the basis of their geometric similarity to hydrothermal vents described elsewhere (e.g. Jamtveit et al., 2004, Hansen, 2006, Svensen et al., 2006, Hansen et al., 2008). They have similar seismic velocities to that of the crater fill (calculated to be ~2,200 m/s) and the surrounding Dingo Claystone, which was penetrated by Falcone-1 south of the mounds (Figure 12).

However, based on the interconnected nature of these flat-topped mounds with the Toro Volcano, and their highly similar seismic response (high amplitude top surface and chaotic, lower amplitude reflectors within the structure), we suggest a shared volcanic origin rather than a hydrothermal origin as proposed by Magee et al. (2016a). This interpretation is consistent with that of Black et al. (2017), who interpret these flat topped mounds as a Tithonian-aged volcanic centre. On this basis we interpret these structures as a continuous chain of volcanoes (that includes the Toro Volcano), which formed contemporaneously on the same surface and were onlapped by Tithonian sedimentary rocks. Low seismic velocities within the structures are explained by the continuation of pervasive alteration observed in the mafic volcanic rocks penetrated by Toro-1.

These truncated volcanoes have a similar 'height' to the Toro Volcano (~330 msTWT). Assuming southward continuation of the alteration encountered in the Toro Volcano, we estimate that these structures are ~475 m high, and, like the Toro Volcano, are likely to have been higher prior to erosion.

4.4.3 Southern Volcanic Province

4.4.3.1 Description of Southern Volcanic Province

In the southwestern part of the Indian 3D seismic reflection survey is a broad (~6 x 13 km) body of chaotically oriented, low amplitude, seismic reflectors, dipping gently north-eastwards within Tithonian strata (Figure 12 and Figure 16). The western part of the body is truncated beneath the KVU (Figure 12 and Figure 16). The eastern portion is not truncated; in this region, the body has a top surface with relatively high amplitude (Figure 16). Variations in topography on the top surface of this body suggest overlapping lobate features that are partially obscured by successive lobes. The base of the body is at ~2.8 s depth, is up to ~300 msTWT thick beneath the KVU; thickness tapers to zero as the body thins towards the northeast (Figure 16).

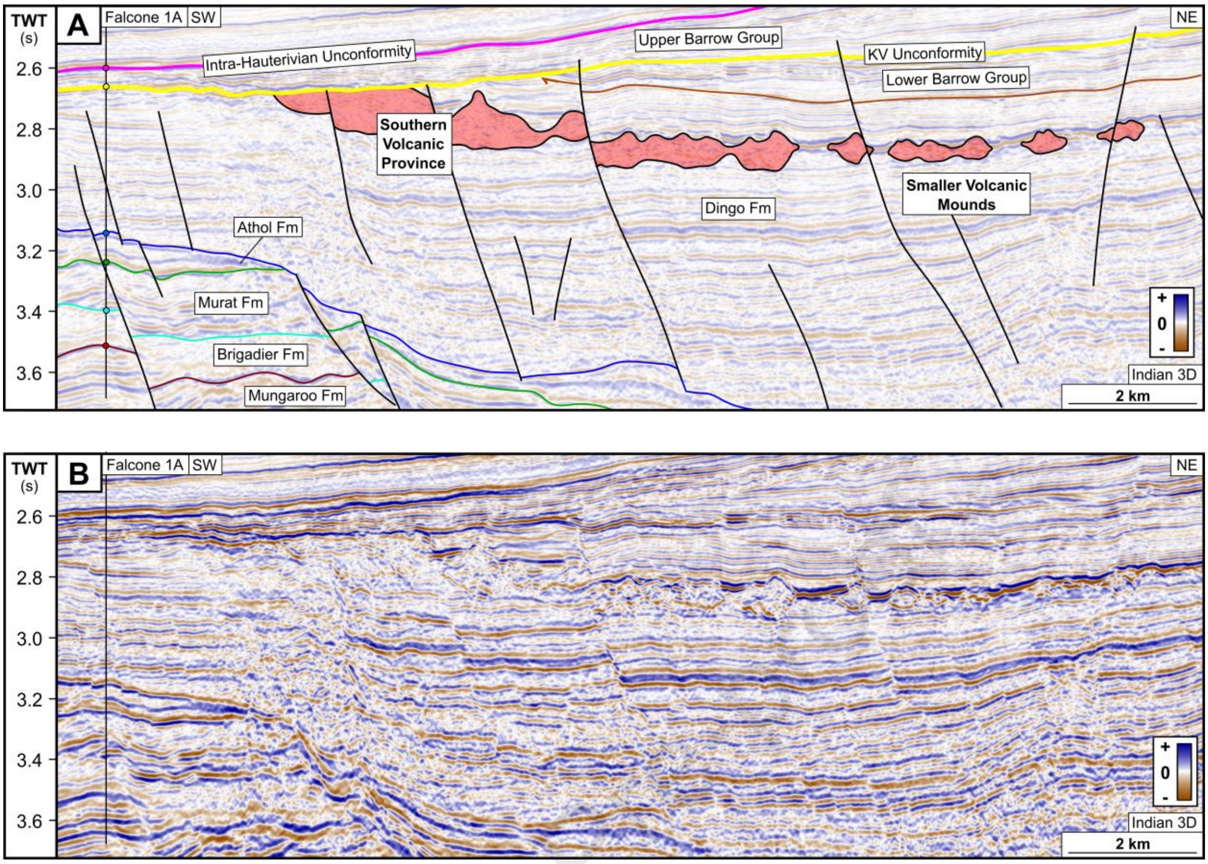

Figure 16: (A) Interpreted and (B) uninterpreted seismic sections from the Indian 3D seismic reflection survey through the Southern Volcanic Province (SVP) and part of the region containing smaller volcanic mounds. The line of section is shown on Figure 9. The SVP is tilted, and its western section was completely removed following Early Cretaceous uplift and erosion prior to the onset of deposition responsible for the Upper Barrow Group. In this vicinity the Toro Volcanic Complex is overlain by the Dingo Formation.

4.4.3.2 Interpretation of the Southern Volcanic Province

The southernmost body of chaotic reflectors connects laterally to the chain of flat-topped volcanoes, which have a similar seismic expression (Figure 16). It is therefore also interpreted to be volcanic in origin. Much of this volcanic body has been removed by erosion, making it hard to determine the original form. However, overlapping lobate features identified on its top surface (Figure 12) suggest that the feature is likely predominantly composed of lava (after Holford et al., 2012). The amplitude response is likely to indicate pervasive alteration of mafic lava flows, as seen at Toro-1. Assuming a seismic velocity similar to that of the volcanic rocks at Toro-1 (~2,850 ms^{-1}), we estimate that this volcanic body has a maximum thickness of ~430 m beneath the KVU.

4.4.4 Smaller mounds to the east of the volcano chain

4.4.4.1 Description of smaller mounds to the east of volcano chain

Roughly 7.5 km to the east of the volcano chain, between ~2,800 and 2,900 msTWT within the Dingo Formation, is a roughly 3.5 x 8 km region containing irregularly shaped mounds (Figure 12 and Figure 14). These mounds range in diameter from roughly 100 to 700 m and have a maximum 'height' of ~120 msTWT. The mounds feature a hard-to-soft top surface reflection event and low amplitude, chaotically oriented internal seismic reflectors. Seismic signatures of individual mounds often interconnect beneath the top surface. Immediately surrounding the mounds and connecting with lavas from the Southern Volcanic Province, are areas of low amplitude with lobate edges.

4.4.4.2 Interpretation of smaller mounds to the east of the volcano chain

These mounds have previously been interpreted as material infilling craters formed by violent expulsion of hydrothermal fluids at the seabed (Magee et al., 2016a). However we interpret these features as volcanic in origin due to (I) the similar internal seismic characteristics these structures share with the Toro Volcano, implying they represent a chain of flat topped volcanoes associated with the Southern Volcanic Province, and (II) their close spatial association this volcanic system. Assuming these structures also comprise altered mafic igneous material similar to that of the Toro Volcano (with an internal seismic velocity of ~2,850 ms^{-1}), we estimate their maximum height to be ~340 m.

4.4.5 Definition of the Toro Volcanic Complex

The north-south trending chain of volcanos (including The Toro Volcano), the Southern Volcanic Province, and the smaller mounds to the east are the largest complex of extrusive igneous rocks recorded in the NCB and cover an area of ~300 km^2. The Toro Volcano and volcano chain have previously been defined as the Toro Volcanic Complex (e.g. Grain et al., 2015, Black et al., 2017). However, with the inclusion of the Southern Volcanic Province and the smaller volcanic mounds, we feel this extrusive system is best described not as a "volcanic centre" (which implies a point source of extruded magma), but as a "volcanic complex" (which implies multiple sources of extruded magma spread over a broad area). Henceforth, we will refer to this extrusive system as the Toro Volcanic Complex (TVC).

4.4.6 Volume of Toro Volcanic Complex

To calculate an estimate of the volume of the TVC, we multiplied the TWT difference grid between the top and bottom TVC surfaces by 0.5 (to convert to one-way time), then by the seismic velocity of altered mafic material reported at the Toro-1 petroleum exploration well (2,850 m/s). This gave a volume of ~50 km^3. This must be regarded as a minimum volume, as it is possible that the entire TVC is not altered. If a velocity of 6,000 m/s is applied (the fastest reported by Lesage et al. (2018), representing the composition of unaltered basalt) a volume of ~100 km^3 is estimated.

4.4.7 Faults intersecting the Toro Volcanic Complex

A set of normal faults offset the TVC (see Figure 2, Figure 13, Figure 14 and Figure 15). They are oriented north-south in the vicinity of the Southern Volcanic Province, and NNE-SSW near the volcano chain (Figure 4) (Black et al., 2017). These faults dip at approximately 70°, offsetting strata towards the east, and they commonly terminate beneath the KVU. These faults have been studied in detail by Black et al. (2017), who reported displacements of ~150 m within Upper Jurassic strata occurring during the Late Tithonian to Valanginian. Fault displacement at the TVC is less than on faults at the Pyrenees Volcano.

4.4.8 High amplitude seismic reflectors beneath the Toro Volcanic Complex

4.4.8.1 Description of high amplitude seismic reflectors beneath the Toro Volcanic Complex

Eight high-amplitude seismic reflectors are identified in the immediate vicinity of the TVC within Late Jurassic rocks (Figure 12). These range in diameter from ~1.5 to ~6 km. Two are present beneath the Toro Volcano and volcano chain; one above Volcano 1, truncated below the KVU; and four beneath the Southern Volcanic Province. Several of these reflections extend beyond the bounds of the Indian 3D seismic reflection survey, with two imaged on the HE94 2D survey lines 108 and 110 to the north (Figure 11). The reflections are concave upwards in morphology with abrupt lateral terminations, and vertically transgress stratigraphy between ~2.6 and ~3.5 sTWT. Attenuation of seismic signal caused by the high amplitude reflections has resulted in a region of low seismic amplitude below each one. The bright reflectors cross-cut and are present along parts of the NNE-SSW faults described above.

4.4.8.2 Interpretation of high amplitude seismic reflections beneath the Toro Volcanic Complex

Due to the high amplitude of reflectors, abrupt lateral termination and similar morphology to intrusions observed elsewhere, we agree with Magee et al. (2013a,c, and 2016a) and Black et al. (2017) that these high amplitude reflection events should be interpreted as boundaries of igneous intrusions. These intrusions both traverse, and are emplaced across, the NNE-SSW oriented fault planes that offset the TVC (Figure 13 and Figure 15) (Magee et al., 2013c, Magee et al., 2016a). This implies emplacement following Late Tithonian to Valanginian displacement recorded on these faults as reported by Black et al. (2017). Because the intrusion above Volcano 1 is emplaced into the Lower Barrow Group but is truncated by the KVU, this implies intrusion emplacement occurred between the late Tithonian (the onset of LBG deposition) and early Valanginian (age of KVU).

4.4.9 Environment of emplacement of the Toro Volcanic Complex

Two petroleum wells penetrate Tithonian-aged host strata in the vicinity of the TVC: Toro-1, which intersects the Toro Volcano (Figure 12 and Figure 13) and Falcone-1A, which is located ~3 km from the eroded western edge of the Southern Volcanic Province (Figure 12 and Figure 13). Pollen spores of the from Dingo Formation claystones interbedded with volcanic rocks at the bottom of the Toro Volcano, and Lower Barrow Group mudstones immediately overlying the volcano, have been interpreted to indicate that the Toro Volcano, and hence the TVC, formed in a nearshore to marginal marine setting (Taylor, 2014). At Falcone-1A, the Dingo Formation beneath the Southern Volcanic Province is composed of claystone containing spores associated with a nearshore environment. The 'nearshore' is the zone above the fair-weather wave base, the depth below which bottom particles cannot be moved by wave action (Davis, 1985), The 'marginal marine' setting is the zone of transition from continental to marine depositional regimes, characterised by beaches, deltas and lagoons (Boggs Jr, 2014).

In Longley et al. (2002)'s regional palaeogeographic reconstructions, the area in which the TVC is situated is not interpreted to be located in a region of *such* shallow water as the nearshore through the Tithonian, but a region straddling the outer edge of a clay dominated shelf (Figure 10C). Water depths on clay-dominated continental shelves are typically >120 m (Nittrouer and Sternberg, 1981) extending to depths of ~200 m at the shelf break (the pint of onset of the continental slope) (Allen, 1980).

The palynological data from wells close to the TVC and palaeogeographic reconstructions are somewhat inconsistent. It is conceivable that terrestrial pollen could have blown or floated ~100 km from the palaeoshoreline to site of the TVC. Despite this, we feel it can be stated with reasonable confidence that water here was, relatively, much shallower than above the Pyrenees Volcano (likely 0 to 200 m), and that the TVC, with heights of at least 470 m, and up to 630 m, would have been exposed sub-aerially during its formation.

5. DISCUSSION

This study has described two regions of Tithonian, rift-related extrusive igneous rocks within the Exmouth Sub-Basin, Western Australia. The Pyrenees Volcano in the central Exmouth Sub-Basin is described here for the first time. It comprises a volcanic edifice and lava flows that are offset by normal faults, but is otherwise apparently near-completely preserved. In contrast, the contemporaneous Toro Volcanic Complex in the western Exmouth Sub-Basin is incomplete, and is characterised by peneplantion beneath the Valanginian-aged KV Unconformity. The comparative preservation and regional setting of these volcanic features is shown on an east-west oriented cross-section across the Exmouth Sub-Basin in Figure 5. In the following section we discuss the processes and events that led to the contrast in preservation states of these extrusive igneous rocks.

5.1 Controls on the preservation of the Toro Volcanic Complex and the Pyrenees Volcano

5.1.1 Paleoenvironmental conditions and potential for erosion at the time of volcanic activity

Palynological analysis of samples from nearby wells indicates that the Pyrenees Volcano likely formed in shelfal to open marine conditions. Water depths were hundreds of metres at the onset of volcanic activity. Assuming the Pyrenees Volcano is composed of altered mafic igneous rocks, like all other igneous rocks sampled in the NCB (Curtis et al., 2022), we estimate that its maximum height was likely ~240 m. Hence, there is ample scope for the Pyrenees Volcano to have been submerged and protected from surficial weathering and erosion processes prior to burial, likely having erupted onto the seabed below the storm wave base (typically ~20 m from the ocean surface; (Embry and Klovan, 1972)). These factors possibly contributed to the minimal impact of erosion on the Pyrenees Volcano following the cessation of eruption.

In contrast, the TVC formed and developed in nearshore to shelfal environment, in water depths of >tens of metres. Hence for much of the period in which the TVC was active and subsequently buried, through the Tithonian, at least part of it would likley have been exposed to subaerial weathering and erosion. This is suggested on the basis of the following observations:

1. Volcanic activity at the TVC was restricted to the Tithonian, supported by (i) palynological data from the Toro-1 well indicating that pollen immediately beneath the Toro Volcano is from the O.montgomeryi dinocyst zone and immediately overlying the volcano is from the D. jurassicum dinocyst zone (Longley et al., 2002, Helby et al., 2004, Taylor, 2014); and (ii) Tithonian aged-ashfall deposits intersected in nearby petroleum exploration wells can be correlated to the TVC (Curtis et al., 2022). Mt Aneto grew to between ~470 and ~630 m in height during this time, and was likely located between the shoreline and continental shelf break.
2. The thickness of the Dingo Claystone that onlaps the Toro Volcano is ~130 msTWT (Figure 14). The Dingo Claystone has an average seismic velocity of ~3100 m/s in the

Toro-1 well. This suggests that during D. jurassicum times, a further ~200 m of Dingo Claystone was deposited onto the volcano. Hence, by the onset of the deposition of the Lower Barrow Group, the top section of the Toro Volcano protruded at least ~270 m, and possibly up to 430 m, above the seabed.

3. The maximum clinoform height in the Exmouth Sub-basin depocentre in the P. iehiense sequence of the LBG is 180 to 360 m (Paumard et al., 2018), suggesting that in the deepest part of the basin, water depths were up to 360 m during P. iehense times. Water depths over the Exmouth Terrace (along the north western edge of the main depocentre, on which the TVC is located), where only bottomsets of the P, iehiense sequence (25 to 50 m thick) are preserved (Paumard et al., 2018), would have been shallower. Therefore, at least part of the Toro Volcano was likely exposed above sea level during much of the Latest Tithonian and possibly into the Earliest Berriasian.

We note that contemporary subaerial erosion rates at the San Miguel mafic volcanic province, in the Azores (surface area of ~750 km^2) have been estimated to be in the range of ~60 to 175 km^3/myr (Louvat and Allègre, 1998). However it is very difficult, and beyond the scope of this study, to extrapolate what erosion rates, and hence total volume loss by erosion prior to burial, may have occurred at the Toro Volcanic Complex, which has an area of ~300 km^2 and for which we have calculated a preserved volume of between 50 and 100 km^3. Factors such as the topography of the volcanic complex, seawater chemistry at the time, its latitude, global average temperatures and prevailing weather patterns are likely to have a role in governing erosion rates of the exposed igneous rocks. However, as the various elements of the TVC have retained their distinct volcano-like morphology, we suggest that any weathering and erosion caused by subaerial exposure was minor in relation to its total volume, and did not severely impact its preservation potential prior to burial.

5.1.2 Timing of Jurassic to Early Cretaceous uplift in the Northern Carnarvon Basin

Two phases of Late Jurassic to Early Cretaceous uplift have been documented in the Northern Carnarvon Basin, which are pertinent to the preservation of rift-related igneous rocks:

5.1.2.1 Uplift Phase 1

A broad region uplift is centred to the west of the study area (Black et al., 2017) (Figure 4B). This uplift initiated at ~165 Ma (Callovian) and culminated at ~136 Ma (Valanginian), and was possibly caused by an impinging mantle plume (Rohrman, 2015, Black et al., 2017). This uplifted the Australian hinterland and a portion of the Indian continent to the west of the present Cape Range Fracture Zone (Reeve et al., 2022).

5.1.2.2 Uplift Phase 2

During the Valanginian, the Ningaloo Arch (trending east-west along a broad ~50 km corridor centred ~50 km to the south of the TVC) was uplifted (Tindale et al., 1998, Reeve et al., 2016, Paumard et al., 2018, Reeve et al., 2022). This Valanginian uplift event is separate to the plume-related uplift of Phase 1, which initiated in the Callovian (Rohrman, 2015; Black et al., 2017).

From their interpretation of the KVU erosional surface, Reeve et al. (2022) imply that the Novara Arch (trending N-S, centred immediately west of the Pyrenees Volcano) and the Resolution Arch (along the boundary of the central Exmouth Sub-Basin and the southern Exmouth Plateau) (Figure 4) were also uplifted during this event. This contradicts earlier work by Tindale et al. (1998), who instead suggest that the formation of the Novara and Resolution arches occurred later, and was associated with regional inversion in the Santonian through to the Oligocene.

The TVC is situated on the eastern flank of the region of domal uplift, north of the Ningaloo Arch, in the west of the study area (Figure 4). Once this uplift had occurred, the volcanic rocks of the TVC would have been located within regions that were topographic highs, contributing to their increased likelihood of removal by immediate and later erosion.

The Pyrenees Volcano is located on the western flank of the Novara Arch. If the Novara Arch was not uplifted until the Santonian to Oligocene, as suggested by Tindale et al. (1998), the host rocks of the Pyrenees Volcano may have been located in a relative topographic low compared to the TVC, and hence less likely to have been impacted by erosion following regional Valanginian uplift. If however, the Novara Arch was uplifted contemporaneously with the Ningaloo Arch, rocks overlying the Pyrenees Volcano would have likely also been subject to erosion.

5.1.3 Early Cretaceous unconformity development and regional erosion

The Ningaloo Arch, and possibly also the Novara and Resolution arches, formed in a region already thermally active and uplifted during Uplift Phase 1 and subject to erosion firstly in the Valanginian during the formation of the KV Unconformity (KVU) that sourced the Upper Barrow Group; and later in the Hauterivian as recorded by the formation of the Intra-Hauterivian Unconformity (IHU) (Figure 4) (Reeve et al., 2022). The IHU truncates the KVU across the central Exmouth Sub-Basin (Figure 4). Together, the KVU and IHU form an angular erosional surface above Jurassic and Early Cretaceous strata across much of the Exmouth Sub-Basin (Reeve et al., 2022) (Figure 4). Isopach mapping between the base Tithonian surface and the KVU within the Indian 3D seismic reflection survey by Black et al. (2017) indicates that at least 900 m of Lower Barrow Group was removed by erosion during the Valanginian. More regionally, Rohrman (2015) used an Airy isostatic approach to calculate erosion across the Exmouth Plateau and Exmouth Sub-Basin related to plume-related uplift (during Uplift Phase 1 as described above). Their calculation used observations from seismic and well data, and estimated over 2 km of erosion centred in the southern Exmouth Sub-Basin. At the Palta-1 petroleum exploration well, located on the Ningaloo Arch in the southern Exmouth Sub-Basin (Figure 1 and Figure 4 and Figure 18), roughly 2,500 m of Upper Triassic, Jurassic and Lower Cretaceous strata are missing (Dale, 2015). Hence it appears that the erosional events manifested by the KVU and IHU are the most significant controls on volcano preservation in the study area. They were responsible for peneplanation of the TVC and removal of all bar ~200 m of overburden from above the peak of the Pyrenees Volcano.

5.1.4 Thickness of Lower Barrow Group, Upper Barrow Group and Birdrong Formation and localised erosion.

In this section we attempt to reconstruct the possible thickness of Lower Barrow Group (deposited above the volcanoes following Uplift Phase 1, prior to erosion associated with the KVU), Upper Barrow Group and Birdrong Formation (deposited following Uplift Phase 2, onto the KVU surface, and prior to erosion associated with the IHU) strata deposited above the TVC and the Pyrenees Volcano. It was the original thickness of these formations that buffered the volcanic centres from erosion associated with the KVU and IHU. By subtracting the remaining thicknesses of these strata from their postulated original thicknesses, we are able to estimate how much material was removed during these erosional events, though we acknowledge the uncertainties associated with stratigraphic correlation-based approaches for estimating missing section (cf. Corcoran & Doré, 2005).

Late Jurassic uplift (during Uplift Phase 1) and resulting erosion sourced deltaic deposits of the Lower Barrow Group (LBG) (Dale, 2015, Reeve et al., 2016, Paumard et al., 2018, Paumard et al., 2019), which is over 3,000 m thick in the centre of the Exmouth Sub-Basin (Reeve et al., 2016). However, towards the hinterland in the south of our study area, there are large areas where the LBG is very thin, or not preserved at all (Figure 10). This is due to Valanginian uplift and subsequent erosion associated with the KVU and IHU (Reeve et al., 2022).

The closest well to the TVC that intercepts a fully preserved thickness of LBG is Ragnar 1A, where it is ~760 m (~450 msTWT) thick (Taylor et al., 2013, Paumard et al., 2018). Ragnar 1A is located between 25 and 30 km northwest of the TVC (Figure 10), hence we tentatively suggest that the original thickness of the LBG above the TVC was likely similar. Our analysis suggests that the highest point of the TVC, the peak of the Toro Volcano, was higher than ~470 m (the height at which it is truncated), and possibly up to ~630 m. We have also calculated that ~200 m of Dingo Claystone onlap the Toro Volcano. Assuming a total thickness for the LBG of ~760 m we suggest that the original thickness of LBG deposited above the Toro Volcano may have been at least 330 m and possibly up to 490 m. As the Toro Volcano is truncated from ~470 m above its base and onlapped by ~200 m Dingo Claystone, onto which was deposited ~760 m of LBG, this implies ~480 m of LBG may have been eroded from above the TVC.

Only part of the P. iehense sequence is preserved in the vicinity of the Pyrenees Volcano (Spry, 1994). The most complete section of LBG penetrated in a petroleum exploration well close the Pyrenees Volcano is that intersected in Novara-1 ST1, ~35 km north of the igneous centre, which contains deposits from the K. wisemaniae to the B. reticulatum sequences (Paumard et al., 2018) (Figure 10). The top of the B. reticulatum sequence in at Novara-1 ST1 is intersected at 1270 mMD (Brooks, 1983). At the Novara-1 ST1 location, Paumard et al. (2018) predict the basal depth of the P. iehiense sequence to be at ~3200 mMD based on seismic correlation of this surface between the Eskdale-1 and Altair-1 petroleum exploration wells (Figure 10). Hence it is likely that ~1930 m of LBG currently exist at the site of Novara-1 ST1. The uppermost part of the LBG, the E. torynum sequence, is not preserved at the Novara-1 ST1 well. During E. torynum times, topsets of the E. torynum sequence were deposited at the location of the Pyrenees Volcano (Figure 10E). Where they *are* preserved, topsets of the E. torynym sequence are between ~70 and ~180 m thick across the depocentre of the Exmouth Sub-Basin (Paumard et al., 2018). Assuming a similar thickness of LBG was deposited above the Pyrenees Volcano as at the site of the Novara-1 ST1 well, it is therefore possible that a vertical thickness of up to ~2000 to ~2080 m of LBG was once present above the Pyrenees Volcano.

We now consider the deposition of Upper Barrow Group and Birdrong Formation, which where preserved in the Exmouth Sub-Basin, are present between the KVU and IHU. In a scenario where the Novara Arch was not uplifted in the Valanginian (after Tindale et al. (1998)), topsets of the Upper Barrow Group (S. areolata sequence of Paumard et al, (2018)) would have been deposited above the Pyrenees Volcano (Figure 10). Where preserved, they are 215 to 305 m thick (Paumard et al, (2018). Where it is penetrated by petroleum exploration wells, the overlying Birdrong Formation is seldom separated from the underlying Upper Barrow Group and overlying Mardie Greensand, as it is particularly thin in the Exmouth Sub-Basin, however, Hocking et al. (1988) report its thickness in exposures onshore to be ~25 m. Therefore, it is possible that ~240 to ~330 m of Upper Barrow Group and Birdrong Formation were present above the location of the Pyrenees Volcano by prior to the onset of erosion associated with the IHU. We also note that if the Novara Arch *was* uplifted in the Valanginian, coeval with the Ningaloo Arch (after Reeve et al. (2022)), the region containing the

Pyrenees Volcano would have been a topographic high during Upper Barrow Group and Birdrong Formation deposition (Figure 17). These formations may have instead onlapped the Novara Arch west of the Pyrenees Volcano, adding no protection to the volcanic centre against continued erosion of LBG strata above.

As the Pyrenees Volcano was overlain by ~90 m Dupuy Formation and ~110 m of LBG, this implies ~1890 to ~1970 m of LBG, and possibly up to ~330 m of Upper Barrow Group and Birdrong Formation were eroded in this area between the Valanginian (beneath the KVU) and Hauterivian (beneath the IHU). As the IHU surface truncates the KVU surface in this region, it is impossible to assign what thickness of strata was eroded beneath each unconformity close to the Pyrenees Volcano. We suggest that such a significant thickness of strata removed from this location in the Valanginian is consistent with uplift of the Novara Arch (on which the Pyrenees Volcano is located; Figure 4 and Figure 5) during this time period, and supports the conclusion of Reeve et al. (2022) that the Novara Arch was uplifted along with the Ningaloo Arch in the Valanginian.

The presence of a ~2 km thick package of LBG strata likely acted to buffer the Pyrenees Volcano from erosion following Uplift Phase 2, which we also suggest here included the Novara Arch. However, where the TVC is located, we suggest that only ~760 m of LBG was deposited. The peak of the Toro Volcano possibly protruded upwards into 430 m of this LBG deposit. In contrast, the Pyrenees Volcano is completely buried by deposits of the Dupuy Formation. The buffer provided by the comparatively thinner LBG sequence covering the top of the Toro Volcano was not great enough to completely protect the TVC from erosion associated with the uplift of the Ningaloo Arch (~50 km to the south; Figure 4B), the possible uplift of the Resolution Arch (immediately to the north; Figure 4B) and the domal uplift (centred ~40 km southwest; Figure 4B) that culminated in the Late Valanginian.

5.2 Relationship with ashfall deposits encountered in Exmouth Sub-Basin and Barrow Sub-Basin petroleum exploration wells

Three petroleum exploration wells (Stybarrow-2, Enfield-3 and Enfield-4) located in the central Exmouth Sub-Basin, and two scientific boreholes: (ODP (Ocean Drilling Program) 263 A & B) located in the eastern Exmouth Plateau (Figure 1), intersected altered volcanic ash deposits within Tithonian aged sedimentary rocks of the Dupuy Formation, Dingo Claystone and Lower Barrow Group (Curtis et al., 2022). Due to the close proximity of these wells to the TVC and the Pyrenees Volcano (~50 and ~30 km respectively), and similar age of the intersected ash to the volcanism, we suggest that the TVC and the Pyrenees Volcano could represent possible sources of the ash deposits in Stybarrow-2, Enfield-3 and Enfield-4. Furthermore, Tithonian-aged volcanic ash deposits have also been interpreted from smectite bands encountered in the Dupuy Formation in four wells in the Barrow Sub-Basin to the east (Tait, 1985): Tortoise-1, Thevenard-1, Koolinda-1 and Flag-1 (Figure 1). No evidence for the presence of volcanic features has been reported in the Barrow Sub-Basin. Due to their similar age, we tentatively suggest that these ash deposits might be sourced from the TVC or the Pyrenees Volcano in the Exmouth Sub-Basin.

5.3 Model for the formation, burial and erosion of the Toro Volcanic Complex and Pyrenees Volcano

In this section, we summarize our model for the formation, burial and erosion of the two volcanic centres preserved in the Exmouth Sub-Basin, which we highlight in Figure 17. The TVC and the Pyrenees volcano formed in the Tithonian, during deposition of the Dingo Claystone in the west of the study area, and the Dupuy Formation in the east (Figure 17A). The Toro Volcano, the largest individual volcano within the TVC, possibly grew to ~630 m in height, and may have protruded above sea level on a relatively shallow continental shelf. Meanwhile, the Pyrenees Volcano formed in the basin setting to the east of the TVC, and likely grew to ~240 m in height; the volcano was probably submerged below sea level. The volcanic centres erupted lava and ash which were deposited across the Exmouth and Barrow sub-basins. At the onset of deposition of the LBG at ~147 Ma (Late Tithonian) (Marshall & Lang, 2013)), the Dupuy Formation covered the peak of the Pyrenees Volcano, whilst the Dingo Formation onlapped the TVC 200 m from its base (Figure 17A); the Toro Volcano possibly protruded ~430 m above the ocean bottom at this time.

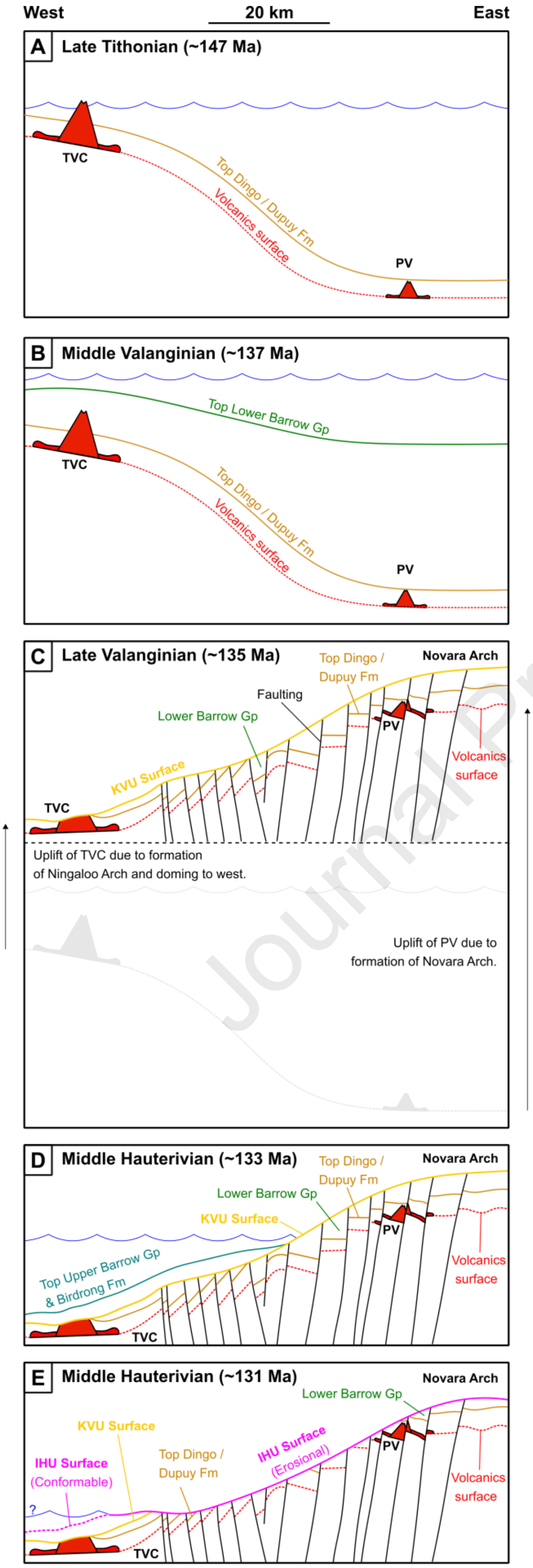

1229 Vertical domain not to scale.

Figure 17: Schematic showing burial, uplift and erosion of the Toro Volcanic Complex (TVC) and Pyrenees Volcano (PV). Approximate line of section shown on Figure 4A. (A) Contemporaneous deposition of Dingo Claystone onto TVC and burial of PV by Dupuy Formation during the Late Tithonian. (B) Deposition of Lower Barrow Group from Late Tithonian to Middle Valanginian. (C) Middle to Late Valanginian: normal faulting of Exmouth Sub-Basin strata, followed by uplift of Ningaloo Arch and, in this model, the Novara Arch, resulting in sub-aerial exposure and erosion of Lower Barrow Group, Dingo Claystone and Dupuy Formation strata, and truncation of the TVC, to form the KVU surface. (D) Late Valanginian to Middle Hauterivian deposition of the Upper Barrow Group and Birdrong Sandstone above the TVC, possibly onlapping strata of the exposed Novara Arch to the east. (E) Continued erosion and relative sea level fall, causing truncation of the KVU west of the TVC beneath the IHU surface.

The Toro Volcano was completely buried during deposition of the LBG (Figure 17B), a complex system of rivers and deltas that carried and deposited sediment from uplifted continent to the south and east. Between ~147 and ~137 Ma (Late Tithonian to Middle Valanginian), ~760 m of LBG strata may have been deposited above the TVC, whilst up to ~2000 m of LBG strata was deposited above the Pyrenees Volcano (Figure 17B). During deposition of the Lower Barrow Group, between ~145 and 138 Ma, strata of the Exmouth Sub-Basin were subject to rift-related normal faulting. These faults downthrew the edifices of the Pyrenees Volcano westwards by ~250 m, and the TVC eastwards to a lesser extent, by ~150 m.

In the Late Valanginian, strata host to both volcanic centres were uplifted by the formation of the Ningaloo Arch ~50 km to the south of the TVC, and also, in our preferred interpretation, the Novara Arch, immediately west of the Pyrenees Volcano (Figure 17C). This uplift event exposed strata above the TVC and Pyrenees Volcano to subaerial erosion. We estimate that between ~1890 to ~1970 m of LBG strata may have been eroded from above the Pyrenees Volcano, and ~480 m LBG strata may have been removed from above the TVC by ~135 Ma. This erosive event truncated volcanos of the TVC, removing up to ~160 m from the peak of the Toro Volcano. The erosive surface forms the KVU (Figure 17C), and represents breakup on the Cuvier Margin southwest of the Exmouth Sub-Basin (Figure 1).

The regions subject to uplift in the Late Valanginian became source areas for the Upper Barrow Group and the Birdrong Formation, deposits of which are between ~240 and 330 m thick where preserved in the Exmouth Sub-Basin. These formations were deposited above the TVC, but may have onlapped the Novara Arch in the central Exmouth Sub-Basin (Figure 17D).

Marine regression, or renewed uplift (possibly related to breakup on the Gascoyne Margin), through the Hauterivian, exposed strata of the Exmouth Sub-Basin to subaerial erosion once again. Erosion continued on the Novara Arch, above the Pyrenees Volcano, and towards the west, to where the resultant IHU unconformity surface truncates that of the KVU (Figure 6 and Figure 17E). Upper Barrow Group and Birdrong Formation strata immediately above the TVC were not eroded (Figure 6 and Figure 17E), possibly protected by being submerged at this time.

5.3 Implications for the broader preservation of volcanic centres in the Exmouth Sub-Basin

We note that the spatial extent of preserved pre-breakup extruded igneous rocks in the NCB (the Pyrenees Volcano at ~25 km^2 and the TVC at ~300 km^2) is proportionally very small compared to that of the pre-breakup intrusive igneous rocks emplaced into the Exmouth Plateau and the Exmouth Sub-Basin (over areas of ~30,000 and ~14,000 km^2 respectively, Figure 1). Hence, the magmatic system has been referred to as a Large *Intrusive* Igneous Province; e.g. Rohrman, 2013. Whilst quantifying the volume of intrusive rocks in the NCB is beyond the scope of this study (and in many basins is challenging due to uncertainties in the ratio of seismically resolvable to unresolvable intrusions (Mark et al., 2019)), typically one-quarter to one-third of igneous material is extruded on volcanic rifted margins (White et al., 2006, Reynolds et al., 2018). Rohrman (2013) notes that no extrusive volcanic centres have been observed in the Exmouth Plateau, and suggests that here, ascent of magma was arrested by a thick sequence of low density host rocks (namely the Triassic Mungaroo Formation) which decreased the overpressure gradient of the magma to the point that it stopped rising.

The volcanic centres we have investigated in the Exmouth Sub-Basin are Tithonian in age, as are reported volcanic ash deposits. This suggests that any volcanic activity elsewhere in the Exmouth Sub-basin was likely also Tithonian in age. It follows that any other extrusive igneous rocks that were erupted during this time will not be preserved in the Exmouth Sub-Basin in areas where Upper Jurassic strata were uplifted and eroded prior to breakup of Greater India and Australia in the Valanginian, such as the western and southern portions of the sub-basin. This region was the focus of Late Jurassic to Early Cretaceous doming (Uplift Phase 1; (Rohrman, 2015, Black et al., 2017) and contains the uplifted Ningaloo Arch (part of Uplift Phase 2; (Tindale et al., 1998).

The scale of erosion beneath the KVU and IHU in the south-western Exmouth Sub-Basin is clearly seen on a regional N-S seismic line through the southern Exmouth Sub-Basin (Figure 18). In the vicinity of the Palta-1 petroleum exploration well, located on the Ningaloo Arch, erosion following Uplift Phases 1 and 2 (resulting in the KVU) removed up to 2,250 m of Jurassic and Triassic rocks before deposition of the Hauterivian Zeepard and Birdrong sandstones (Dale, 2015). This is consistent with findings by Rohrman (2015) who suggests there was over 2 km of erosion in this part of the Exmouth Sub-Basin. Hence it is possible that any Late Jurassic extrusive volcanic rocks that were once present in this region have subsequently been removed.

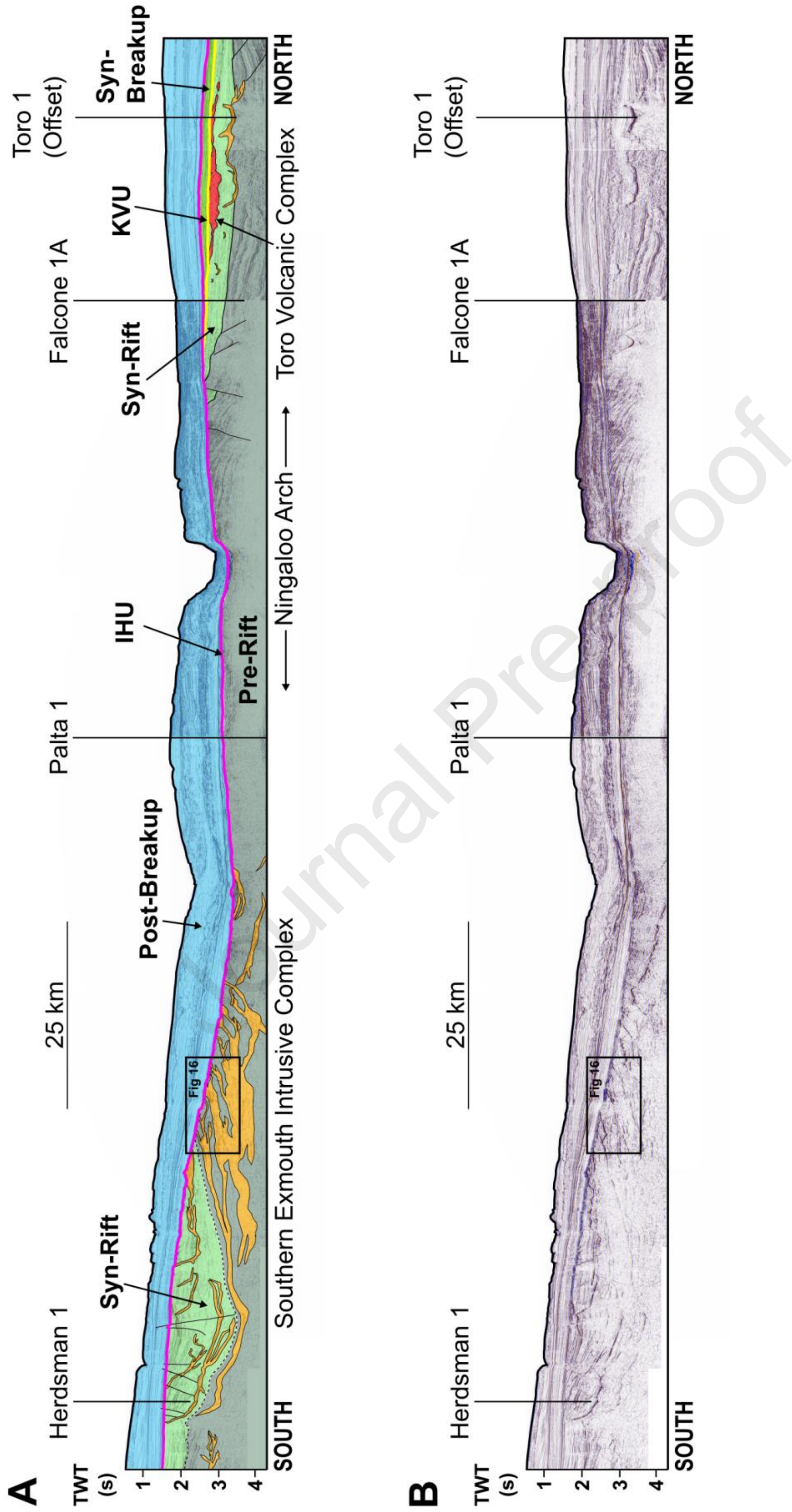
A
TWT (s)
1
2
3
4
Herdsman 1
Syn-Rift
25 km
Fig 16
Post-Breakup
Palta 1
IHU
Pre-Rift
Ningaloo Arch
Falcone 1A
Syn-Rift
KVU
Toro 1 (Offset)
Syn-Breakup
SOUTH
Southern Exmouth Intrusive Complex
Toro Volcanic Complex
NORTH
B
TWT (s)
1
2
3
4
Herdsman 1
25 km
Fig 16
Palta 1
Falcone 1A
Toro 1 (Offset)
SOUTH
NORTH

Figure 18: (A) Interpreted and (B) uninterpreted regional 2D seismic survey line composed of seismic reflection data from the Tortilla 2D, Salsa 2D, Jawa 2D, HE94 2D, Eendract Extracts 2D and Indian 3D seismic reflection surveys through the central and southern Exmouth Sub-Basin. The line of section is shown on Figure 4A and Figure 20. Jurassic and Early Cretaceous syn-rift strata, host to Tithonian-aged volcanism, were completely removed by erosion associated with uplift of the Ningaloo Arch. Triassic pre-rift strata are also missing beneath the KV and Intra-Hauterivian Unconformities (which combine along much of the section) at the Palta-1 petroleum exploration well. This strongly suggests that large volumes of igneous rock, likely including Late Jurassic volcanoes, were removed by erosion during uplift associated with breakup on the Cuvier and Gascoyne Margins in the Early Cretaceous.

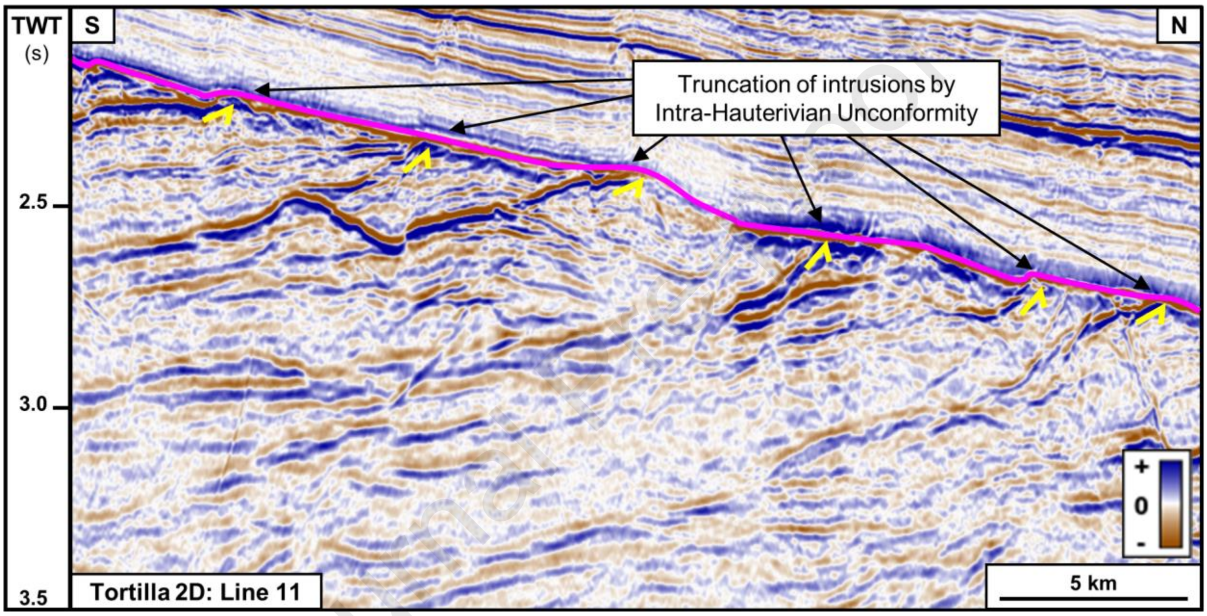

Figure 19: Section of Line 11 from the Tortilla 2D seismic reflection survey; location shown as inset in Figure 18. Intrusions (represented by high amplitude seismic reflections, with brown upper reflectors) hosted by Triassic strata are truncated by the Intra-Hauterivian Unconformity.

At the southern end of this regional seismic line is a large interconnected intrusive igneous complex, with a lateral extent of ~60 km. The southern extent of this intrusive complex is described by McClay et al. (2013) and Mark et al. (2020) who noted both strong control by pre-existing faults on intrusion morphology, and the termination of shallow intrusions beneath a breakup unconformity (e.g. Figure 19). Reeve et al. (2022) suggest the IHU is the dominant breakup-related unconformity in this part of the basin, implying that the youngest age of the intrusions is Hauterivian. The Herdsman-1 petroleum exploration well was drilled above the intrusive complex (Mark et al., 2020). The well penetrates Lower Jurassic sedimentary rocks of the Athol Formation beneath the unconformities, above which is the Barremian Muderong Formation (Willis, 2003). The entire Valanginian to Oxfordian section has been removed at this location. It is possible that magma from this intrusive complex in the southern Exmouth Sub-Basin reached the surface and was erupted, forming a volcanic centre, which was subsequently removed by rift-related uplift and subsequent erosion.

Figure 20 depicts the potential spatial extent of a zone where volcanic rocks may have been uplifted and eroded from the Exmouth Sub-Basin from the Late Jurassic to the Early Cretaceous. The extent of this zone is constrained primarily by the region of erosion beneath the IHU and KVU mapped by Reeve et al. (2022), except in the northern and central Exmouth Sub-Basin, where the outline is further constrained by the subcrop of the top volcanic surface beneath the IHU and KVU that we have mapped as part of this study, and in the eastern Exmouth Sub-basin, where we have incorporated the region of domal uplift identified by Black et al. (2017). According to Rohrman (2015), much of the southern Exmouth Sub-Basin was subject to at least 1 km of uplift during the period we have ascribed to Uplift Phase 1. We have also indicated areas where erosion may have removed intrusions that were emplaced at relatively shallow depths (i.e. <2 km), based on earlier mapping of the extent of intrusions by Symonds et al. (1998), McClay et al. (2013) and Mark et al. (2020).

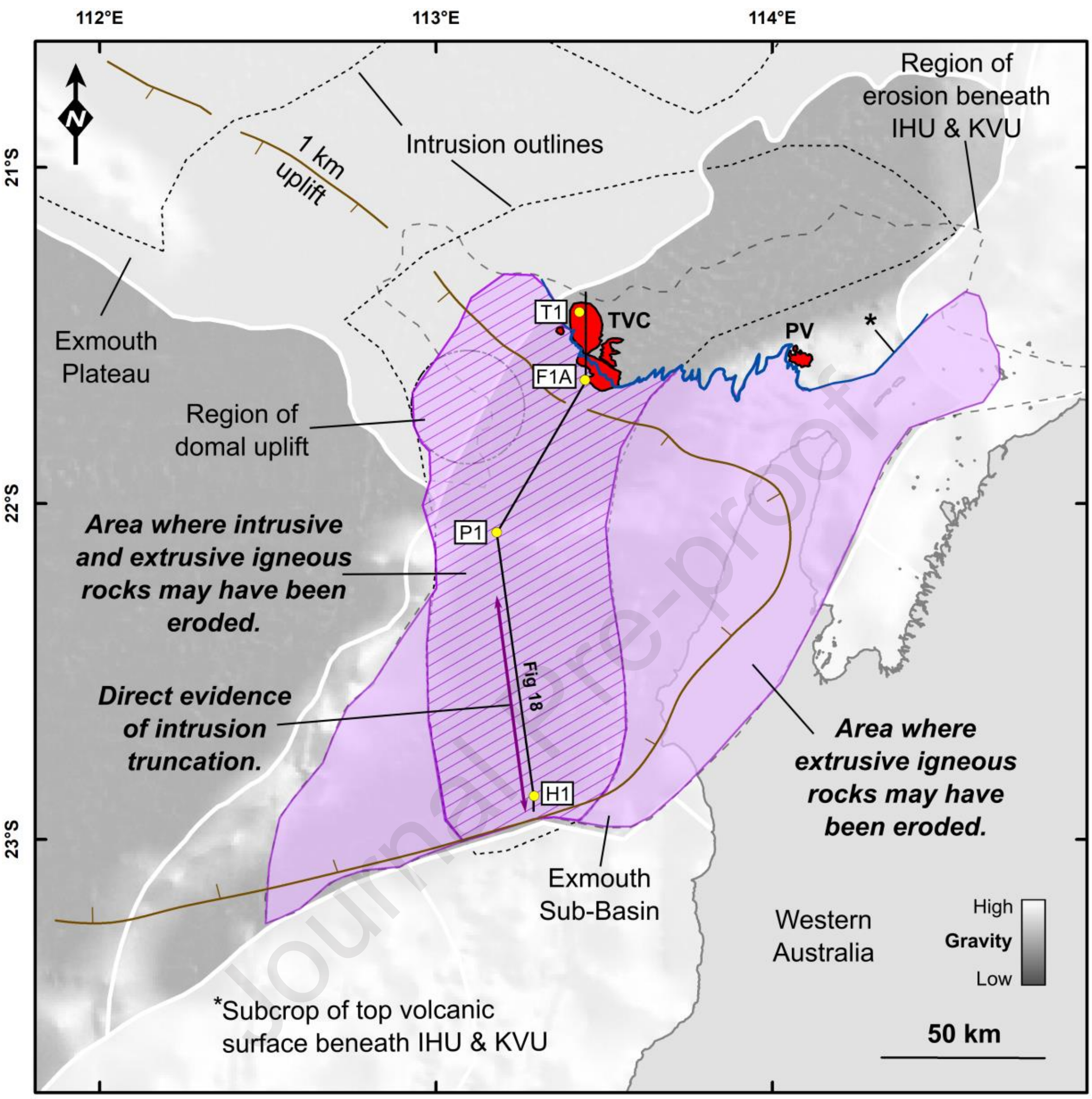

Figure 20: Regions of possible erosion of volcanic (pink) and intrusive igneous (pink hatching) rocks in the Exmouth Sub-Basin. TVC – Toro Volcanic Complex; PV – Pyrenees Volcano; IHU – Intra-Hauterivian Unconformity, KVU – Early Cretaceous (Valanginian) Unconformity; F1A – Falcone-1A, H1 – Herdsman-1, P1 – Palta-1, T1 – Toro-1. Intrusion outlines (stippled lines) are after Symonds et al. (1998); the region of domal uplift (dash-dot-dot line) after Black et al. (2017); the region of erosion beneath IHU and KVU (dashed line) after Reeve et al. (2022). The approximate location of the contour of 1 km uplift related to mantle plume activity and underplate emplacement mapped by Rohrman (2015) is also shown (brown line), with tick marks pointing toward direction of increasing uplift.

5.4 Where is this eroded material now? Implications for petroleum exploration

If significant volumes of mafic volcanic rocks have been eroded along the Ningaloo Arch and in the southern Exmouth Sub-Basin, there is the question of where this material was redeposited. Paumard et al. (2018) suggest that the material eroded from the uplifted Ningaloo Arch was re-deposited during the Early Cretaceous within the Upper Barrow Group (UBG) that overlies the KV Unconformity. The Upper Barrow Group extends across much of the Exmouth Sub-Basin and southern Exmouth Plateau (Reeve et al., 2022). It hence follows that the UBG might contain a portion of this eroded volcanic material.

In a detrital zircon study of the Late Cretaceous Ceduna Delta system in the Bight Basin, South Australia, MacDonald et al. (2013) show that while primary igneous minerals (e.g. plagioclase feldspars, pyroxenes and amphiboles, and volcanic glass altered to zeolite), can survive local weathering and incorporation into proximal volcanogenic sediments (e.g. in the Otway Basin; (Duddy, 2003)), these phases are often too soft or unstable to survive transport by fluvial systems and deposition in delta systems hundreds of kilometres away. For example, it is only apatite, quartz and zircon crystals derived from intermediate to felsic volcanism in the Southern Magmatic Province (Eromanga, Otway and Gippsland basins, southern and eastern Australia; (Duddy, 2003) and possibly the Whitsunday Volcanic Province (offshore central Queensland; (Veevers, 2000) that have been preserved in the Ceduna Delta at the Gnarlyknots-1A petroleum exploration well following up to 1,000 to 1,500 km of fluvial transport and subsequent deposition (MacDonald et al., 2013). Softer minerals, such as mica, have broken down due to weathering processes during transit.

While sediment transport distances from the Ningaloo Arch and the southern Exmouth Sub-Basin to the outer bounds of the UBG are 200 to 350 km, shorter than from the Southern Magmatic Province and Whitsunday Volcanic Province to the Ceduna Delta, we consider it unlikely that significant quantities of primary igneous minerals will remain within delta deposits of the UBG. Igneous rocks in the Exmouth Sub-Basin are mafic in composition (Curtis et al., 2022), hence their mineralogy is dominated by plagioclase feldspar and pyroxene, and devoid of quartz and apatite. Pyroxene and plagioclase feldspar are readily hydrated and altered to clay (Curtis et al., 2022), a process which could have occurred following eruption, during weathering and erosion, during transport and following deposition. Although not common in mafic igneous rocks from rifted margins, zircon crystals *may* be a possible primary igneous component of the proposed volcanic system remaining within the UBG. If zircon crystals could be collected from UBG deposits intersected in petroleum exploration wells, absolute dating to Late Jurassic and/or Early Cretaceous ages may be indicative of sourcing from a postulated eroded volcanic province.

As weathered material from the postulated volcanic province would likely be highly altered at present (all intersected mafic igneous rocks in the Northern Carnarvon basin are altered; (Curtis et al., 2022)), and as remnants of the volcanic province may be present in the UBG, this presents a potential source of clay in UBG deposits. This elevated clay content may reduce the porosity, and hence permeability, of nearshore delta sandstone deposits in the UBG (Zhou et al., 1996, Griffiths et al., 2019, Usman et al., 2020), which are often targeted as petroleum reservoirs in the Northern Carnarvon Basin.

5.5 Bias towards preservation of post-rift volcanism on rifted margins

This study has shown that the preservation potential of syn-rift, pre-breakup volcanic rocks in sedimentary depocentres on rifted margins can be low, due to their eruption in a dynamic tectonic and geomorphic setting where basins are typically subject to complex vertical motions encompassing extensive uplift, erosion, redeposition and deformation (e.g. Holford et al., 2009, Alves et al., 2020). We suggest that it is possible that the majority of pre-breakup extrusive volcanic rocks that were once present in the Exmouth Sub-Basin were uplifted and eroded prior to deposition of post-breakup sedimentary rocks, and hence they have not been preserved.

On margins where pre- and syn-rift volcanism *is* preserved, rifting tends to be associated with vast outpourings of plume-related continental flood volcanism, for example, in Afar, Ethiopia, where ~750,000 km^2 of mafic lava up to 4 km thick were erupted between 31 and 13 Ma (Mohr, 1983, Ukstins et al., 2002). Even with the presence of a breakup unconformity in Afar (Ukstins et al., 2002), and recent plateau uplift and significant erosion in the Pleistocene (Mohr, 1971, McDougall et al., 1975), the current geographic extent of the LIP is ~600,000 km^2 (Mohr, 1983). We suggest it likely that the sheer volume of extrusive volcanic rocks is what enabled their preservation. Although a plume-related supply of magma to the Carnarvon pre-breakup intrusive system is plausible (Rohrman, 2015), there is scant evidence of volcanism preserved beneath the breakup unconformity beyond what is documented in this study.

Pre-breakup tectonic settings on rift margins are often dynamic, subjecting local strata to one or more phases of uplift and erosion, as has occurred in the Northern Carnarvon Basin (Reeve et al., 2022). Pre-breakup volcanism on extensional margins therefore has high potential for removal by erosion. This may explain the lack of preservation, and apparent scarcity, of pre-breakup volcanic features in similar rift settings worldwide (Duddy, 2003). Current approaches for calculating the ratio of intrusive to extrusive igneous rock volume in volcanic rifted margins (e.g. White et al., 2006, Reynolds et al., 2018) do not account for this 'eroded' component of extrusive rock, and could therefore result in inaccurate estimates of the relative volume of original magmatic vs. volcanic rock in these settings.

In contrast, post-breakup volcanism generally occurs in a stable tectonic setting i.e. on a subsiding margin following rifting, and is typically not subject to such extensive uplift, deformation and erosion. Such volcanism is typically better preserved than pre-breakup volcanism, and hence is more often imaged in seismic reflection data. This is the case both on the outboard North West Australian Margin (e.g. the Wallaby Plateau, Quokka Rise, and Sonne and Sonja ridges; (Symonds et al., 1998, Müller et al., 2002)), in rift basins on other Australian margins (e.g. the Bass Basin; (Watson et al., 2019); and the Bight Basin; (Jackson, 2012, Reynolds et al., 2017a)) and other rift basins worldwide (e.g. the UK Faroe Shetland Basin; (Hardman et al., 2018)). This better state of preservation and ease of seismic characterisation likely accounts for the disproportionate number of studies in the scientific literature documenting post- rather than pre-breakup volcanism in rifted margins.

6. CONCLUSIONS

The Northern Carnarvon Basin has been described as host to a "Large Intrusive Igneous Province" (Rohrman, 2013). This was based on the presence of an extensive network of igneous intrusions emplaced into the crust of the Exmouth Plateau and the Exmouth Sub-Basin from the Late Jurassic to the Early Cretaceous, with the assumption that there was no extrusive component to the igneous system. This study shows that not to be the case. For the first time, we describe the Pyrenees Volcano, a well preserved volcano in the eastern Exmouth Sub-Basin. We also highlight the recently recognised Toro Volcanic Complex, composed of the Toro Volcano; a chain of peneplaned mounds previously interpreted as infilled hydrothermal vents (Magee et al., 2016a) that we have re-interpreted as eroded volcanic edifices; and an elevated volcanic plateau truncated by the KV Unconformity.

We have shown that preservation of the Pyrenees Volcano was strongly dependent on its burial by ~2000+ m accumulation of Tithonian to Valanginian LBG strata prior to Valanginian uplift (possibly related to the formation of the Novara Arch. The Pyrenees Volcano's preservation was further enhanced by its eruption and growth in submarine conditions in the Tithonian and its downthrow by multiple normal faults. These factors protected the volcano from ~1890 m of erosion following tilting and uplift in the Early Cretaceous, likely related to the formation of the Novara Arch. These conditions were not afforded to the Toro Volcanic Complex, which is peneplaned and truncated beneath the regional KV Unconformity. Here, the volcanoes formed in a shallower shelfal environment, and were subject to limited subaerial erosion. The ~760 m thickness of the overlying Lower Barrow Group and minor downthrow during the same episode of faulting that contributed to preservation of the Pyrenees Volcano, was not enough to protect the Toro Volcanic Complex from ~480 m erosion associated with the KVU following Valanginian uplift along the Ningaloo Arch to the south, and Callovian to Valanginian domal uplift to the southwest.

A significant implication is that Early Cretaceous uplift and erosion in this region are the key controls on where Tithonian aged volcanism might have been preserved. Along the Ningaloo Arch, Upper Jurassic strata have been removed. We suggest that these eroded strata may have been host to a larger volcanic province associated with syn-rift, pre-breakup magmatism, contemporaneous with the Pyrenees Volcano and the Toro Volcanic Complex. The intrusive system in the southern Exmouth Sub-Basin, hosted in Triassic and Early Jurassic sedimentary rocks that have been incised by the breakup unconformity, is also missing an extrusive component that may possibly have been eroded.

Hence the current the ratio of extrusive to intrusive igneous rocks associated with pre-breakup rifting in the Northern Carnarvon Basin is almost certainly biased towards the preserved intrusive component of magmatism. Our study thus has implications for rifted margins host to uncommonly high volumetric ratios of intrusive to extrusive igneous rock elsewhere in the world. In regions characterised by complex rift histories involving significant uplift prior to breakup, and lack of early burial of volcanic rock by contemporaneous sedimentation, it is possible that significant volumes of syn-rift, pre-breakup volcanism may have been eroded.

ACKNOWLEDGEMENTS

We would like to thank Iain Campbell, formerly Chief Petroleum Geophysicist at the South Australian Department for Energy and Mining for arranging the stitching together of multiple SEGY component files for the Indian 3D seismic reflection survey which was instrumental for interpretation of the Toro Volcanic Complex. We would also like to thank both Simon Lang and particularly Victorien Paumard of the Centre for Energy Geoscience, University of Western Australia, for numerous discussions around the development of the Barrow Delta in the Exmouth Sub-Basin and Exmouth Plateau. We thank Tiago Alves for editorial guidance, and the constructive reviews provided by Victorien Paumard, Natasha Stanton, Gerome Calves, Chris Elders, Kamaldeen Omosanya and one anonymous referee.

FUNDING

This work was supported by a postgraduate scholarship from the University of Adelaide's Faculty of Engineering Computer and Mathematical Sciences, and also by ASEG Research Foundation Grant no. RF19P01. SPH acknowledges funding support from the South Australian Department for Energy and Mining.

DATA AVAILABITY STATEMENT

All well and seismic reflection data used in this study was accessed through the National Offshore Petroleum Information Management System (NOPIMS; https://nopims.dmp.wa.gov.au/Nopims/) and the West Australian Petroleum Information Management System (WAPIMS; https://wapims.dmp.wa.gov.au/WAPIMS/).

REFERENCES

ADAMSON, K., LANG, S., MARSHALL, N., SEGGIE, R., ADAMSON, N. & BANN, K. Understanding the Late Triassic Mungaroo and Brigadier Deltas of the Northern Carnarvon Basin, North West Shelf, Australia. West Australian Basins Symposium 2013 Proceedings, Perth, WA, 2013.

ALLEN, J. 1980. Models of wind-driven currents on the continental shelf. *Annual Review of Fluid Mechanics,* 12**,** 389-433.

ALVES, T., FETTER, M., BUSBY, C., GONTIJO, R., CUNHA, T. A. & MATTOS, N. H. 2020. A tectono-stratigraphic review of continental breakup on intraplate continental margins and its impact on resultant hydrocarbon systems. *Marine and Petroleum Geology,* 117**,** 104341.

ALVES, T. M., FETTER, M., BUSBY, C., CUNHA, T. A. & MATTOS, N. H. 2023. Stratigraphic record of continental breakup, offshore NW Australia—Discussion. *Basin Research,* 35**,** 470-482.

ARDITTO, P. A. 1993. Depositional sequence model for the post-Barrow Group Neocomian succession, Barrow and Exmouth sub-basins, Western Australia. *The APPEA journal,* 33**,** 151-160.

BARBER, P. M. 1982. PALAEOTECTONIC EVOLUTION AND HYDROCARBON GENESIS OF THE CENTRAL EXMOUTH PLATEAU. *The APPEA Journal,* 22**,** 131-144.

BATIZA, R., WHITE, J. D. & SIGURDSSON, H. 2000. Submarine lavas and hyaloclastite. *Encyclopedia of volcanoes***,** 361-381.

BISCHOFF, A. P., NICOL, A. & BEGGS, M. 2017. Stratigraphy of architectural elements in a buried volcanic system and implications for hydrocarbon exploration. *Interpretation,* 5**,** SK141-SK159.

BLACK, M., MCCORMACK, K., ELDERS, C. & ROBERTSON, D. 2017. Extensional fault evolution within the Exmouth Sub-basin, North West Shelf, Australia. *Marine and Petroleum Geology,* 85**,** 301-315.

BOGGS JR, S. 2014. *Principles of sedimentology and stratigraphy*, Pearson Education.

BRAUN, J. & BEAUMONT, C. 1989. A physical explanation of the relation between flank uplifts and the breakup unconformity at rifted continental margins. *Geology,* 17**,** 760-764.

BROOKS, D. 1983. Well Completion Report, Novara-1, Carnarvon Basin, Western Australia. Esso Australia Limited.

CALVÈS, G., TORVELA, T., HUUSE, M. & DINKLEMAN, M. G. 2012. New evidence for the origin of the Porcupine Median Volcanic Ridge: Early Cretaceous volcanism in the Porcupine Basin, Atlantic margin of Ireland. *Geochemistry, Geophysics, Geosystems,* 13.

CHONGZHI, T., GUOPING, B., JUNLAN, L., CHAO, D., XIAOXIN, L., HOUWU, L., DAPENG, W., YUAN, W. & MIN, L. 2013. Mesozoic lithofacies palaeogeography and petroleum prospectivity in North Carnarvon Basin, Australia. *Journal of Palaeogeography,* 2**,** 81-92.

COLLIER, J. & WATTS, A. 2001. Lithospheric response to volcanic loading by the Canary Islands: constraints from seismic reflection data in their flexural moat. *Geophysical Journal International,* 147**,** 660-676.

CURTIS, M. S., HOLFORD, S. P., BUNCH, M. A. & SCHOFIELD, N. J. 2022. Seismic, petrophysical and petrological constraints on the alteration of igneous rocks in the Northern Carnarvon Basin, Western Australia: implications for petroleum exploration and drilling operations. *The APPEA Journal,* 62**,** 196-222.

DALE, M. 2015. Palta 1 & Palta 1 ST1 Final Well Completion Report. Shell Development (Australia) Pty Ltd.

DAVIES, R., BELL, B. R., CARTWRIGHT, J. A. & SHOULDERS, S. 2002. Three-dimensional seismic imaging of Paleogene dike-fed submarine volcanoes from the northeast Atlantic margin. *Geology,* 30**,** 223-226.

DAVIS, R. A. 1985. Beach and nearshore zone. *Coastal sedimentary environments.* Springer.

DEMPSEY, C., BENSON, R., O'HALLORAN, G. & DAVIES, C. 2019. A Summary of the Tectonic and Sedimentological History of the Exmouth Sub Basin.: BHP Petroleum Pty Ltd.

DIREEN, N., STAGG, H., SYMONDS, P. & COLWELL, J. 2008. Architecture of volcanic rifted margins: new insights from the Exmouth–Gascoyne margin, Western Australia. *Australian Journal of Earth Sciences,* 55, 341-363.

DRISCOLL, N. W. & KARNER, G. D. 1998. Lower crustal extension across the Northern Carnarvon basin, Australia: Evidence for an eastward dipping detachment. *Journal of Geophysical Research: Solid Earth,* 103, 4975-4991.

DUDDY, I. 2003. Mesozoic: a time of change in tectonic regime. Geological Society of Australia Victoria Division.

EMBRY, A. F. & KLOVAN, J. E. 1972. Absolute water depth limits of Late Devonian paleoecological zones. *Geologische Rundschau,* 61, 672-686.

EXON, N. F., BUFFLER, R. T., GRADSTEIN, F. & LUDDEN, J. Mesozoic seismic stratigraphy and tectonic evolution of the western Exmouth Plateau. Proceedings of the Ocean Drilling Program, Scientific Results, 1992. ODP Ocean Drilling Program, 61-81.

FELTON, E. A., MIYAZAKI, S., DOWLING, L., PAIN, L., VUCKOVIC, V. & LE POIDEVIN, S. R. 1992. Carnarvon Basin, W.A. *Australian Petroleum Accumulations,* 8.

FOMIN, T., GONCHAROV, A., SYMONDS, P. & COLLINS, C. 2000. Acoustic structure and seismic velocities in the Carnarvon Basin, Australian North West Shelf: towards an integrated study. *Exploration Geophysics,* 31, 579-583.

FREY, Ø., PLANKE, S., SYMONDS, P. A. & HEEREMANS, M. 1998. Deep crustal structure and rheology of the Gascoyne volcanic margin, Western Australia. *Marine Geophysical Researches,* 20, 293-311.

GA. 2022. *National Offshore Petroleum Information Mangagement System* [Online]. National Offshore Petroleum Titles Administrator, Geoscience Australia. Available: https://nopims.dmp.wa.gov.au/Nopims/.

GHORI, K. 1999. *Silurian-Devonian petroleum source-rock potential and thermal history, Carnarvon Basin, Western Australia*, Geological Survey of Western Australia.

GIBSON, P. 2014. Palta 1 & Palta 1 ST1 Initial Well Completion Report. Shell Development (Australia) Pty Ltd.

GRAIN, S., FOLKERS, T., ROBERTSON, D., MACKAY, S. & MAGEE, T. 2015. Drilling a Volcanic Complex at Toro-1 Provides Insights Into Jurassic Rifting in the Exmouth Sub-Basin, Western Australia. *International Conference and Exhibition.* Melbourne: Society of Exploration Geophysicists.

GRIFFITHS, J., WORDEN, R. H., WOOLDRIDGE, L. J., UTLEY, J. E., DULLER, R. A. & EDGE, R. L. 2019. Estuarine clay mineral distribution: modern analogue for ancient sandstone reservoir quality prediction. *Sedimentology,* 66, 2011-2047.

HANSEN, D. M. 2006. The morphology of intrusion-related vent structures and their implications for constraining the timing of intrusive events along the NE Atlantic margin. *Journal of the Geological Society,* 163, 789-800.

HANSEN, D. M. & CARTWRIGHT, J. 2006a. Saucer-shaped sill with lobate morphology revealed by 3D seismic data: implications for resolving a shallow-level sill emplacement mechanism. *Journal of the Geological Society,* 163, 509-523.

HANSEN, D. M. & CARTWRIGHT, J. 2006b. The three-dimensional geometry and growth of forced folds above saucer-shaped igneous sills. *Journal of Structural Geology,* 28, 1520-1535.

HANSEN, D. M., REDFERN, J., FEDERICI, F., DI BIASE, D. & BERTOZZI, G. 2008. Miocene igneous activity in the Northern Subbasin, offshore Senegal, NW Africa. *Marine and Petroleum Geology,* 25, 1-15.

HARDMAN, J., SCHOFIELD, N., JOLLEY, D., HARTLEY, A., HOLFORD, S. & WATSON, D. 2018. Controls on the distribution of volcanism and intra-basaltic sediments in the Cambo–Rosebank region, West of Shetland. *Petroleum Geoscience.*

HELBY, R., MORGAN, R. & PARTRIDGE, A. D. 2004. Updated Jurassic–Early Cretaceous dinocyst zonation, NWS Australia. *Geoscience Australia Publication,* 1, 01.

HELDREICH, G., REDFERN, J., LEGLER, B., GERDES, K. & WILLIAMS, B. 2017. Challenges in characterizing subsurface paralic reservoir geometries: a detailed case study of the

Mungaroo Formation, North West Shelf, Australia. *Geological Society, London, Special Publications,* 444**,** 59-108.

HOCKING, R., VOON, J. & COLLINS, L. Stratigraphy and sedimentology of the basal Winning Group, northern Carnarvon Basin. The North West shelf, Australia. Symposium, 1988. 203-224.

HOCKING, R. M. 1992. *Jurassic deposition in the southern and central North West Shelf, Western Australia*, Geological Survey of Western Australia.

HOLFORD, S., SCHOFIELD, N., JACKSON, C.-L., MAGEE, C., GREEN, P. & DUDDY, I. 2013. Impacts of igneous intrusions on source reservoir potential in prospective sedimentary basins along the western Australian continental margin.

HOLFORD, S. P., GREEN, P. F., DUDDY, I. R., TURNER, J. P., HILLIS, R. R. & STOKER, M. S. 2009. Regional intraplate exhumation episodes related to plate-boundary deformation. *Geological Society of America Bulletin,* 121**,** 1611-1628.

HOLFORD, S. P., SCHOFIELD, N. & REYNOLDS, P. 2017. Subsurface fluid flow focused by buried volcanoes in sedimentary basins: Evidence from 3D seismic data, Bass Basin, offshore southeastern Australia. *Interpretation,* 5**,** SK39-SK50.

HOLFORD, S. S., N.; MACDONALD, JD; DUDDY, IR; GREEN PF 2012. Seismic analysis of igneous systems in sedimentary basins and thier impacts on hydrocarbon prospectivity: examples from the Southern Australian Margin. *APPEA Journal*.

JABLONSKI, D. 1997. Recent advances in the sequence stratigraphy of the Triassic to Lower Cretaceous succession in the northern Carnarvon Basin, Australia. *The APPEA Journal,* 37**,** 429-454.

JACKSON, C. A.-L. 2012. Seismic reflection imaging and controls on the preservation of ancient sill-fed magmatic vents. *Journal of the Geological Society,* 169**,** 503-506.

JAMTVEIT, B., SVENSEN, H., PODLADCHIKOV, Y. Y. & PLANKE, S. 2004. Hydrothermal vent complexes associated with sill intrusions in sedimentary basins. *Physical Geology of High-Level Magmatic Systems. Geological Society, London, Special Publications,* 234**,** 233-241.

JOHNSON, J., GIBSON, S., THOMPSON, R. & NOWELL, G. 2005. Volcanism in the Vitim volcanic field, Siberia: Geochemical evidence for a mantle plume beneath the Baikal rift zone. *Journal of Petrology,* 46**,** 1309-1344.

JOLLEY, D. W., MILLETT, J. M., SCHOFIELD, N. & BROADLEY, L. 2021. Stratigraphy of volcanic rock successions of the North Atlantic rifted margin: the offshore record of the Faroe–Shetland and Rockall basins. *Earth and Environmental Science Transactions of the Royal Society of Edinburgh,* 112**,** 61-88.

KIØRBOE, L. Stratigraphic relationships of the Lower Tertiary of the Faeroe basalt plateau and the Faeroe–Shetland Basin. Geological Society, London, Petroleum Geology Conference series, 1999. Geological Society of London, 559-571.

KJELLGREN, G., HOLLAMS, R., MARKS, T. & WHITE, H. 1982. Yardie East 1, Well Completion Report. Perth, WA: Mesa Australia Limited.

LEBEDEV, S., MEIER, T. & VAN DER HILST, R. D. 2006. Asthenospheric flow and origin of volcanism in the Baikal Rift area. *Earth and Planetary Science Letters,* 249**,** 415-424.

LESAGE, P., HEAP, M. J. & KUSHNIR, A. 2018. A generic model for the shallow velocity structure of volcanoes. *Journal of Volcanology and Geothermal Research,* 356**,** 114-126.

LIPSKI, P. 1993. TECTONIC SETTING, STRATIGRAPHY AND HYDROCARBON POTENTIAL OF THE BEDOUT SUB-BASIN, NORTH WEST SHELF. *The APPEA Journal,* 33**,** 138-150.

LOCKE, A. 2004. Stybarrow 2: Well Completion Report, Interpretive Volume. Perth: BHP Billiton.

LONGLEY, I., BUESSENSCHUETT, C., CLYDSDALE, L., CUBITT, C., DAVIS, R., JOHNSON, M., MARSHALL, N., MURRAY, A., SOMERVILLE, R. & SPRY, T. The North West Shelf of Australia–a Woodside perspective. The Sedimentary Basins of Western Australia 3: Proceedings of the Petroleum Exploration Society of Australia Symposium, Perth, 2002. Pet. Explor. Soc. of Aust. Perth, 27-88.

LOUVAT, P. & ALLÈGRE, C. J. 1998. Riverine erosion rates on Sao Miguel volcanic island, Azores archipelago. *Chemical Geology,* 148**,** 177-200.

MACDONALD, J. D., HOLFORD, S. P., GREEN, P. F., DUDDY, I. R., KING, R. C. & BACKÉ, G. 2013. Detrital zircon data reveal the origin of Australia's largest delta system. *Journal of the Geological Society,* **170,** 3-6.

MAGEE, C., BRIGGS, F. & JACKSON, C. A. L. 2013a. Lithological controls on igneous intrusion-induced ground deformation. *Journal of the Geological Society,* **170,** 853-856.

MAGEE, C., DUFFY, O. B., PURNELL, K., BELL, R. E., JACKSON, C. A. L. & REEVE, M. T. 2016a. Fault-controlled fluid flow inferred from hydrothermal vents imaged in 3D seismic reflection data, offshore NW Australia. *Basin Research,* **28,** 299-318.

MAGEE, C., HUNT-STEWART, E. & JACKSON, C. A. L. 2013b. Volcano growth mechanisms and the role of sub-volcanic intrusions: Insights from 2D seismic reflection data. *Earth and Planetary Science Letters,* **373,** 41-53.

MAGEE, C. & JACKSON, C. A. L. 2020. Seismic reflection data reveal the 3D structure of the newly discovered Exmouth Dyke Swarm, offshore NW Australia. *Solid Earth,* **11,** 579-606.

MAGEE, C., JACKSON, C. A. L., HARDMAN, J. P. & REEVE, M. T. 2017. Decoding sill emplacement and forced fold growth in the Exmouth Sub-basin, offshore northwest Australia: Implications for hydrocarbon exploration. *Interpretation,* **5,** SK11-SK22.

MAGEE, C., JACKSON, C. A. L. & SCHOFIELD, N. 2013c. The influence of normal fault geometry on igneous sill emplacement and morphology. *Geology,* **41,** 407-410.

MAGEE, C., MUIRHEAD, J. D., KARVELAS, A., HOLFORD, S. P., JACKSON, C. A. L., BASTOW, I. D., SCHOFIELD, N., STEVENSON, C. T. E., MCLEAN, C., MCCARTHY, W. & SHTUKERT, O. 2016b. Lateral magma flow in mafic sill complexes. *Geosphere,* **12,** 809-841.

MARK, N., HOLFORD, S., SCHOFIELD, N., EIDE, C. H., PUGLIESE, S., WATSON, D. & MUIRHEAD, D. 2020. Structural and lithological controls on the architecture of igneous intrusions: examples from the NW Australian Shelf. *Petroleum Geoscience***,** petgeo2018-067.

MARK, N., SCHOFIELD, N., GARDINER, D., HOLT, L., GROVE, C., WATSON, D., ALEXANDER, A. & POORE, H. 2019. Overthickening of sedimentary sequences by igneous intrusions. *Journal of the Geological Society,* **176,** 46-60.

MARK, N. J., SCHOFIELD, N., PUGLIESE, S., WATSON, D., HOLFORD, S., MUIRHEAD, D., BROWN, R. & HEALY, D. 2018. Igneous intrusions in the Faroe Shetland basin and their implications for hydrocarbon exploration; new insights from well and seismic data. *Marine and Petroleum Geology,* **92,** 733-753.

MARSHALL, N. & LANG, S. A new sequence stratigraphic framework for the North West Shelf, Australia. The Sedimentary Basins of Western Australia 4: Proceedings PESA Symposium. Perth, 2013. 1-32.

MCCAFFREY, J. C., WALLACE, M. W. & GALLAGHER, S. J. 2020. A cenozoic great barrier reef on Australia's north west shelf. *Global and Planetary Change,* **184,** 103048.

MCCLAY, K., SCARSELLI, N. & JITMAHANTAKUL, S. 2013. Igneous Intrusions in the Carnarvon Basin, NW Shelf, Australia. *West Astralian Basins Symmposium*.

MCDOUGALL, I., MORTON, W. & WILLIAMS, M. 1975. Age and rates of denudation of Trap Series basalts at Blue Nile Gorge, Ethiopia. *Nature,* **254,** 207-209.

MIHUT, D. & MÜLLER, R. D. 1998. Volcanic margin formation and Mesozoic rift propagators in the Cuvier Abyssal Plain off Western Australia. *Journal of Geophysical Research: Solid Earth,* **103,** 27135-27149.

MITCHUM, R., VAIL, P. R. & SANGREE, J. B. 1977a. Seismic stratigraphy and global changes of sea level: Part 6. Stratigraphic interpretation of seismic reflection patterns in depositional sequences: Section 2. Application of seismic reflection configuration to stratigraphic interpretation.

MITCHUM, R., VAIL, P. R. & THOMPSON III, S. 1977b. Seismic stratigraphy and global changes of sea level: Part 2. The depositional sequence as a basic unit for stratigraphic analysis: Section 2. Application of seismic reflection configuration to stratigraphic interpretation.

MOHR, P. 1983. Ethiopian flood basalt province. *Nature,* **303,** 577-584.

MOHR, P. A. 1971. *The geology of Ethiopia*, Haile Selassie I University Press.

MÜLLER, R., MIHUT, D., HEINE, C., O'NEILL, C., RUSSELL, I., KEEP, M. & MOSS, S. Tectonic and volcanic history of the Carnarvon Terrace: Constraints from seismic interpretation and geodynamic modelling. The Sedimentary Basins of Western Australia 3: Proceedings of the Petroleum Exploration Society of Australia Symposium, 2002. Petroleum Exploration Society of Australia, Perth, Australia, 719-740.

MUTTER, J. C. & LARSON, R. L. 1989. Extension of the Exmouth Plateau, offshore northwestern Australia: Deep seismic reflection/refraction evidence for simple and pure shear mechanisms. *Geology,* 17**,** 15-18.

NITTROUER, C. & STERNBERG, R. 1981. The formation of sedimentary strata in an allochthonous shelf environment: the Washington continental shelf. *Developments in Sedimentology.* Elsevier.

O'HALLORAN, G., BENSON, R. & DEMPSEY, C. 2019. Jurassic igneous activity in the Exmouth Sub-basin: Insights from new 3D seismic. *ASEG Extended Abstracts,* 2019**,** 1-6.

OLIEROOK, H. K., MERLE, R. E., JOURDAN, F., SIRCOMBE, K., FRASER, G., TIMMS, N. E., NELSON, G., DADD, K. A., KELLERSON, L. & BORISSOVA, I. 2015. Age and geochemistry of magmatism on the oceanic Wallaby Plateau and implications for the opening of the Indian Ocean. *Geology,* 43**,** 971-974.

PAUMARD, V., BOURGET, J., PAYENBERG, T., AINSWORTH, R. B., GEORGE, A. D., LANG, S., POSAMENTIER, H. W. & PEYROT, D. 2018. Controls on shelf-margin architecture and sediment partitioning during a syn-rift to post-rift transition: Insights from the Barrow Group (Northern Carnarvon Basin, North West Shelf, Australia). *Earth-Science Reviews,* 177**,** 643-677.

PAUMARD, V., BOURGET, J., PAYENBERG, T., GEORGE, A. D., AINSWORTH, R. B. & LANG, S. 2019. From quantitative 3D seismic stratigraphy to sequence stratigraphy: insights into the vertical and lateral variability of shelf-margin depositional systems at different stratigraphic orders. *Marine and Petroleum Geology,* 110**,** 797-831.

PAYENBERG, T., WILLIS, B., FOWLER, J., LANG, S., POWELL, A., MARSH, T., SIXSMITH, P. & VAKARELOV, B. 2019. Morphometrics of channel belts from the Mungaroo Formation, NWS, Australia.

PLANKE, S., RASMUSSEN, T., REY, S. S. & MYKLEBUST, R. Seismic characteristics and distribution of volcanic intrusions and hydrothermal vent complexes in the Vøring and Møre basins. Geological Society, London, Petroleum Geology Conference series, 2005. Geological Society of London, 833-844.

PLANKE, S., SYMONDS, P. A., ALVESTAD, E. & SKOGSEID, J. 2000. Seismic volcanostratigraphy of large‐volume basaltic extrusive complexes on rifted margins. *Journal of Geophysical Research: Solid Earth,* 105**,** 19335-19351.

QUILTY, P. G. 1977. Cenozoic sedimentation cycles in Western Australia. *Geology,* 5**,** 336-340.

QUIRIE, A. K., SCHOFIELD, N., HARTLEY, A., HOLE, M. J., ARCHER, S. G., UNDERHILL, J. R., WATSON, D. & HOLFORD, S. P. 2019. The Rattray Volcanics: Mid-Jurassic fissure volcanism in the UK Central North Sea. *Journal of the Geological Society,* 176**,** 462-481.

REEVE, M. T., JACKSON, C. A. L., BELL, R. E., MAGEE, C. & BASTOW, I. D. 2016. The stratigraphic record of prebreakup geodynamics: Evidence from the Barrow Delta, offshore Northwest Australia. *Tectonics,* 35**,** 1935-1968.

REEVE, M. T., MAGEE, C., BASTOW, I. D., MCDERMOTT, C., JACKSON, C. A.-L., BELL, R. E. & PRYTULAK, J. 2021. Nature of the Cuvier Abyssal Plain crust, offshore NW Australia. *Journal of the Geological Society*.

REEVE, M. T., MAGEE, C., JACKSON, C. A. L., BELL, R. E. & BASTOW, I. D. 2022. Stratigraphic record of continental breakup, offshore NW Australia. *Basin Research*.

REY, S. S., PLANKE, S., SYMONDS, P. A. & FALEIDE, J. I. 2008. Seismic volcanostratigraphy of the Gascoyne margin, Western Australia. *Journal of Volcanology and Geothermal Research,* 172**,** 112-131.

REYNOLDS, P., HOLFORD, S., SCHOFIELD, N. & ROSS, A. 2017a. The shallow depth emplacement of mafic intrusions on a magma-poor rifted margin: An example from the Bight Basin, southern Australia. *Marine and Petroleum Geology,* 88**,** 605-616.

REYNOLDS, P., HOLFORD, S., SCHOFIELD, N. & ROSS, A. 2017b. Three-Dimensional Seismic Imaging of Ancient Submarine Lava Flows: An Example From the Southern Australian Margin. *Geochemistry, Geophysics, Geosystems,* 18**,** 3840-3853.

REYNOLDS, P., HOLFORD, S., SCHOFIELD, N. & ROSS, A. 2018. The importance of subsurface lithology in controlling magma storage v. eruption: an example from offshore southern Australia. *Journal of the Geological Society,* 175**,** 694-703.

REYNOLDS, P., SCHOFIELD, N., BROWN, R. J. & HOLFORD, S. P. 2017c. The architecture of submarine monogenetic volcanoes - insights from 3D seismic data. *Basin Research,* 30**,** 437-451.

RIERA, R. 2020. Stratigraphic evolution of Miocene carbonate platforms of the North West Shelf (Exmouth-Barrow Sub-basins, Australia).

ROBB, M. S., TAYLOR, B. & GOODLIFFE, A. M. 2005. Re-examination of the magnetic lineations of the Gascoyne and Cuvier Abyssal Plains, off NW Australia. *Geophysical Journal International,* 163**,** 42-55.

ROHRMAN, M. 2013. Intrusive large igneous provinces below sedimentary basins: An example from the Exmouth Plateau (NW Australia). *Journal of Geophysical Research: Solid Earth,* 118**,** 4477-4487.

ROHRMAN, M. 2015. Delineating the Exmouth mantle plume (NW Australia) from denudation and magmatic addition estimates. *Lithosphere,* 7**,** 589-600.

SANDWELL, D. & SMITH, W. 1997. Marine gravity anomaly from Geosat and ERS 1 satellite altimetry: Journal of Geophysical Research. *B, Solid Earth and Planets,* 102**,** 10,039-10,054.

SAYERS, J., BORISSOVA, I., SYMONDS, P. A. & RAMSAY, D. C. 2002. *Geological framework of the Wallaby Plateau and adjacent areas*, Geoscience Australia.

SCHMIEDEL, T., GALLAND, O., HAUG, Ø. T., DUMAZER, G. & BREITKREUZ, C. 2019. Coulomb failure of Earth's brittle crust controls growth, emplacement and shapes of igneous sills, saucer-shaped sills and laccoliths. *Earth and Planetary Science Letters,* 510**,** 161-172.

SCHOFIELD, N., HEATON, L., HOLFORD, S. P., ARCHER, S. G., JACKSON, C. A. L. & JOLLEY, D. W. 2012a. Seismic imaging of 'broken bridges': linking seismic to outcrop-scale investigations of intrusive magma lobes. *Journal of the Geological Society,* 169**,** 421-426.

SCHOFIELD, N., HOLFORD, S., MILLETT, J., BROWN, D., JOLLEY, D., PASSEY, S. R., MUIRHEAD, D., GROVE, C., MAGEE, C., MURRAY, J., HOLE, M., JACKSON, C. A. L. & STEVENSON, C. 2017. Regional magma plumbing and emplacement mechanisms of the Faroe-Shetland Sill Complex: implications for magma transport and petroleum systems within sedimentary basins. *Basin Research,* 29**,** 41-63.

SCHOFIELD, N. J., BROWN, D. J., MAGEE, C. & STEVENSON, C. T. 2012b. Sill morphology and comparison of brittle and non-brittle emplacement mechanisms. *Journal of the Geological Society,* 169**,** 127-141.

SHIPBOARD SCIENTIFIC PARTY 1990. Site 763. *In:* HAQ, B. U., VON RAD, U., O'CONNELL, S. & AL, E. (eds.) *Proceedings of the Ocean Drilling Program, Initial Reports, 122: College Station, Texas.*

SINHA, S., ROUTH, P. S., ANNO, P. D. & CASTAGNA, J. P. 2005. Spectral decomposition of seismic data with continuous-wavelet transform. *Geophysics,* 70**,** P19-P25.

SMALLWOOD, J. R. & MARESH, J. 2002. The properties, morphology and distribution of igneous sills: modelling, borehole data and 3D seismic from the Faroe-Shetland area. *Geological Society, London, Special Publications,* 197**,** 271-306.

SMITH, N., DEMPSEY, C., JACKSON, M. & PRESTON, J. 2003. Overcoming historical bias: an integrated geological and engineering assessment of the Coniston prospect, Exmouth Sub-basin. *The APPEA Journal,* 43**,** 363-383.

SOMOZA, L., DıAZ-DEL-RıO, V., LEÓN, R., IVANOV, M., FERNÁNDEZ-PUGA, M., GARDNER, J., HERNÁNDEZ-MOLINA, F., PINHEIRO, L., RODERO, J. & LOBATO, A. 2003. Seabed morphology and hydrocarbon seepage in the Gulf of Cadiz mud volcano area: Acoustic imagery, multibeam and ultra-high resolution seismic data. *Marine geology,* 195**,** 153-176.

SPRY, T. 1994. WA-155-P, Pyrenees-1 Well Completion Report: Interpretive Volume.: BHP Petroleum.

STURROCK, V. 2014. Toro 1 (WA-430-P, Carnarvon Basin) Initial Well Completion Report. Woodside Energy Ltd.

SVENSEN, H., JAMTVEIT, B., PLANKE, S. & CHEVALLIER, L. 2006. Structure and evolution of hydrothermal vent complexes in the Karoo Basin, South Africa. *Journal of the Geological Society,* 163**,** 671-682.

SYMONDS, P., PLANKE, S., FREY, O. & SKOGSEID, J. 1998. Volcanic Evolution of the Western Australian Continental Margin and its Implications for Basin Development. *In:* PURCELL, P. P., RR; (ed.) *The Sedimentary Basins of West Australia 2.* Perth: West Australin Basins Symposium.

TAIT, A. M. 1985. A depositional model for the Dupuy Member and the Barrow Group in the Barrow Sub-basin, Northwestern Australia. . *The APPEA Journal,* 25**,** 282-290.

TAYLOR, L. 2014. Toro 1 (WA-430-P, Carnarvon Basin) Final Well Completion Report. Woodside Energy Ltd.

TAYLOR, L., KITTIKKAT, M., CARTER, T. & HULL, J. 2013. Ragnar-1 and 1A Final Well Completion Report. Woodside Energy Ltd.

THOMSON, K. 2005. Volcanic features of the North Rockall Trough: application of visualisation techniques on 3D seismic reflection data. *Bulletin of Volcanology,* 67**,** 116-128.

TINDALE, K., NEWELL, N., KEALL, J., SMITH, N., PURCELL, P. & PURCELL, R. 1998. Structural evolution and charge history of the Exmouth Sub-basin, northern Carnarvon Basin, Western Australia. *The Sedimentary Basins of Western Australia,* 2.

UKSTINS, I. A., RENNE, P. R., WOLFENDEN, E., BAKER, J., AYALEW, D. & MENZIES, M. 2002. Matching conjugate volcanic rifted margins: 40Ar/39Ar chrono-stratigraphy of pre-and syn-rift bimodal flood volcanism in Ethiopia and Yemen. *Earth and Planetary Science Letters,* 198**,** 289-306.

UNDERSCHULTZ, J., HILL, R. & EASTON, S. 2008. The hydrodynamics of fields in the Macedon, Pyrenees, and Barrow sands, Exmouth Sub-basin, Northwest Shelf Australia: identifying seals and compartments. *Exploration Geophysics,* 39**,** 85-93.

USMAN, M., SIDDIQUI, N. A., MATHEW, M., ZHANG, S., EL-GHALI, M. A., RAMKUMAR, M., JAMIL, M. & ZHANG, Y. 2020. Linking the influence of diagenetic properties and clay texture on reservoir quality in sandstones from NW Borneo. *Marine and Petroleum Geology,* 120**,** 104509.

VEEVERS, J. 2000. *Billion-year earth history of Australia and neighbours in Gondwanaland*, GEMOC Press, Macquarie University Sydney.

VELAYATHAM, T., HOLFORD, S. & BUNCH, M. 2018. Linear Trends of Paleo-Pockmarks and Fluid Flow Pipes in the Jurassic and Triassic Sediments of Offshore Northwest Australia. *ASEG Extended Abstracts,* 2018**,** 1-3.

VON STACKELBERG, U., EXON, N., VON RAD, U., QUILTY, P., SHAFIK, S., BEIERSDORF, H., SEIBERTZ, E. & VEEVERS, J. 1980. Geology of the Exmouth and Wallaby Plateaus off northwest Australia: sampling of seismic sequences. *BMR J. Aust. Geol. Geophys,* 5**,** 113-140.

WADGE, G. & LOPES, R. 1991. The lobes of lava flows on Earth and Olympus Mons, Mars. *Bulletin of Volcanology,* 54**,** 10-24.

WATSON, D., HOLFORD, S., SCHOFIELD, N. & MARK, N. 2019. Failure to predict igneous rocks encountered during exploration of sedimentary basins: a case study of the Bass Basin, Southeastern Australia. *Marine and Petroleum Geology,* 99**,** 526-547.

WHITE, R. & MCKENZIE, D. 1989. Magmatism at rift zones: the generation of volcanic continental margins and flood basalts. *Journal of Geophysical Research: Solid Earth,* 94**,** 7685-7729.

WHITE, S. M., CRISP, J. A. & SPERA, F. J. 2006. Long-term volumetric eruption rates and magma budgets. *Geochemistry, Geophysics, Geosystems,* 7.

WILKINS, M. 2002. Indian 2000 3D Seismic Interpretation Report, WA-271-P, Exmouth Sub-basin, Australia. Perth: Woodside Energy Ltd.

WILLIS, S. 2001. Enfield 3, Well Completion Report, Interpretive Data. Woodside Energy Ltd.

WILLIS, S. 2002. Enfield 4, Well Completion Report, Interpretive Data Woodside Energy Ltd.

WILLIS, S. 2003. Herdsman-1 Well Completion Report - Interpretive Data (WA-299P, Carnarvon Basin). Perth, Western Australia: Woodside Ltd.

ZHOU, Z., GUNTER, W., KADATZ, B. & CAMERON, S. 1996. Effect of clay swelling on reservoir quality. *Journal of Canadian Petroleum Technology,* 35.

HIGHLIGHTS

Two Late Jurassic volcanic centres: the Pyrenees Volcano and the Toro Volcanic Complex, are present in the inboard Exmouth Sub-Basin (ESB), part of the Carnarvon Basin, Western Australia.

The Pyrenees Volcano is well preserved, whilst the Toro Volcanic Complex has been peneplaned following Late Jurassic to Early Cretaceous uplift and erosion.

The proximity of preserved volcanic centres to arches uplifted from the Late Jurassic to the Early Cretaceous suggests a broader volcanic province in the southern ESB was uplifted and eroded.

Geologists may be underestimating the significance of pre-breakup extrusive volcanic rocks on magma-rich rifted margins worldwide.

Declaration of interests

☒ The authors declare that they have no known competing financial interests or personal relationships that could have appeared to influence the work reported in this paper.

☐ The authors declare the following financial interests/personal relationships which may be considered as potential competing interests: